MICROCOPY RESOLUTION TEST CHART

NATIONAL BUREAU OF STANDARDS-1963-A

DTIC
ELECTE
S
MAR 1 1 1986
D
D

AIRCRAFT PERFORMANCE OPTIMIZATION

WITH THRUST VECTOR CONTROL

THESIS

Mark S. Fellows

AFIT/GAE/AA/85D-6

DEPARTMENT OF THE AIR FORCE

AIR UNIVERSITY

AIR FORCE INSTITUTE OF TECHNOLOGY

Wright-Patterson Air Force Base Ohio

AFIT/GAE/AA/85D-6

AIRCRAFT PERFORMANCE OPTIMIZATION

WITH THRUST VECTOR CONTROL

THESIS

Mark S. Fellows

AFIT/GAE/AA/85D-6

AIRCRAFT PERFORMANCE OPTIMIZATION

WITH THRUST VECTOR CONTROL

THESIS

Presented to the Faculty of the School of Engineering

of the Air Force Institute of Technology

Air University

In Partial Fulfillment of the

Requirements for the Degree of

Master of Science in Aeronautical Engineering

Mark S. Fellows, B.S.A.E.

December 1985

Accesion For		
NTIS CRA&I		☑
DTIC TAB		☐
Unannounced		☐
Justification		
By		
Dist ibution /		
Availability Codes		
Dist	Avail and / or Special	
A-1		

Approved for public release; distribution unlimited

Table of Contents

Acknowledgements

I would like to thank my thesis advisor, Dr Curtis Spenny, for contributing much time and effort in helping me complete this project. I also appreciate the help and advice given by my thesis committee, consisting of Dr Robert Calico, Capt Lanson Hudson and Dr Peter Torvik. I would also like to thank the members of the sponsoring organization that contributed to this effort, in particular, Jerome Forner, Richard Dyer, Jacqueline Harris, Richard Johnson and Lt Charles Brink. Finally, I would like to thank my wife, Kathy, for her support and understanding during the 18 month program at AFIT.

List of Figures

List of Tables

List of Symbols

C_D	— drag coefficient
C_L	— lift coefficient
C_{L_α}	— lift curve slope due to angle of attack
$C_{L_{\delta_c}}$	— lift curve slope due to canard deflection
D	— drag
E	— energy
F_g	— gross thrust
F_N	— net thrust
g	— gravitational constant
h	— altitude
K	— induced drag coefficient
l_{c_x}	— distance from canard to center of gravity parallel to x-axis
l_{c_z}	— distance from canard to center of gravity parallel to z-axis
l_{N_x}	— distance from nozzle to center of gravity parallel to x-axis
l_{N_z}	— distance from nozzle to center of gravity parallel to z-axis
L	— lift
m	— aircraft mass
M	— Mach number
n	— load factor
P_s	— specific excess power
q	— dynamic pressure
Q	— sideforce
sfc	— specific fuel consumption
S	— wing reference area
t_{ff}	— fuel flow slope with thrust

t_0 - fuel flow at zero thrust

T - thrust

V - velocity

W - aircraft weight

X - downrange

Y - crossrange

α - angle of attack

γ - flight path angle

δ_c - canard deflection angle

δ_N - nozzle deflection angle

ε - thrust angle of attack

μ - bank angle

ν - thrust sideslip angle

π - thrust power setting

ρ - air density

τ - aircraft angle

χ - heading angle

Subscripts

c   - canard

WB   - wing/body

0   - zero lift condition

Abstract

The objective of this investigation is to determine to what extent a highly-maneuverable aircraft's overall performance capability is enhanced by thrust-vectoring nozzles. The resulting performance capabilities are compared to a baseline configuration with non-thrust-vectoring nozzles to determine the effects and advantages of thrust vectoring.

The results indicate that the use of vectored thrust can significantly increase an aircraft's performance capability in turning flight. The greater the demand on the aircraft in a turning combat scenario, the more the aircraft utilizes its thrust-vectoring capability to complete the task. The results also indicate that the use of vectored thrust in other phases of flight -- such as cruise, acceleration and climb -- only slightly increases an aircraft's performance capability.

AIRCRAFT PERFORMANCE OPTIMIZATION WITH THRUST VECTOR CONTROL

I. Introduction

Background

A fighter aircraft's performance capability mainly consists of a combat mission radius associated with its close-in combat maneuverability. By evaluating the aircraft's performance characteristics in segments which, when added together, define the combat mission profile, the design of the fighter aircraft can be broken down into three parts: climb, cruise and combat. The aircraft's maximum climb performance is determined by the engine's maximum available thrust; optimum cruise performance is determined by its aerodynamic and propulsive efficiency; and combat performance is determined by maximum turning capabilities -- dictated by structural and angle of attack limits.

In an effort to improve a fighter aircraft's performance without changing the basic design, the Air Force is currently investigating the use of vectored engine thrust by developing the F-15 short takeoff and landing (STOL) demonstrator. By installing advanced aerodynamic and propulsion control concepts on an "off-the-shelf" F-15, the Air Force expects the F-15 STOL/maneuver technology aircraft to "yield combat performance and runway flexibility improvements of a magnitude normally associated with the development of an entirely new aircraft" (1). The primary modifications to the F-15B two-seat flight test aircraft will be "the addition of controllable canards above the engine inlets forward of the main wing of the aircraft" and "two-dimensional nozzles at the rear

1

of the F-15's Pratt and Whitney F100 engines." The F-15 STOL

demonstrator is expected to begin flying in 1988, testing these

"potential applications to the next generation of Air Force combat

aircraft." The Advanced Tactical Fighter, nicknamed as a

"superfighter," might employ vectored engine thrust -- "an especially

welcome feature in a superfighter because of its small wings" (2).

Several studies present optimal controls and trajectories to

minimize an aircraft's turning time, one aspect of an aircraft's overall

performance capability. Humphreys, Hennig, Bolding and Helgeson (3)

investigated three-dimensional aircraft dynamics. Johnson (4) included

the possibility of in-flight thrust reversal. Finnerty (5) constrained

the maneuver to the vertical plane. Brinson (6) considered the effects

of sideforce and Schneider (7) considered the effects of vectored thrust

in reducing the time to turn. Johnson, Brinson and Schneider all found

substantial benefits in utilizing additional controls to reduce an

aircraft's turning time in three-dimensional flight. This study, in

contrast, investigates a highly-maneuverable tactical aircraft's overall

performance capability enhanced by thrust-vectoring nozzles and

restricts turning flight to the horizontal plane.

Problem Statement

This investigation seeks the thrust vector angle schedules which

will optimize various air combat energy maneuverability parameters --

including specific excess power, maximum sustained and instantaneous

turn rate, and the power setting required to sustain a given load factor

and energy level.

2

The controls to be optimized are nozzle deflection angle and thrust sideslip angle (where applicable). These controls are to be considered unconstrained initially and subsequently constrained to practical physical limits as dictated by the F-15 STOL demonstrator design.

To evaluate the effects of thrust vectoring on fighter aircraft performance, the optimal thrust vector angle schedules and associated performance results will be obtained and compared against the results of a non-thrust-vectoring configuration.

Assumptions

Several assumptions regarding the aircraft, its dynamics and the controls are incorporated into this study. These assumptions are not only necessary to reduce the complexity of the problem to manageable proportions, but are common in this type of study as a source of meaningful comparison of results. The assumptions are:

1. the aircraft is a point mass

2. flat, non-rotating earth

3. NASA 1962 Standard Atmosphere (8)

4. constant gravitational acceleration

5. coordinated turn (no sideforce)

6. instantaneous controls

Summary of Current Knowledge

Aircraft performance analyses done within the Air Force and industry have traditionally been done using graphical and analytical methods with underlying assumptions that the angle of attack and thrust vector angle are small and consequently neglected. In the case of highly-

3

maneuverable aircraft utilizing large angles of attack and high thrust-to-weight ratios (such as the F-15 and F-16), the negligible angle of attack assumption becomes less accurate but will yield acceptable conservative results. In the case of the F-15 STOL demonstrator where thrust-vectoring nozzles will be used, the thrust vector angle becomes a primary control variable and will directly influence the canard deflection.

Current aircraft performance computer programs in use throughout the Air Force are typically generic -- meaning that they are applicable to nearly every type of Air Force aircraft, such as cargo, transport, trainer, attack and fighter aircraft. To keep the programs from becoming too complex, the small angle of attack and thrust vector angle assumptions were built into the logic since there was no real need for these capabilities at the time. With the advent of the F-15 STOL demonstrator program and its eventual Advanced Tactical Fighter applications, the inclusion of angle of attack and thrust vector angle as additional control variables in optimal performance analyses has become a necessity for aircraft performance engineers.

There is only one aircraft currently in production and service in the United States that utilizes thrust-vectoring nozzles -- the AV-8 Harrier, flown by the United States Marine Corps. The Harrier is capable of vectoring its four exhaust nozzles through angles of approximately 100 degrees, giving it vertical and short takeoff and landing capability (V/STOL). Low speed pitch, roll and yaw attitudes are controlled by six small reaction control jets placed in appropriate locations on the aircraft and are integrated into the flight control

system. The Harrier uses its thrust-vectoring capabilities mainly to provide direct lift since the exhaust nozzles are symmetrically located about the aircraft's center of gravity. The F-15 STOL demonstrator, on the other hand, uses its thrust-vectoring capabilities to provide both direct lift and pitch control through its integrated control system that governs the nozzle deflection angle/canard deflection interaction.

Approach

Definitions of all aspects of the aircraft performance problem including models and constraints are discussed in Section II. The derivations of the equations of motion of an aircraft in straight and level flight, climbing flight and turning flight are presented in Section III. These equations of motion include the angle of attack and thrust vector angle contributions which are traditionally neglected. A direct comparison of the traditional equations of motion is also covered in this section. The changes necessary to transform the traditional equations of motion in an existing aircraft performance computer program to those that include angle of attack and thrust vector angle are discussed in Section IV. The methods used in optimizing the aircraft's performance with vectored thrust are presented in Section V. The results of this study are then discussed and the use of thrust vectoring is compared to the non-thrust-vectoring baseline in Section VI. Finally, conclusions and recommendations are given in Section VII.

II. The Aircraft Performance Problem

Before results can be analyzed and compared, it is necessary to completely define all aspects of the problem. The problem will be defined in terms of the different phases of flight to be investigated, the characteristics which model the aircraft, atmospheric properties, and practical physical constraints on the control variables.

Phases of Flight

The different phases of flight are determined by setting certain state variables and/or their derivatives equal to zero and letting the other state variables vary within the optimization. The phases of flight included in this study are:

1. straight and level flight

    a. acceleration

    b. cruise

2. climbing flight

3. turning flight

    a. sustained turn

    b. instantaneous turn

The takeoff and landing phases are not included since they require an optimal trajectory analysis beyond the scope of this study. This study concentrates on the aircraft's mission performance applications, which treat the takeoff and landing portions of a mission profile as segments of flight that use fuel with no time or range considerations. With the

phases of flight included in this study and appropriate approximations
for takeoff and landing, a typical fighter aircraft mission profile can
be analytically performed.

Equations of Motion

The equations of motion for flight of a point mass aircraft over a
flat, non-rotating earth are derived by Miele (9:42-49) as

$$\dot{X} = V \cos\gamma \cos\chi \tag{1}$$

$$\dot{Y} = V \cos\gamma \sin\chi \tag{2}$$

$$\dot{h} = V \sin\gamma \tag{3}$$

$$m\dot{V} = T \cos\epsilon \cos\nu - D - mg \sin\gamma \tag{4}$$

$$\dot{\chi} \cos\mu \cos\gamma - \dot{\gamma} \sin\mu = \frac{1}{mV} \{T \cos\epsilon \sin\nu - Q + mg \sin\mu \cos\gamma\} \tag{5}$$

$$\dot{\chi} \sin\mu \cos\gamma + \dot{\gamma} \cos\mu = \frac{1}{mV} \{T \sin\epsilon + L - mg \cos\mu \cos\gamma\} \tag{6}$$

The definitions of all the variables used in this study are contained in
the List of Symbols preceding the Abstract and are shown pictorially in
Figure 1. Since this study does not allow for sideforce, $Q = 0$.
Rearranging, the equations of motion become

$$\dot{X} = V \cos\gamma \cos\chi \tag{7}$$

7

$$\dot{Y} = V \cos \gamma \sin \chi \tag{8}$$

$$\dot{h} = V \sin \gamma \tag{9}$$

$$\dot{V} = g \left\{ \frac{T}{W} \cos \epsilon \cos \nu - \frac{D}{W} - \sin \gamma \right\} \tag{10}$$

$$\dot{\chi} = \frac{g}{V \cos \gamma} \left\{ \frac{T}{W}(\cos \epsilon \sin \nu \cos \mu + \sin \epsilon \sin \mu) + \frac{L}{W} \sin \mu \right\} \tag{11}$$

$$\dot{\gamma} = \frac{g}{V} \left\{ \frac{T}{W} (\sin \epsilon \cos \mu - \cos \epsilon \sin \nu \sin \mu) + \frac{L}{W} \cos \mu - \cos \gamma \right\} \tag{12}$$

These equations are written in the wind axes and describe the aircraft motion with respect to an earth-fixed coordinate frame. The state variables are X, Y, h, V, χ and γ. The variables μ, ϵ and ν are control variables. The aircraft weight (W) is considered constant for the point performance calculations, but will vary when used in quasi-steady integrations.

The lift, drag and thrust forces will be discussed in the next paragraphs and will give rise to three more control variables.

8
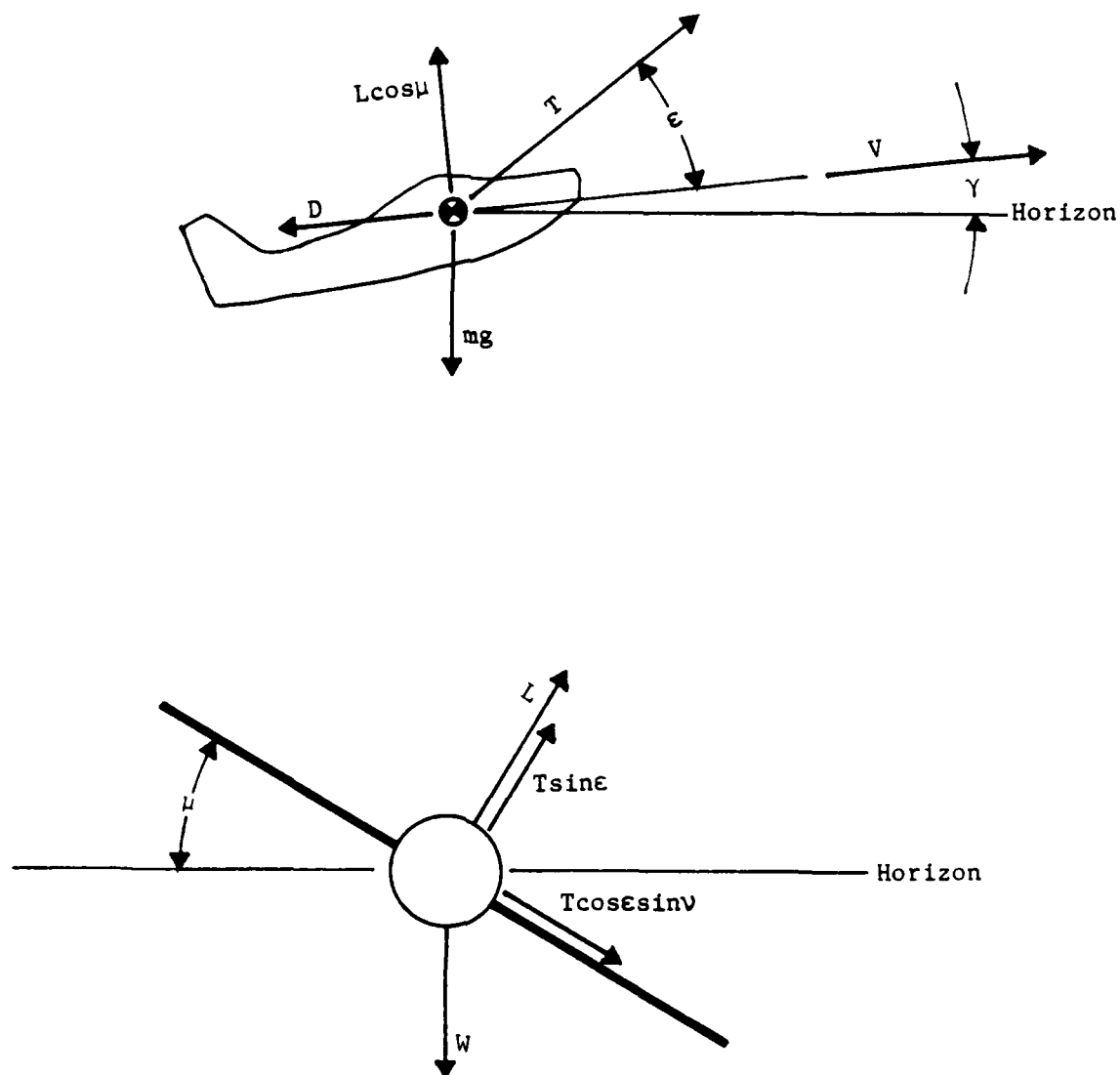
Figure 1 -- Aircraft Performance Problem

9

Aircraft Characteristics

The common coefficient forms of the aerodynamic lift and drag forces are

$$L = \tfrac{1}{2}\rho V^2 S C_L \tag{13}$$

$$D = \tfrac{1}{2}\rho V^2 S C_D \tag{14}$$

From incompressible aerodynamic and thin airfoil theories, the lift and drag coefficients can be expressed as

$$C_L = C_{L_{WB}} + C_{L_c} = C_{L_{0_{WB}}} + C_{L_{\alpha_{WB}}} \alpha + C_{L_{0_c}} + C_{L_{\delta_c}} \delta_c \tag{15}$$

$$C_D = C_{D_{WB}} + C_{D_c} = C_{D_{0_{WB}}} + K_{WB} C_{L_{WB}}^2 + C_{D_{0_c}} + K_c C_{L_c}^2 \tag{16}$$

which shows that the lift coefficient is a linear function of angle of attack (α) and canard deflection angle (δ_c) and that the drag coefficient varies parabolically with lift coefficient. These simple yet descriptive relationships give rise to the terms "linear lift curve slope" and "parabolic drag polar" and identify the control variables associated with the aircraft's aerodynamics. The aerodynamic lift and drag data used to model the aircraft in this study, however, have been derived from flight test and analytical methods and exhibit the same trends as the linear lift curve slope and parabolic drag polar. These

10

data, contained in Appendix A, realistically model the aircraft's aerodynamics with angle of attack and canard deflection angle as control variables.

The engine data is also derived from flight test and analytical methods and does not resemble the ideal jet theory where engine thrust is considered only as a function of altitude. The thrust and fuel flow characteristics can be written ideally as

$$T = T_{max} \pi \qquad (17) \qquad\qquad sfc = \frac{1}{T}(t_{ff} T + t_0) \qquad (18)$$

where T_{max} is a function of velocity and altitude and the thrust power setting (π) is the control variable associated with the aircraft's propulsion system. These data are also contained in Appendix A.

The formulation of the lift, drag and thrust relationships has introduced several aircraft parameters and three control variables: α, δ_c and π. Approximate values for the aircraft parameters in the case of the F-15 STOL demonstrator at a Mach number of 0.8 and an altitude of 30,000 feet are:

$$C_{L_{0_{WB}}} = 0.1 \qquad\qquad C_{L_{0_c}} = 0$$

$$C_{D_{0_{WB}}} = 0.0200 \qquad\qquad C_{D_{0_c}} = 0.0013$$

$$C_{L_\alpha} = 0.05 \text{ (1/degree)} \qquad\qquad C_{L_{\delta_c}} = 0.0145 \text{ (1/degree)}$$

$$K_{WB} = 0.25 \qquad\qquad K_c = 0.105$$

11

$$S = 608 \text{ ft}^2 \qquad\qquad W = 35{,}000 \text{ lb}$$

$$T_{max} = 10{,}900 \text{ lb}_T \qquad\qquad \text{(Military Power)}$$

$$T_{max} = 22{,}968 \text{ lb}_T \qquad\qquad \text{(Maximum Afterburner)}$$

$$t_{ff} = 0.833 \text{ lb}_f/(\text{lb}_T \text{ hr}) \qquad \text{(Military Power and below)}$$

$$t_{ff} = 2.142 \text{ lb}_f/(\text{lb}_T \text{ hr}) \qquad \text{(Maximum Afterburner)}$$

$$t_0 = 1000 \text{ lb}_f/\text{hr}$$

These values were used initially with the linear lift curve slope, parabolic drag polar and engine thrust equations to test the techniques developed for optimizing aircraft performance with thrust vector angle, while the results presented in this study are based on the data in Appendix A.

Atmospheric Model

The NASA 1962 Standard Atmosphere (8) was used for this study and is limited to the first two layers of the lower atmosphere. This atmosphere is modelled from sea level to the tropopause (36,089 feet) as a linearly decreasing temperature layer, and above the tropopause as an isothermal layer -- the troposphere and stratosphere, respectively. The aircraft performance program used in this study is programmed with the complete set of equations to model the NASA 1962 Standard Atmosphere.

12

Control Variable Constraints

Three control variables -- the throttle setting (π), angle of attack (α) and canard deflection (δ_c) -- are constrained by physical considerations. The thrust can neither be greater than the maximum thrust nor less than the minimum thrust of the particular power setting being used. The F-15 is capable of throttling both the military and afterburner power settings. The minimum thrust for the military power setting is taken to be zero, while the minimum thrust for the afterburner power setting is taken to be 100% military power. The scope of this study, however, will only be concerned with throttling military and not the afterburner power setting for cruise and turning performance calculations. Since the throttle setting is defined in equation (17) in terms of the maximum thrust, the throttle setting is limited to

$$0 \leq \pi \leq 1 \quad \text{for military power}$$
$$\pi = 1 \quad \text{for afterburner power}$$

Each lifting surface is limited by its own aerodynamic lift limit and the total lift generated is limited by the aircraft's maximum load factor. Individually, the angle of attack and canard deflection can not exceed their stall points; collectively, the angle of attack and canard deflection can not generate more lift than is tolerated by the aircraft's maximum load factor. Since the canard is used to trim out the pitching moment caused by the deflection of the thrust vector, the canard surface is assumed to be designed such that its stall point is never reached in normal thrust vectoring applications to maintain pitch

13

control authority. In this case, the aircraft is constrained by an angle of attack limit (defined by a $C_{L_{max}}$ of 1.6) and a thrust vector angle limit and not constrained by a canard deflection limit.

In turning performance, the velocity where the aircraft is at its maximum angle of attack and maximum load factor is the corner velocity. The corner velocity is the velocity at which the aircraft achieves its maximum turn rate. At speeds below the corner velocity, the aircraft is limited by its maximum angle of attack. At speeds above the corner velocity, the aircraft is limited by its maximum load factor (9 g's).

No constraints were placed on the thrust angle of attack (ε) and thrust sideslip angle (ν). While the F-15 STOL demonstrator will have limits on its nozzle deflection angle (δ_N)

$$-20^{o} \leq \delta_N \leq +20^{o}$$

this angle was allowed full range in order to determine how much range of thrust vectoring would be exploited if it were available. The effects of constraining the two thrust vector angles were later examined and are discussed in Section VII.

The aircraft's velocity is constrained by the lesser of the following: a dynamic pressure limit determined by the aircraft's structural and flutter characteristics ($q = 2131$ lb/ft^2); or the aircraft's Mach number limit determined by temperature or engine limits ($M = 2.5$). No constraint was placed on the bank angle (μ).

14

III. Aircraft Performance Equations of Motion

Miele's equations of motion for flight of a point mass aircraft over a flat, non-rotating earth as discussed in Section II use the thrust sideslip angle (ν) and thrust angle of attack (ε) as the angles of successive rotation to which the wind axes must be subjected in order to turn the velocity vector in a direction parallel to the thrust vector. When a pair of body-fixed reference lines are introduced into the derivation of the equations of motion (as depicted in Figure 2), the thrust angle of attack control variable is found to be dependent upon the aircraft's angle of attack (α) -- a control variable derived from the aircraft's aerodynamic characteristics.
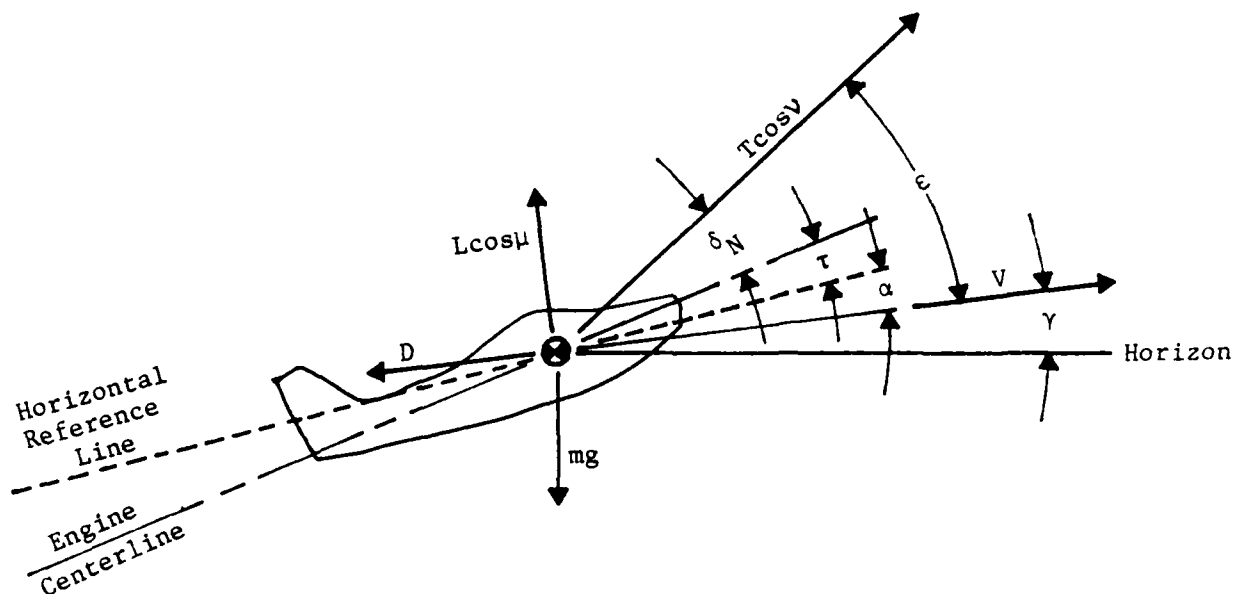
Figure 2 -- Definition of Thrust Vector Angle

15

The nozzle deflection angle (δ_N) replaces the thrust angle of attack as the second angle of rotation in the definition of the thrust vector orientation, with the body-fixed engine centerline replacing the velocity vector as the reference orientation. Since this study allows for no sideslip, the thrust sideslip angle definition is unchanged. The nozzle deflection angle and thrust angle of attack are related by the equality

$$\varepsilon = \delta_N + \tau + \alpha \ .$$

(19)

The equations of motion now become

$$\dot{X} = V \cos \gamma \cos \chi$$

(20)

$$\dot{Y} = V \cos \gamma \sin \chi$$

(21)

$$\dot{h} = V \sin \gamma$$

(22)

$$\dot{V} = g \ \{\frac{T}{W} \cos(\delta_N + \tau + \alpha) \cos \nu - \frac{D}{W} - \sin \gamma\}$$

(23)

$$\dot{\chi} = \frac{g}{V \cos \gamma} \ \{\frac{T}{W}[\cos(\delta_N + \tau + \alpha) \sin \nu \cos \mu + \sin(\delta_N + \tau + \alpha) \sin \mu] + \frac{L}{W} \sin \mu\}$$

(24)

$$\dot{\gamma} = \frac{g}{V}\{\frac{T}{W}[\sin(\delta_N + \tau + \alpha) \cos \mu - \cos(\delta_N + \tau + \alpha) \sin \nu \sin \mu] + \frac{L}{W} \cos \mu - \cos \gamma\}$$

(25)

16

The first three equations are kinematic relationships and the second three equations are dynamic relationships.

Trimmed Flight

Since the aircraft is considered to be a point mass with all forces acting at the center of gravity, there must be no net moments acting on the aircraft. In the case of the F-15 STOL demonstrator, however, a deflection of the nozzle will cause a moment since the nozzle's point of action is not at the center of gravity. The addition of the canard in the F-15 STOL demonstrator design allows for balancing the moment induced by the nozzle deflection by deflecting the canard appropriately. This interaction results in an additional constraint equation relating the canard deflection and the nozzle deflection. Since the F-15 STOL demonstrator design does not have a sideforce generator to balance a moment caused by deflecting the nozzle out of the aircraft's plane of symmetry, the thrust sideslip angle (ν) must be set to zero for trimmed flight.

The additional constraint equation relates the canard's aerodynamic characteristics to the thrust (T), nozzle deflection angle, the aircraft angle of attack and the aircraft's dimensional characteristics (1_{c_x}, 1_{c_z}, 1_{N_x}, 1_{N_z}) by balancing the moments induced by the nozzle and canard deflections:

$$1_{c_x} [L_c \cos\alpha + D_c \sin\alpha] + 1_{c_z} [L_c \sin\alpha - D_c \cos\alpha]$$

$$+ 1_{N_x} [T \sin(\delta_N + \tau)] \quad + 1_{N_z} [T \cos(\delta_N + \tau)] = 0 \qquad (26)$$

The lift and drag of the canard (L_c and D_c) are functions of the canard deflection control variable in the same manner as the lift and drag of the aircraft are functions of the angle of attack control variable.

Figure 3 -- Trimmed Flight

Functional Relationships

The final set of equations governing the motion of the point mass aircraft is composed of three kinematic relationships, three dynamic relationships and one trim constraint equation. The trim constraint equation transforms the aerodynamic characteristics of the aircraft from a function of four variables to a function of six variables:

$$L = L(h, V, \alpha, \delta_c) \quad \text{trim} \quad L = L(h, V, \alpha, \delta_c, \delta_N, \pi)$$

$$D = D(h, V, \alpha, \delta_c) \quad \text{constraint} \quad D = D(h, V, \alpha, \delta_c, \delta_N, \pi)$$

The kinematic and dynamic equations have the following functional relationships:

18

$$\dot{X} = X(V, \gamma, \chi)$$

$$\dot{Y} = Y(V, \gamma, \chi)$$

$$\dot{h} = h(V, \gamma)$$

$$\dot{V} = V(h, V, \gamma, \alpha, \delta_c, \delta_N, \pi)$$

$$\dot{\chi} = \chi(h, V, \gamma, \alpha, \delta_c, \delta_N, \pi, \mu)$$

$$\dot{\gamma} = \gamma(h, V, \gamma, \alpha, \delta_c, \delta_N, \pi, \mu)$$

The aircraft performance computer program used in this study utilizes point performance optimization, treating the kinematic equations as integrals of motion and the dynamic equations as the differential system. To accomplish this, the aircraft's downrange (X) and crossrange (Y) locations along with its altitude (h) and velocity (V) must be known prior to optimization. Since the program already has routines to optimize the various aircraft performance parameters with altitude and velocity, the optimization of the aircraft's performance with thrust vectoring can be considered as a point sub-optimization problem, or an optimization within an optimization.

Of the twelve state and control variables, seven remain unspecified and are considered dependent variables. Since there are four equations in the differential system (including the trim constraint equation), there are three degrees of freedom in which to optimize the aircraft's performance (9: 48-51). By restricting flight to the vertical and horizontal planes and defining a phase of flight by constraining certain variables within that plane, the number of degrees of freedom in which to optimize the aircraft's performance can be reduced significantly.

19

Flight in the Vertical Plane

This category of trajectories is represented by a vertical plane of symmetry which implies

$$Y = \text{constant} \tag{27}$$

$$\mu = 0 \tag{28}$$

Equation (27) implies that $\dot{Y} = 0$, and equation (21) implies that $\chi = \dot{\chi} = 0$. The equations of motion become

$$\dot{X} = V \cos \gamma \tag{29}$$

$$\dot{h} = V \sin \gamma \tag{30}$$

$$\dot{V} = \frac{g}{W} [T \cos(\delta_N + \tau + \alpha) - D - W \sin\gamma] \tag{31}$$

$$\dot{\gamma} = \frac{g}{WV} [T \sin(\delta_N + \tau + \alpha) + L - W \cos\gamma] \tag{32}$$

$$\dot{\chi} = 0 \tag{33}$$

$$0 = 1_{c_x} [L_c \cos\alpha + D_c \sin\alpha] + 1_{c_z} [L_c \sin\alpha - D_c \cos\alpha] $$
$$+ 1_{N_x} [T \sin(\delta_N + \tau)] \quad + 1_{N_z} [T \cos(\delta_N + \tau)] \tag{34}$$

Rewriting, the remaining equations of motion are

$$\dot{X} = V \cos \gamma \qquad (35)$$

$$\dot{h} = V \sin \gamma \qquad (36)$$

$$\dot{V} = \frac{g}{W} [T \cos(\delta_N + \tau + \alpha) - D - W \sin\gamma] \qquad (37)$$

$$\dot{\gamma} = \frac{g}{WV} [T \sin(\delta_N + \tau + \alpha) + L - W \cos\gamma] \qquad (38)$$

$$0 = 1_{c_x} [L_c \cos\alpha + D_c \sin\alpha] + 1_{c_z} [L_c \sin\alpha - D_c \cos\alpha]$$
$$+ 1_{N_x} [T \sin(\delta_N + \tau)] \quad + 1_{N_z} [T \cos(\delta_N + \tau)] \qquad (39)$$

This reduced system of equations for flight in the vertical plane has
two kinematic relationships and three dynamic equations. Of the
seven dependent variables previously unspecified for point performance
optimization, five variables -- π, δ_N, α, δ_c and γ -- remain
unspecified, yielding two degrees of freedom.

One common application of flight in the vertical plane is that of
straight and level flight, where the flight path angle (γ) and its
derivative ($\dot{\gamma}$) are set to zero. This implies that the aircraft will
maintain a constant altitude during this flight phase. The equations of
motion reduce to

$$\dot{X} = V \qquad (40)$$

$$\dot{V} = \frac{g}{W} [T \cos(\delta_N + \tau + \alpha) - D] \qquad (41)$$

$$0 = T \sin(\delta_N + \tau + \alpha) + L - W \qquad (42)$$

$$\begin{aligned}
0 = &1_{c_x}[L_c \cos\alpha + D_c \sin\alpha] + 1_{c_z}[L_c \sin\alpha - D_c \cos\alpha] \\
&+ 1_{N_x}[T \sin(\delta_N + \tau)] + 1_{N_z}[T \cos(\delta_N + \tau)] \qquad (43)
\end{aligned}$$

with dependent variables π, δ_N, α and δ_c. Two cases of straight and level flight are of primary interest to the aircraft performance engineer -- acceleration and cruise. Although the equations of motion are the same, the techniques involved in finding the aircraft's optimal acceleration and cruise controls are entirely different.

In the case of maximizing an aircraft's acceleration, the throttle setting control variable is set at some constant value (normally at the maximum -- $\pi = 1$ for maximum acceleration). This reduces the number of dependent variables to three (δ_N, α and δ_c), but since the performance parameter to be optimized ($\dot{V}$) is solved for explicitly in the first dynamic equation (41), the number of equations in the differential system is also reduced by one. The resultant differential system has three dependent variables and two equations, leaving just one degree of freedom in optimizing the aircraft's acceleration capability. Since this study is interested in finding the effects of thrust vectoring on the performance of an aircraft, the one control variable chosen to be the degree of freedom is the nozzle deflection angle (δ_N).

In the constant altitude cruise case, the throttle setting (π) is the parameter that is to be minimized. Since the cruise condition is a

22

non-accelerating flight phase, the aircraft's acceleration ($\dot{V}$) must be set to zero. The throttle setting appears explicitly in all three dynamic equations but also appears implicitly in the first two as a functional dependency. Thus the differential system has four dependent variables and three equations, leaving just one degree of freedom. Again the nozzle deflection angle is the control variable that is chosen to be the single degree of freedom.

The traditional equations of motion for level flight in the vertical plane neglect the angle of attack and thrust vector angle contributions:

$$\dot{X} = V \tag{44}$$

$$\dot{V} = \frac{g}{W} [T - D] \tag{45}$$

$$L = W \tag{46}$$

Since the aircraft weight is known, the lift, drag and subsequently the aircraft's acceleration or cruise throttle setting are easily calculated -- results from a system of equations with no degrees of freedom.

Another common application of flight in the vertical plane is that of climbing flight, where the parameter to be optimized is the time rate of change of the altitude or climb rate ($\dot{h}$). The climb rate is solved for explicitly in the second kinematic equation but can be inserted into the first dynamic equation by a direct substitution. The equations of motion reduce to

23

$$\dot{X} = V \cos \gamma \tag{47}$$

$$\dot{h} = \frac{V}{W} [T \cos(\delta_N + \tau + \alpha) - D - \frac{W}{g} \dot{V}] \tag{48}$$

$$\dot{\gamma} = \frac{g}{WV} [T \sin(\delta_N + \tau + \alpha) + L - W \cos\gamma] \tag{49}$$

$$0 = 1_{c_x} [L_c \cos\alpha + D_c \sin\alpha] + 1_{c_z} [L_c \sin\alpha - D_c \cos\alpha]$$
$$+ 1_{N_x} [T \sin(\delta_N + \tau)] + 1_{N_z} [T \cos(\delta_N + \tau)] \tag{50}$$

An alternate way of expressing the climb rate is

$$\dot{h} = \frac{[T \cos(\delta_N + \tau + \alpha) - D]}{1 + \frac{V}{g} \frac{dV}{dh}} \frac{V}{W} \tag{51}$$

where $\frac{V}{g} \frac{dV}{dh}$ is the acceleration correction term. For climbing flight at a constant true airspeed, the acceleration terms are zero:

$$\frac{V}{W}[\frac{W}{g} \dot{V}] = \frac{V}{g} \dot{V} = \frac{V}{g} \frac{dV}{dh} \dot{h} = 0 \tag{52}$$

or $\quad \frac{W}{g} \dot{V} = 0 \quad$ and $\frac{V}{g} \frac{dV}{dh} = 0$ (53)

The equations of motion for non-accelerating climbing flight become

$$\dot{X} = V \cos \gamma \tag{54}$$

24

$$\dot{h} = \frac{V}{W} [T \cos(\delta_N + \tau + \alpha) - D] \qquad (55)$$

$$\dot{\gamma} = \frac{g}{WV} [T \sin(\delta_N + \tau + \alpha) + L - W \cos\gamma] \qquad (56)$$

$$0 = 1_{c_x} [L_c \cos\alpha + D_c \sin\alpha] + 1_{c_z} [L_c \sin\alpha - D_c \cos\alpha]$$

$$+ 1_{N_x} [T \sin(\delta_N + \tau)] \qquad + 1_{N_z} [T \cos(\delta_N + \tau)] \qquad (57)$$

The climb rate equation (55) is identical to the equation for the aircraft's level acceleration (41) when multiplied by a constant factor. Since the non-accelerating climb rate and level acceleration are the parameters to be optimized in their respective cases, their optimizations should result in the same values for the control variables.

This relationship between the constant altitude acceleration and the non-accelerating climb is the basis for the specific energy concept described by Rutowski (10). In his approach to the performance problem using energy concepts, the author computes the time rate of change of the aircraft's energy in terms of its climb rate and acceleration:

$$\frac{d}{dt}(\frac{E}{W}) = P_s = \dot{h} + \frac{V}{g} \dot{V} = \frac{V}{W} [T \cos(\delta_N + \tau + \alpha) - D] \qquad (58)$$

For the constant altitude case, $P_s = \frac{V}{g} \dot{V}$. For the non-accelerating case, $P_s = \dot{h}$. Optimizing the specific excess power (P_s) optimizes the accelerating climb rate or the varying altitude acceleration providing

25

"the desired simplification with no loss in accuracy."

Since the optimization of the specific excess power can be done by the techniques developed for the level acceleration, the dynamic equation for the time rate of change of the flight path angle (γ) is not used when optimizing climb rate. This parameter can be calculated, however, for the non-accelerating climb by making use of the relationship between the climb rate and the flight path angle:

$$\dot{h} = V \sin\gamma \qquad (59)$$

Once P_S and $\dot{h}$ are optimized by the techniques developed for the level acceleration, the flight path angle and its derivative can be calculated directly.

The traditional equations for non-accelerating flight in the vertical plane neglect the angle of attack and thrust vector angle contributions:

$$\dot{X} = V \cos\gamma \qquad (60)$$

$$\dot{h} = V \sin\gamma = \frac{V}{W} (T - D) \qquad (61)$$

$$\dot{\gamma} = \frac{g}{WV} (L - W \cos\gamma) \qquad (62)$$

Once the optimal climb rate is found, the flight path angle and its derivative are easily calculated.

26

Flight in the Horizontal Plane

This category of trajectories is represented by the mathematical condition

$$h = \text{constant} \tag{63}$$

Equation (63) implies that $\dot{h} = 0$, and equation (30) implies that $\gamma = \dot{\gamma} = 0$. The remaining equations of motion are

$$\dot{X} = V \cos \chi \tag{64}$$

$$\dot{Y} = V \sin \chi \tag{65}$$

$$\dot{V} = \frac{g}{W} [T \cos(\delta_N + \tau + \alpha) - D] \tag{66}$$

$$\dot{\chi} = \frac{g}{WV} [T \sin(\delta_N + \tau + \alpha) \sin\mu + L \sin\mu] \tag{67}$$

$$0 = T \sin(\delta_N + \tau + \alpha) \cos\mu + L \cos\mu - W \tag{68}$$

$$
0 = 1_{c_x} [L_c \cos\alpha + D_c \sin\alpha] + 1_{c_z} [L_c \sin\alpha - D_c \cos\alpha]
$$
$$
+ 1_{N_x} [T \sin(\delta_N + \tau)] \quad + 1_{N_z} [T \cos(\delta_N + \tau)] \tag{69}
$$

This reduced system of equations for flight in the horizontal plane has two kinematic relationships and four dynamic equations. Of the seven dependent variables previously unspecified for point performance

optimization, six variables -- π, δ_N, α, δ_c, μ and χ -- remain unspecified. The heading angle (χ) is only used in the kinematic relationships and is not included in the dynamic equations, so the differential system has only five dependent variables, yielding one degree of freedom.

A common application of flight in the horizontal plane is that of the instantaneous turn, where the aircraft is accelerating or decelerating ($\dot{V} \neq 0$). This implies that the aircraft will maintain a prescribed turn rate at the specified throttle setting but will not turn at a constant altitude, constant velocity combination (energy state) during this flight phase. Since this study restricts the aircraft to turn only in the horizontal plane, the altitude must remain constant and any change from the initial energy state will be reflected in a change in velocity. By maximizing the aircraft's acceleration (or minimizing its deceleration), the aircraft's energy gain (or loss) is optimized. The performance parameter to be optimized ($\dot{V}$) is solved for explicitly in the first dynamic equation (66), so the number of equations in the differential system is reduced by one. Since the throttle setting is specified, this leaves one degree of freedom: the nozzle deflection angle (δ_N).

Another application of flight in the horizontal plane is that of the sustained turn, where the aircraft is not accelerating or decelerating ($\dot{V} = 0$). This implies that the aircraft will maintain a constant altitude and velocity during the flight phase. The equations of motion reduce to

$$\dot{X} = V \cos X \tag{70}$$

$$\dot{Y} = V \sin X \tag{71}$$

$$0 = T \cos(\delta_N + \tau + \alpha) - D \tag{72}$$

$$\dot{\chi} = \frac{g}{WV} [T \sin(\delta_N + \tau + \alpha) \sin\mu + L \sin\mu] \tag{73}$$

$$0 = T \sin(\delta_N + \tau + \alpha) \cos\mu + L \cos\mu - W \tag{74}$$

$$0 = 1_{c_x}[L_c \cos\alpha + D_c \sin\alpha] + 1_{c_z}[L_c \sin\alpha - D_c \cos\alpha]$$
$$+ 1_{N_x}[T \sin(\delta_N + \tau)] + 1_{N_z}[T \cos(\delta_N + \tau)] \tag{75}$$

with dependent variables $\pi, \delta_N, \alpha, \delta_c$ and μ. There are two cases of the sustained turn flight phase that are of primary interest to the aircraft performance engineer -- the maximum sustained turn rate and the minimum throttle setting required to maintain a specified sustained turn rate. Although the equations of motion are the same, the techniques involved in finding the maximum sustained turn rate and the minimum throttle setting are entirely different.

In the case of maximizing the aircraft's sustained turn rate, the throttle setting control variable is set at some constant value (normally at the maximum -- $\pi = 1$). This reduces the number of dependent variables to four ($\delta_N, \alpha, \delta_c$ and μ), but since the performance parameter to be optimized ($\dot{\chi}$) is solved for explicitly in the second

29

dynamic equation (73), the number of equations in the differential system is also reduced by one. The resultant differential system has one degree of freedom and again will be chosen to be the nozzle deflection angle.

In the case of finding the minimum throttle setting required to maintain a specified sustained turn rate, the throttle setting appears explicitly in all four dynamic equations but also appears implicitly in the first three as a functional dependency. Thus the differential system has five dependent variables and four equations, and will use the same control variable as the degree of freedom as the other turn cases.

The traditional equations for turning flight in the horizontal plane neglect the angle of attack and thrust vector angle contributions:

$$n = \frac{L}{W} \tag{76}$$

$$\dot{X} = V \cos X \tag{77}$$

$$\dot{Y} = V \sin X \tag{78}$$

$$\dot{V} = \frac{g}{W} [T - D] \tag{79}$$

$$\dot{X} = \frac{g}{WV} L \sin\mu = \frac{g}{V} [n^2 - 1]^{\frac{1}{2}} \tag{80}$$

For a sustained turn the thrust is equal to the drag, which determines the load factor through the drag polar and in turn determines the turn rate. For an instantaneous turn the specified turn rate determines the

load factor, which in turn determines the drag and the aircraft's acceleration.

Summary

Restricting flight to the vertical and horizontal planes greatly reduces the magnitude and complexity of the aircraft performance problem. Applications of this study reduces the flight in the vertical and horizontal planes to optimization problems with one degree of freedom.

IV. Aircraft Performance Computer Program

NSEG (11), a segmented aircraft performance analysis program widely
in use throughout the Air Force, uses the traditional equations of
motion to calculate an aircraft's performance capability. Implementing
the full equations of motion discussed in Section III would require a
major overhaul of the existing equations which would necessitate a
complete checkout for all applications. On the other hand, adjusting
the thrust and drag data to account for the changes in the equations of
motion would leave the existing equations intact while only changing the
data lookup routines. Currently, the aircraft's aerodynamic drag data
is input as a function of the required lift force, Mach number,
altitude, drag index and center of gravity. The engine's propulsion
characteristics (net thrust and fuel flow data) are input as a function
of power setting, Mach number and altitude.

The NSEG program utilizes a thrust-drag accounting system that
treats the airframe and throttle-dependent drags (ram, spillage and
nozzle drag) as separate and unrelated. This system, when coupled with
the small angle of attack and thrust vector angle assumptions, reduces
Miele's equations of motion (20-25) to the traditional equations of
motion (60-62 and 76-80), where the thrust (T) is actually the net
thrust (F_N) defined by

$$F_N = F_g - D_{ram} - D_{spillage} - D_{nozzle} \tag{81}$$

and is the resultant propulsive effort of the engine. The thrust and
drag appear in the traditional equations of motion only as the quantity

32

(T - D), which renders the thrust-drag accounting system arbitrary as long as it remains consistent.

This thrust-drag accounting system becomes very important, however, when the complete equations of motion are used. In this case, the thrust (T) is the engine's gross thrust (F_g), which is the actual force being exerted through the nozzle. The total drag (D) will then have to include the throttle-dependent drags as discussed above. As the gross thrust is vectored through a positive angle ($\delta_N + \tau + \alpha$), there is a loss in thrust corresponding to a gain in lift. To illustrate this point, part of Figure 1 is repeated here with additional definitions.
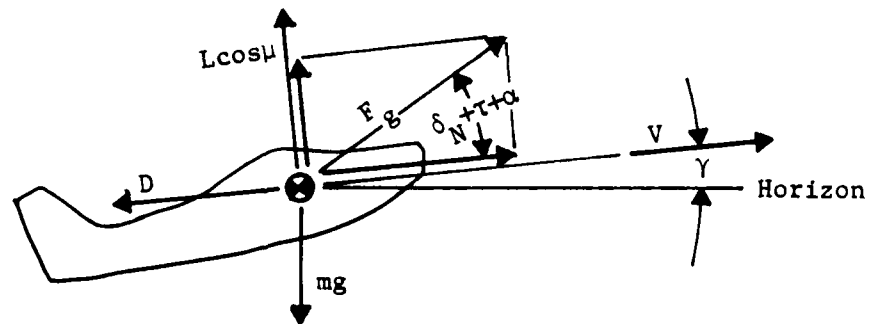
Figure 4 — Thrust's Contribution to Lift

When ($\delta_N + \tau + \alpha$) = 0, the engine's propulsive force is just F_g. When ($\delta_N + \tau + \alpha$) > 0, the propulsive force along the flight path is $F_g \cos(\delta_N + \tau + \alpha)$. The loss in thrust along the flight path is then the difference between these two forces:

$$F = F_g \left[1 - \cos(\delta_N + \tau + \alpha)\right] \qquad (82)$$

In flight, this loss in thrust may be expressed as an increase in drag. In drag coefficient form, this increase is given by

$$\Delta C_D = \frac{F_g \left[1 - \cos(\delta_N + \tau + \alpha)\right]}{\frac{1}{2}\, \rho\, V^2\, S} \qquad (83)$$

The corresponding increase in lift due to vectoring the thrust, as shown in Figure 4, is

$$\Delta L = F_g \sin(\delta_N + \tau + \alpha) \qquad (84)$$

In lift coefficient form, this increase is given by

$$\Delta C_L = \frac{F_g \sin(\delta_N + \tau + \alpha)}{\frac{1}{2}\, \rho\, V^2\, S} \qquad (85)$$

The total lift and drag can then be expressed as

$$C_L = C_{L_{aero}} + \Delta C_L \qquad (86)$$

$$C_D = C_{D_{aero}} + \Delta C_D \qquad (87)$$

where $C_{L_{aero}}$ is the lift generated by the aircraft's aerodynamics and $C_{D_{aero}}$ is its corresponding drag. For $\nu = 0$, NSEG's traditional equations of motion and thrust-drag accounting system defined by equation (81), along with these adjustments to the aerodynamic data will provide the same

34

results as if the complete set of equations of motion were reprogrammed into NSEG. The required data now includes the aircraft's aerodynamic data and the engine's net thrust and fuel flow characteristics as before, as well as the aircraft's lift curve slopes and the engine's gross thrust characteristics. The program uses the gross thrust data to adjust the aeodynamic data accordingly and uses the net thrust as before. For $\nu \neq 0$, the turn rate equation (24) and the time rate of change of the flight path equation (25) each have an additional term to be considered and programmed. Since ν has been determined to be zero for this aircraft in Section III, the $\nu = 0$ case has not been addressed.

Included in the programming changes to account for thrust vectoring is the trim constraint equation (26). The moment induced by vectoring the thrust is counteracted by inducing an equal and opposite moment with the canard. With the canard deflection, additional lift and drag are added and taken into account in $C_{L_{aero}}$ and $C_{D_{aero}}$ respectively. The thrust (T) in the trim equation is actually the gross thrust (F_g) being exerted through the nozzle that creates the moment about the center of gravity.

V. Optimization Techniques

As discussed in Section III, the aircraft performance problem can be broken down into several distinct phases of flight, each of which are one degree of freedom optimization problems. Since the functional form of the performance parameters to be optimized are not explicitly known, numerical techniques must be used to search for the optimal control values. Two techniques -- equal interval search and quadratic interpolation -- were coupled together to provide an efficient and effective optimization algorithm with an acceptable interval of uncertainty.

The equal interval search technique was used to find the interval in which the optimal solution is located. In this procedure, the control variable chosen to be the degree of freedom is set at some lower bound and is incremented until an upper bound is met or until an optimal interval has been detected. At each point, the performance parameter to be optimized is calculated and compared to its value at the previous point. The optimal interval is detected when the performance parameter calculated is not the optimal value when compared to its previous value. The optimal interval is then defined as the interval bounded by the points on either side of the optimal solution determined by the equal interval search.

The quadratic interpolation technique uses the three points that define the optimal interval along with their functional values to determine the coefficients of a quadratic equation that approximates the performance parameter function in this interval. By elementary calculus, the optimal control value can then be determined analytically

36

and the optimal performance parameter value can be calculated directly. Using a second order Lagrangian interpolation polynomial, the quadratic equation can be represented by

$$F(x) = ax^2 + bx + c = F_1(x) + F_2(x) + F_3(x) \tag{88}$$

where

$$F_1(x) = \frac{x-x_2}{x_1-x_2} \frac{x-x_3}{x_1-x_3} \quad f(x_1) \tag{89}$$

$$F_2(x) = \frac{x-x_1}{x_2-x_1} \frac{x-x_3}{x_2-x_3} \quad f(x_2) \tag{90}$$

$$F_3(x) = \frac{x-x_1}{x_3-x_1} \frac{x-x_2}{x_3-x_2} \quad f(x_3) \tag{91}$$

Equating coefficients, the quadratic equation's coefficients are found to be

$$a = \frac{(x_3-x_2) \ f(x_1) + (x_1-x_3) \ f(x_2) + (x_2-x_1) \ f(x_3)}{(x_3-x_1) \ (x_3-x_2) \ (x_2-x_1)} \tag{92}$$

$$b = \frac{(x_2+x_3)(x_2-x_3)f(x_1) + (x_1+x_3)(x_3-x_1)f(x_2) + (x_1+x_2)(x_1-x_2)f(x_3)}{(x_3-x_1)(x_3-x_2)(x_2-x_1)} \tag{93}$$

$$c = \frac{x_2 x_3 (x_3-x_2) \ f(x_1) + x_1 x_3 (x_1-x_3) \ f(x_2) + x_1 x_2 (x_2-x_1) \ f(x_3)}{(x_3-x_1)(x_3-x_2)(x_2-x_1)} \qquad (94)$$

The quadratic equation is then differentiated once and set to zero, and the optimal control value is easily determined:

$$F(x) = ax^2 + bx + c \qquad (95)$$

$$F'(x) = 2ax + b = 0 \qquad (96)$$

Equation (89) implies that

$$x_{opt} = -\frac{b}{2a} \qquad (97)$$

Even though this optimization algorithm is not the best algorithm that could be used to find a function's optimal value, it was used because the NSEG program already utilizes the quadratic interpolation technique in optimizing simple functions. In these existing applications, NSEG systematically picks three points in a given interval, calculates their functional values, and "curvefits" the function to find an approximate optimal solution. The equal interval search and quadratic interpolation techniques were coupled together in this new application so that a fairly accurate optimal solution would result.

VI. Results

Since the objective of this investigation is to determine to what extent a highly-maneuverable aircraft's overall performance capability is enhanced by thrust-vectoring nozzles, the results are shown against a baseline configuration with non-thrust-vectoring nozzles such that a direct comparison can be made. The results are shown for three cases:

Case 1: Results from using the traditional equations
        of motion with angle of attack and thrust
        vector angle neglected

Case 2: Results from using the complete equations of
        motion with no thrust vectoring

Case 3: Results from using the complete equations of
        motion at the optimum nozzle deflection angle.

With the thrust-vectoring nozzles being used in flight to enhance the aircraft's combat maneuverability, the results are shown for various points throughout the air battle arena. Parrott (12) defines the air battle arena as the part of the fighter aircraft's envelope in which most of its close-in combat maneuvering takes place. The air battle arena definition assumes a threat engagement at a high velocity, high altitude condition. As the dogfight develops, the aircraft dissipates its energy by maneuvering outside of its sustained envelope and eventually ends up at a low velocity, low altitude condition. In order to be effective in a dogfight, the aircraft must be able to maneuver without excess energy loss and must be able to disengage from the

39

opponent at any time. This requires high sustained load factors and high level flight acceleration capabilities throughout the air battle arena.

Figures 5 and 6 illustrate the F-15 STOL's air battle arena superimposed on the aircraft's sustained envelope for various load factors. Tables 1 through 9 show the results for the critical Mach-altitude points of the air battle arena for the cases previously discussed. Appendix B contains graphical data for the first case and Appendix C contains graphical data for the second and third cases. Appendix D contains graphical data for subsonic, high altitude, long range cruise conditions for mission range comparisons. The units for the different aircraft performance parameters are as follows:

Specific Excess Power (P_s) : ft/sec

Sustained Load Factor : g's

Sustained Turn Rate : ^{o}/sec

Thrust Required : lb

Specific Range : NM/lb_f

Figures 27 through 34 show that an aircraft's sustained load factor and turn rate are significantly improved through the use of thrust vectoring, especially at low altitudes and low velocities. The tables of results quantitatively show an increase in sustained load factor as much as 0.5 g at maximum A/B power and 0.25 g at military power, and an increase in sustained turn rate as much as 1.5^o/sec at maximum A/B and 0.5^o/sec at military power in the air battle arena. Figures 35 through

40

42 show that an aircraft's specific excess power is increased substantially through the use of thrust vectoring, especially at higher load factors. The aircraft's specific excess power is shown unchanged at level 1 g flight. Figures 43 through 46 show that lower thrust is required to sustain a specified load factor with thrust vectoring, especially at lower speeds that are not part of the air battle arena. Figures 50 through 52 show that the aircraft's high altitude, subsonic cruise performance is improved slightly with thrust vectoring.

F-15 STOL

SPECIFIC EXCESS POWER (FT/SEC)

CONFIGURATION:

MILITARY POWER
ANGLE OF ATTACK
AND THRUST VECTOR
ANGLE NEGLECTED

GLEVEL=9.00
WEIGHT=35000.
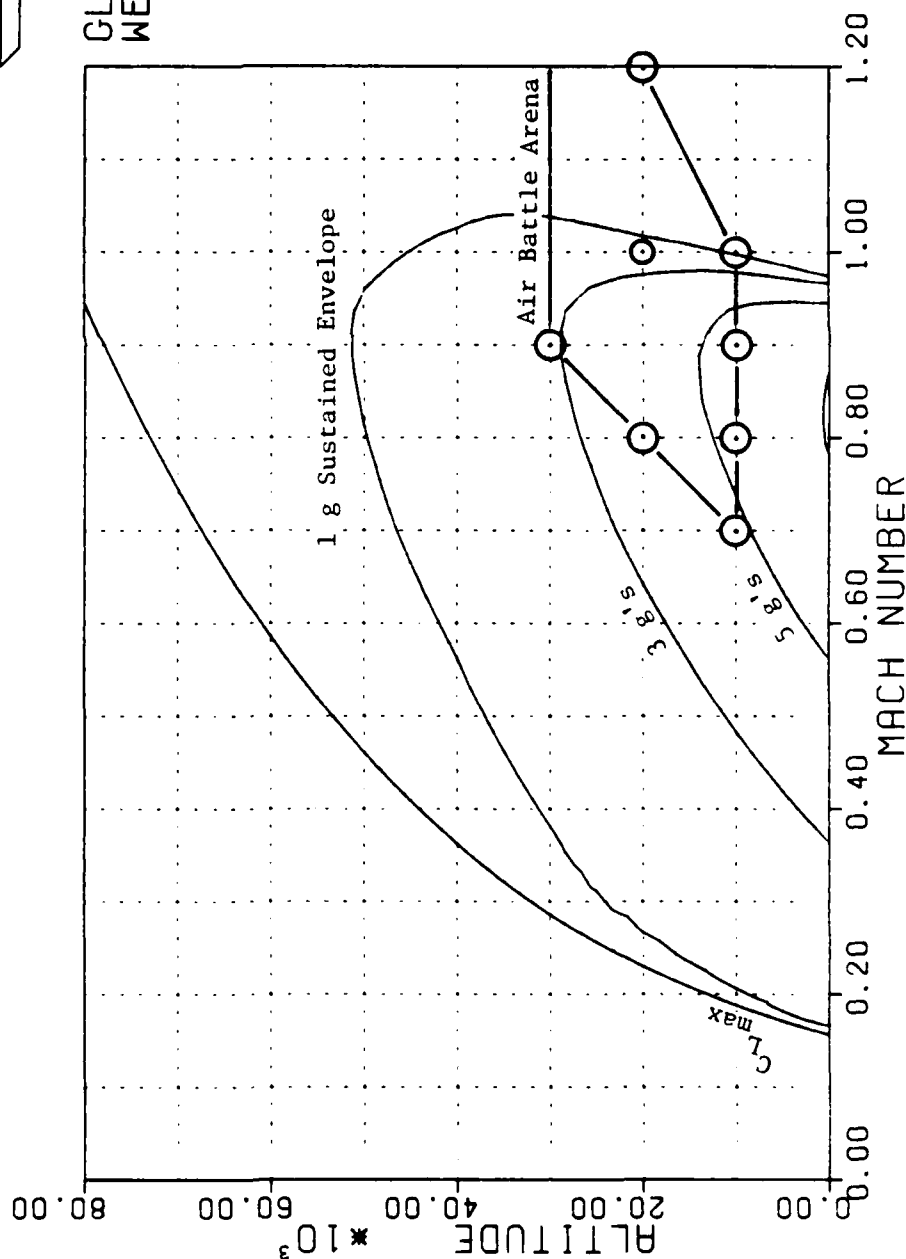
Figure 5 -- Flight Envelope

F-15 STOL

SPECIFIC EXCESS POWER (FT/SEC)

CONFIGURATION:

MAXIMUM A/B POWER
ANGLE OF ATTACK
AND THRUST VECTOR
ANGLE NEGLECTED

GLEVEL=9.00
WEIGHT=35000.
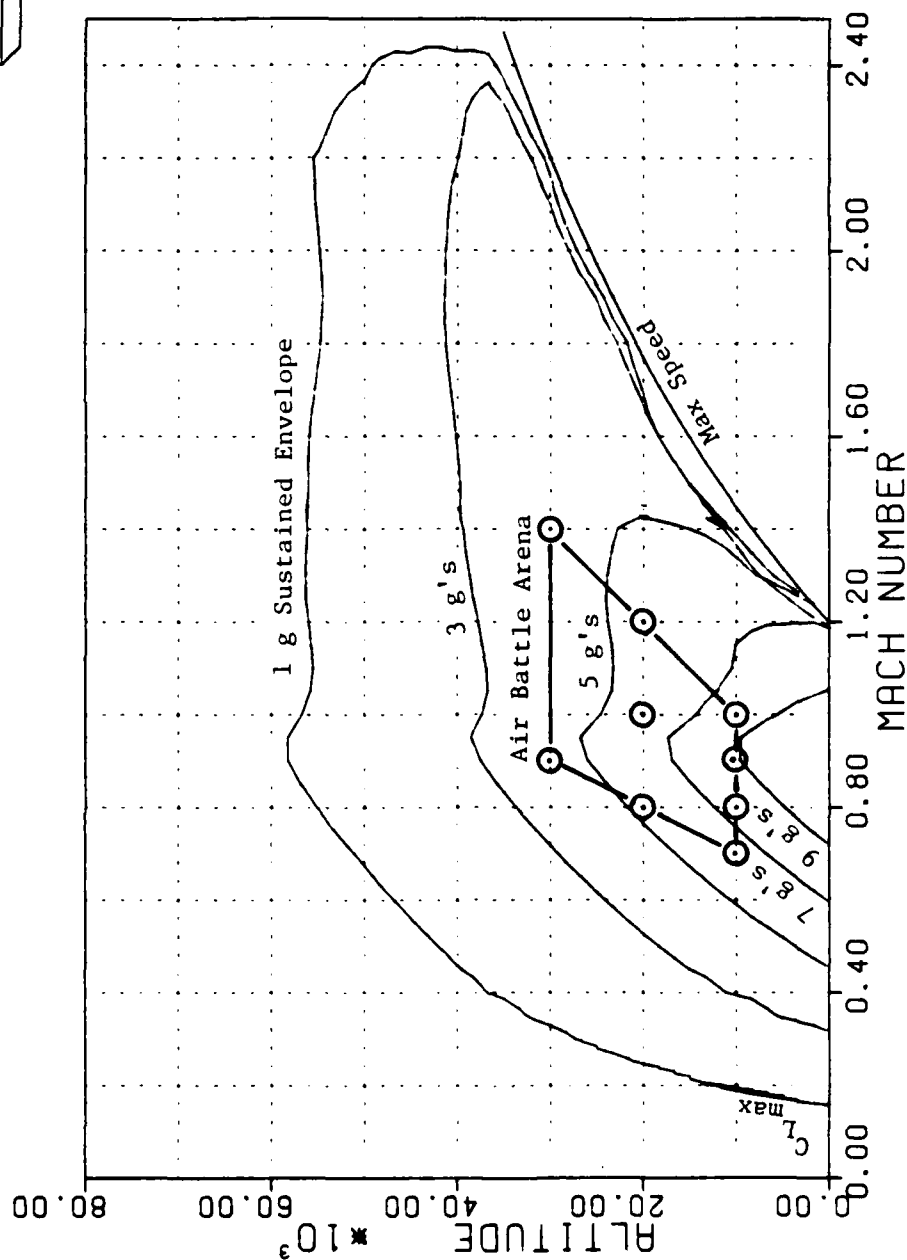
Figure 6 -- Flight Envelope

43

TABLE I

Results: M = 0.7/10,000 feet

	Case 1	Case 2	Case 3
Military Power			
P_S @ 1g	266	267	267 @ 0°
P_S @ 3g	188	190	194 @ 6°
P_S @ 5g	-48	-30	9 @ 14°
Sustained Load Factor	4.74	4.83	5.04 @ 14°
Sustained Turn Rate	11.3	11.6	12.1 @ 14°
% Thrust Required for 3g Sustained Turn	55.0	54.1	53.5 @ 1°
Maximum A/B Power			
P_S @ 1g	687	687	687 @ 0°
P_S @ 5g	372	401	442 @ 8°
P_S @ 9g	-1255	-1064	-678 @ 25°
Sustained Load Factor	6.28	6.47	7.10 @ 21°
Sustained Turn Rate	15.2	15.6	17.2 @ 21°

TABLE II

Results: M = 0.8/10,000 feet

	Case 1	Case 2	Case 3
Military Power			
P_S @ 1g	259	259	259 @ 0°
P_S @ 3g	201	202	204 @ 3°
P_S @ 5g	51	56	65 @ 8°
Sustained Load Factor	5.38	5.45	5.65 @ 10°
Sustained Turn Rate	11.3	11.5	11.9 @ 10°
% Thrust Required for 3g Sustained Turn	57.6	57.5	57.1 @ 4°
Maximum A/B Power			
P_S @ 1g	794	794	794 @ 0°
P_S @ 5g	587	594	606 @ 5°
P_S @ 9g	-595	-484	-169 @ 21°
Sustained Load Factor	7.59	7.78	8.43 @ 19°
Sustained Turn Rate	16.1	16.5	17.9 @ 19°

TABLE III

Results: M = 0.9/10,000 feet

	Case 1	Case 2	Case 3
Military Power			
P_S @ 1g	232	232	232 @ 0°
P_S @ 3g	181	183	184 @ 2°
P_S @ 5g	58	61	67 @ 6°
Sustained Load Factor	5.55	5.61	5.75 @ 9°
Sustained Turn Rate	10.4	10.5	10.8 @ 9°
% Thrust Required for 3g Sustained Turn	67.0	66.6	66.4 @ 2°
Maximum A/B Power			
P_S @ 1g	906	906	906 @ 0°
P_S @ 5g	732	737	747 @ 5°
P_S @ 9g	-40	19	164 @ 15°
Sustained Load Factor	8.86	9.00	9.00 @ 17°
Sustained Turn Rate	16.7	17.0	17.0 @ 17°

TABLE IV

Results: M = 1.0/10,000 feet

	Case 1	Case 2	Case 3
Military Power			
P_S @ 1g	-6	-6	-5 @ 1°
P_S @ 3g	-96	-94	-86 @ 6°
P_S @ 5g	-283	-278	-252 @ 10°
Sustained Load Factor	-	-	-
Sustained Turn Rate	-	-	-
% Thrust Required for 3g Sustained Turn	-	-	-
Maximum A/B Power			
P_S @ 1g	837	837	838 @ 1°
P_S @ 5g	560	569	603 @ 7°
P_S @ 9g	-291	-248	-65 @ 15°
Sustained Load Factor	7.98	8.13	8.73 @ 16°
Sustained Turn Rate	13.6	13.8	14.9 @ 16°

TABLE V

Results: M = 0.8/20,000 feet

	Case 1	Case 2	Case 3
Military Power			
P_S @ 1g	216	216	216 @ 0°
P_S @ 3g	117	119	123 @ 7°
P_S @ 5g	-266	-239	-158 @ 23°
Sustained Load Factor	3.93	3.99	4.17 @ 12°
Sustained Turn Rate	8.5	8.6	9.0 @ 12°
% Thrust Required for 3g Sustained Turn	67.8	67.3	66.4 @ 7°
Maximum A/B Power			
P_S @ 1g	603	604	604 @ 1°
P_S @ 5g	121	163	260 @ 14°
P_S @ 9g	-2473	-2068	-1403 @ 29°
Sustained Load Factor	5.34	5.50	6.00 @ 18°
Sustained Turn Rate	11.7	12.0	13.2 @ 18°

TABLE VI

Results: M = 1.0/20,000 feet

	Case 1	Case 2	Case 3
Military Power			
P_s @ 1g	51	51	52 @ 1°
P_s @ 3g	-80	-77	-67 @ 9°
P_s @ 5g	-399	-386	-337 @ 14°
Sustained Load Factor	2.03	2.05	2.12 @ 7°
Sustained Turn Rate	3.1	3.2	3.3 @ 7°
% Thrust Required for 3g Sustained Turn	-	-	-
Maximum A/B Power			
P_s @ 1g	664	665	665 @ 0°
P_s @ 5g	214	236	300 @ 12°
P_s @ 9g	-1099	-995	-789 @ 21°
Sustained Load Factor	5.82	5.95	6.44 @ 17°
Sustained Turn Rate	10.2	10.4	11.3 @ 17°

TABLE VII

Results: M = 1.2/20,000 feet

	Case 1	Case 2	Case 3
Military Power			
P_S @ 1g	−525	−525	−525 @ 0°
P_S @ 3g	−539	−537	−534 @ 5°
P_S @ 5g	−815	−806	−763 @ 13°
Sustained Load Factor	−	−	−
Sustained Turn Rate	−	−	−
% Thrust Required for 3g Sustained Turn	−	−	−
Maximum A/B Power			
P_S @ 1g	410	410	410 @ 0°
P_S @ 5g	121	136	192 @ 8°
P_S @ 9g	−1262	−1175	−889 @ 21°
Sustained Load Factor	5.50	5.63	6.07 @ 12°
Sustained Turn Rate	8.0	8.2	8.9 @ 12°

TABLE VIII

Results: M = 0.9/30,000 feet

	Case 1	Case 2	Case 3
Military Power			
P_s @ 1g	144	144	144 @ 0°
P_s @ 3g	-18	-12	7 @ 10°
P_s @ 5g	-698	-651	-474 @ 27°
Sustained Load Factor	2.89	2.94	3.05 @ 10°
Sustained Turn Rate	5.6	5.7	5.9 @ 10°
% Thrust Required for 3g Sustained Turn	-	-	99.9 @ 10°
Maximum A/B Power			
P_s @ 1g	479	480	480 @ 0°
P_s @ 5g	-362	-286	-92 @ 20°
P_s @ 9g	-5592	-4777	-3092 @ 48°
Sustained Load Factor	4.23	4.34	4.71 @ 19°
Sustained Turn Rate	8.5	8.7	9.5 @ 19°

TABLE IX

Results: M = 1.4/30,000 feet

	Case 1	Case 2	Case 3
Military Power			
P_S @ 1g	-592	-592	-592 @ 0°
P_S @ 3g	-701	-698	-691 @ 7°
P_S @ 5g	-1197	-1177	-1078 @ 14°
Sustained Load Factor	-	-	-
Sustained Turn Rate	-	-	-
% Thrust Required for 3g Sustained Turn	-	-	-
Maximum A/B Power			
P_S @ 1g	378	378	378 @ 0°
P_S @ 5g	-228	-191	-74 @ 13°
P_S @ 9g	-2366	-2215	-1733 @ 23°
Sustained Load Factor	4.27	4.36	4.71 @ 12°
Sustained Turn Rate	5.5	5.6	6.1 @ 12°

52

VII. Conclusions and Recommendations

Two major conclusions are drawn based upon the results of this study:

1. Thrust-vectoring nozzles can substantially increase a fighter aircraft's turning performance throughout the air battle arena. The $\pm$ 20° nozzle deflection angle constraint would limit the aircraft's optimal performance in only a few instances.

2. Level 1 g flight does not benefit from the use of vectored thrust since the aircraft's wing loading is small compared to that of turning flight.

Two recommendations are offered for future research:

1. This study concentrated on the air-to-air combat applications of a fighter aircraft's performance. Air-to-ground applications should be investigated for the ordnance delivery scenario.

2. Investigate the class of aircraft that might utilize thrust sideslip vectoring and sideforce generation and the type of trajectories that may result.

APPENDIX A

Aircraft Performance Computer Program Data Input

```
...
...    REYNOLD'S NUMBER CORRECTIONS
...

       INDA01=1,
       IA01X=8,
       IA01Y=11,
       ATAB01=0.,10000.,20000.,30000.,40000.,50000.,60000.,70000.,
       .2,.6,.8,1.0,1.2,1.4,1.6,1.8,2.0,2.2,2.5,
       -.0017,-.0012,-.0006,.0,.0009,.0020,.0033,.0047,    $M=.2
       -.0013,-.0009,-.0005,.0,.0007,.0015,.0025,.0036,    $M=.6
       -.0012,-.0008,-.0004,.0,.0006,.0014,.0023,.0033,    $M=.8
       -.0012,-.0008,-.0004,.0,.0006,.0013,.0022,.0031,    $M=1.0
       -.0011,-.0007,-.0004,.0,.0005,.0012,.0020,.0029,    $M=1.2
       -.0010,-.0007,-.0004,.0,.0005,.0012,.0019,.0027,    $M=1.4
       -.0010,-.0006,-.0003,.0,.0005,.0011,.0018,.0025,    $M=1.6
       -.0009,-.0006,-.0003,.0,.0004,.0010,.0017,.0023,    $M=1.8
       -.0008,-.0006,-.0003,.0,.0004,.0010,.0016,.0022,    $M=2.0
       -.0008,-.0006,-.0003,.0,.0003,.0009,.0015,.0021,    $M=2.2
       -.0007,-.0005,-.0002,.0,.0003,.0008,.0013,.0019,    $M=2.5
...
...    F-15 FLIGHT TEST DRAG POLARS
...

       INDA02=1,
       IA02X=27,
       IA02Y=21,
       ATAB02=.0,.05,.1,.15,.2,.25,.3,.35,.4,.45,.5,.55,.6,.65,
          .7,.75,.8,.85,.9,.95,1.0,1.05,1.1,1.15,1.2,1.4,1.6,
             .4,.6,.7,.8,.85,.9,.95,1.0,1.05,1.1,1.2,
             1.3,1.4,1.5,1.6,1.7,1.8,1.9,2.0,2.2,2.4,
 .0228,.0225,.0230,.0242,.0254,.0284,.0320,.0360,.0420,
  .0493,.0580,.0685,.0825,.1005,.1180,.1400,.1630,.1850,
  .2105,.2400,.2715,.2945,.3367,.3810,.4495,.8700,1.3100,
 .0222,.0215,.0220,.0232,.0245,.0273,.0305,.0347,.0390,
  .0450,.0530,.0635,.0780,.0960,.1163,.1396,.1640,.1873,
  .2163,.2465,.2793,.3135,.3565,.4105,.4790,.9000,1.3400,
 .0220,.0213,.0215,.0225,.0242,.0268,.0299,.0341,.0390,
  .0453,.0523,.0625,.0765,.0957,.1156,.1395,.1650,.1904,
  .2203,.2525,.2880,.3285,.3770,.4325,.5040,.9200,1.3650,
 .0217,.0213,.0216,.0225,.0242,.0265,.0298,.0337,.0383,
  .0437,.0520,.0633,.0780,.0946,.1150,.1395,.1668,.1960,
  .2290,.2643,.3000,.3460,.3980,.4550,.5280,.9350,1.4000,
 .0215,.0213,.0220,.0231,.0244,.0269,.0300,.0336,.0386,
  .0445,.0534,.0646,.0783,.0953,.1152,.1400,.1686,.2000,
  .2345,.2700,.3075,.3540,.4075,.4650,.5590,.9400,1.4200,
 .0216,.0213,.0224,.0236,.0249,.0274,.0304,.0343,.0396,
  .0466,.0560,.0673,.0803,.0973,.1163,.1413,.1705,.2045,
  .2400,.2760,.3135,.3630,.4180,.4800,.5900,.9900,1.4700,
 .0230,.0230,.0235,.0256,.0273,.0300,.0330,.0380,.0448,
  .0533,.0650,.0790,.0912,.1065,.1275,.1510,.1740,.2125,
  .2470,.2835,.3220,.3725,.4280,.4850,.6100,1.0500,1.5200,
 .0300,.0299,.0310,.0335,.0367,.0410,.0465,.0540,.0623,
  .0735,.0870,.1000,.1150,.1330,.1485,.1675,.1990,.2275,
  .2565,.2915,.3325,.3825,.4380,.4900,.6330,1.0800,1.5800,
 .0394,.0386,.0389,.0407,.0438,.0484,.0542,.0625,.0728,
  .0848,.0990,.1135,.1333,.1510,.1678,.1865,.2130,.2400,
  .2690,.3060,.3440,.4060,.4630,.5200,.6650,1.1500,1.6200,
 .0435,.0420,.0420,.0434,.0464,.0511,.0580,.0670,.0772,
  .0910,.1050,.1219,.1425,.1610,.1803,.2037,.2313,.2505,
  .2825,.3215,.3600,.4150,.4700,.5400,.6850,1.1000,1.5500,
 .0495,.0473,.0452,.0461,.0489,.0544,.0615,.0715,.0845,
  .0993,.1150,.1340,.1555,.1735,.1975,.2300,.2570,.2780,
```

```
             .3000,..3400,..3700,..4400,..5040,.5800,..6450,1.0471,1.4700,
        .0500,..0481,..0474,..0488,..0517,..0580,..0655,..0765,..0903,
        .1062,..1248,..1450,..1657,..1845,..2093,..2350,..2620,..2830,
        .3075,..3400,..3700,..4300,..4875,..5550,..6150,..9100,1.3500,
   .0496,..0483,..0483,..0497,..0535,..0600,..0690,..0813,..0960,
        .1130,..1328,..1545,..1795,..1995,..2160,..2420,..2670,.2900,
        .3150,..3400,..3700,..4200,..4700,..5300,..5850,..6600,1.2400,
   .0496,..0486,..0490,..0515,..0552,..0622,..0723,..0850,..1010,
        .1200,..1400,..1590,..1810,..2040,..2260,..2470,..2710,.2930,
        .3160,..3400,..3650,..4125,..4500,..4950,..5450,..7700,1.0800,
   .0500,..0493,..0496,..0517,..0550,..0635,..0742,..0890,..1052,
        .1263,..1440,..1645,..1860,..2100,..2300,..2520,..2740,.2960,
        .3170,..3400,..3600,..3950,..4300,..4600,..4900,..6500,0.9300,
   .0486,..0485,..0492,..0524,..0566,..0653,..0765,..0920,..1098,
        .1300,..1505,..1723,..1960,..2190,..2400,..2640,..2860,.3090,
        .3320,..3550,..3800,..4100,..4500,..4800,..5150,..6700,0.91500,
   .0473,..0482,..0490,..0522,..0575,..0668,..0790,..0948,..1142,
        .1330,..1575,..1800,..2040,..2280,..2500,..2750,..3000,.3230,
        .3450,..3700,..3950,..4300,..4550,..4950,..5250,0.6550,0.8950,
   .0474,..0467,..0485,..0519,..0583,..0685,..0816,..0984,..1187,
        .1385,..1645,..1875,..2120,..2370,..2600,..2850,..3100,.3340,
        .3570,..3825,..4075,..4450,..4800,..5200,..5500,0.6970,0.8750,
   .0462,..0463,..0475,..0515,..0584,..0702,..0850,..1025,..1237,
        .1450,..1710,..1950,..2210,..2465,..2700,..2960,..3200,.3450,
        .3700,..3950,..4200,..4580,..4940,..5400,..5700,0.7100,0.8520,
   .0440,..0437,..0455,..0502,..0610,..0740,..0916,..1105,..1300,
        .1600,..1870,..2130,..2380,..2650,..2890,..3150,..3400,.3650,
        .3900,..4160,..4410,..4700,..5000,..5350,..5700,..6800,0.8000,
   .0420,..0410,..0432,..0487,..0629,..0802,..0997,..1225,..1500,
        .1780,..2050,..2300,..2600,..2850,..3100,..3400,..3650,.3940,
        .4200,..4480,..4750,..5000,..5270,..5540,..5800,..6850,0.7900,
   ...
   ...   2 PLACE CANOPY DRAG
   ...
        INDA03=1,
        IA03X=2,
        IA03Y=6,
        ATAB03=0.,80000.,
               0.1,1.31,1.54,1.55,2.05,3.0,
        .00050,..00050,
        .00050,..00050,
        .00075,..00075,
        .00083,..00083,
        .00100,..00100,
        .00100,..00100,
   ...
   ...   F-15 CL-ALPHA CURVES
   ...
        ICLAX=29,
        ICLAY=10,
        CLATAB=0.,..1,..2,..3,..4,..5,..55,..6,..65,..7,
               .75,..8,..85,..9,..95,1.0,1.05,1.1,1.15,1.2,
               1.25,1.3,1.35,1.4,1.45,1.5,1.55,1.6,1.65,
            .2,..6,..85,..9,1.0,1.2,1.6,2.2,2.25,2.5,
   -0.45, 1.07, 2.58, 4.12, 5.63, 7.19, 7.90, 8.68, 9.48,10.30,
   11.17,12.12,13.09,14.04,15.01,16.03,17.30,18.70,20.30,22.50,
   25.25,27.90,30.95,34.00,37.05,39.70,42.10,44.00,44.00, $M=0.2
   -0.45, 1.07, 2.58, 4.12, 5.63, 7.19, 7.90, 8.63, 9.48,10.30,
   11.17,12.12,13.09,14.04,15.01,16.03,17.30,18.70,20.30,22.50,
   25.25,27.90,30.60,33.00,35.30,37.55,39.85,42.00,42.00, $M=0.6
   -0.51, 0.85, 2.28, 3.66, 5.07, 6.45, 7.13, 7.90, 8.64, 9.45,
   10.33,11.44,12.60,13.90,15.30,16.85,18.50,20.25,22.10,24.00,
   26.05,28.10,30.30,32.40,34.50,36.35,38.10,39.50,39.50, $M=.85
   -0.43, 0.88, 2.19, 3.50, 4.80, 6.08, 6.72, 7.42, 8.16, 8.97,
   9.90,11.09,12.37,13.70,15.12,16.67,18.33,20.10,21.90,23.75,
   25.70,27.55,29.45,31.20,32.85,34.30,35.55,36.30,36.80, $M=.9
```

```
        -0.30,  .95, 2.25, 3.50, 4.00, 6.10, 6.75, 7.35, 8.00, 8.75,
         7.70,10.80,12.00,13.30,14.75,16.20,17.70,19.20,20.75,22.30,
        23.70,24.95,26.10,27.20,28.20,29.20,30.20,31.10,31.10, $M=1.0
        -0.35, 1.14, 2.65, 4.17, 5.85, 7.50, 8.30, 9.10, 9.90,10.70,
        11.55,12.50,13.45,14.60,16.00,17.40,19.30,20.75,22.00,23.20,
        24.30,25.30,26.30,27.20,27.20,27.20,27.20,27.20,27.20, $M=1.2
        -0.92, 1.07, 3.10, 5.10, 7.50,10.00,11.25,12.50,13.80,15.10,
        16.30,17.50,18.75,20.30,22.10,23.80,25.90,26.20,26.20,28.20,
        28.20,28.20,28.20,28.20,28.20,28.20,28.20,28.20,28.20, $M=1.6
        -0.06, 2.17, 4.93, 7.85,10.67,13.70,16.00,18.20,20.45,22.70,
        22.70,22.70,22.70,22.70,22.70,22.70,22.70,22.70,22.70,22.70,
        22.70,22.70,22.70,22.70,22.70,22.70,22.70,22.70,22.70, $M=2.2
        -0.66, 2.17, 5.03, 7.67,10.45,13.90,16.20,18.55,20.85,20.85,
        20.85,20.85,20.85,20.85,20.85,20.85,20.85,20.85,20.85,20.85,
        20.85,20.85,20.85,20.85,20.85,20.85,20.85,20.85,20.85, $M=2.25
        -0.25, 2.55, 5.30, 8.10,10.90,14.90,14.90,14.90,14.90,14.90,
        14.90,14.90,14.90,14.90,14.90,14.90,14.90,14.90,14.90,14.90,
        14.90,14.90,14.90,14.90,14.90,14.90,14.90,14.90,14.90, $M=2.5

  ...
  ...     CANARD DRAG POLAR
  ...
        INDA04=11,
        IA04X=23,
        IA04Y=12,
        ATAB04=-.22,-.20,-.18,-.16,-.14,-.12,-.10,-.08,-.06,-.04,-.02,
               0.,.02,.04,.06,.08,.10,.12,.14,.16,.18,.20,.22,
                .2,.4,.6,.8,1.0,1.2,1.4,1.6,1.8,2.0,2.2,2.4,
  $ M=0.2
                .0635,. 0525, .0428, .0340, .0262,
                .0196, .0140, .0093, .0057, .0032, .0016,
                .0011,
                .0016, .0032, .0057, .0093, .0140, .0196,
                .0262, .0340, .0428, .0525, .0635,
  $ M=0.4
                .0717, .0533, .0407, .0324, .0250,
                .0186, .0132, .0088, .0054, .0029, .0015,
                .0010,
                .0015, .0029, .0054, .0088, .0132, .0186,
                .0250, .0324, .0407, .0533, .0717,
  $ M=0.6
                .1013, .0719, .0512, .0362, .0252,
                .0182, .0129, .0086, .0053, .0029, .0014,
                .0010,
                .0014, .0029, .0053, .0086, .0129, .0182,
                .0252, .0362, .0512, .0719, .1013,
  $ M=0.8
                .2732, .1553, .0961, .0616, .0399,
                .0255, .0159, .0094, .0052, .0028, .0014,
                .0009,
                .0014, .0028, .0052, .0094, .0159, .0255,
                .0399, .0616, .0961, .1553, .2732,
  $ M=1.0
                1.181, .3204, .1552, .0876, .0523,
                .0317, .0189, .0109, .0059, .0031, .0017,
                .0014,
                .0017, .0031, .0059, .0109, .0189, .0317,
                .0523, .0876, .1552, .3204, 1.181,
  $ M=1.2
                .0842, .0697, .0565, .0448, .0344,
                .0255, .0180, .0119, .0073, .0040, .0022,
                .0018,
                .0022, .0040, .0073, .0119, .0180, .0255,
                .0344, .0448, .0565, .0697, .0842,
  $ M=1.4
                .1048, .0860, .0702, .0555, .0426,
                .0315, .0221, .0145, .0087, .0046, .0024,
```

```
                        .0019,
                        .0024,  .0046,  .0037,  .0145,  .0221,  .0315,
                        .0426,  .0555,  .0702,  .0866,  .1648,
            $ M=1.6
                        .1255,  .1039,  .0839,  .0662,  .0508,
                        .0374,  .0262,  .0170,  .0101,  .0052,  .0025,
                        .0019,
                        .0025,  .0052,  .0101,  .0170,  .0262,  .0374,
                        .0508,  .0662,  .0839,  .1039,  .1255,
            $ M=1.8
                        .1453,  .1199,  .0970,  .0766,  .0586,
                        .0431,  .0301,  .0195,  .0114,  .0058,  .0026,
                        .0019,
                        .0026,  .0058,  .0114,  .0195,  .0301,  .0431,
                        .0586,  .0766,  .0970,  .1199,  .1453,
            $ M=2.0
                        .1646,  .1358,  .1098,  .0866,  .0662,
                        .0486,  .0338,  .0218,  .0126,  .0063,  .0027,
                        .0019,
                        .0027,  .0063,  .0126,  .0218,  .0338,  .0486,
                        .0662,  .0866,  .1098,  .1358,  .1646,
            $ M=2.2
                        .1835,  .1514,  .1223,  .0964,  .0737,
                        .0540,  .0375,  .0241,  .0139,  .0067,  .0027,
                        .0018,
                        .0027,  .0067,  .0139,  .0241,  .0375,  .0540,
                        .0737,  .0964,  .1223,  .1514,  .1835,
            $ M=2.4
                        .2022,  .1667,  .1347,  .1062,  .0810,
                        .0594,  .0412,  .0264,  .0151,  .0072,  .0028,
                        .0018,
                        .0028,  .0072,  .0151,  .0264,  .0412,  .0594,
                        .0810,  .1062,  .1347,  .1667,  .2022,
    ...
    ...    CANARD LIFT CURVE
    ...
            ICLCX=2,
            ICLCY=8,
            CLCTAB= -0.2,  0.2,
                    .2,.4,.6,.8,1.0,1.2,1.4,2.4,
                    -27.5,  27.5,
                    -27.0,  27.0,
                    -26.0,  26.0,
                    -24.5,  24.5,
                    -22.3,  22.3,
                    -19.6,  19.6,
                    -20.2,  20.2,
                    -20.2,  20.2,
    ...
    ...    F-15 MILITARY POWER   (FN WITH SFC AND FG HOOKS)
    ...
            INDT01= 1,
            IT01X=  6,
            IT01Y=  9,
            TTAB01=  0.,   10000.,   20000.,   30000.,   40000.,   50000.,
            0.00,    .20,     .40,      .60,      .80,     .85,      .90,     .95,   1.00,
                        11790.,    8674.,    6099.,    4134.,    2542.,    1546., $M=0.00
                        12030.,    9117.,    6099.,    4134.,    2542.,    1546., $M= .20
                        11970.,    9339.,    6360.,    4134.,    2542.,    1546., $M= .40
                        12160.,    9521.,    6986.,    4558.,    2794.,    1722., $M= .60
                        12090.,    9642.,    7620.,    5160.,    3195.,    1971., $M= .80
                        12050.,    9775.,    7654.,    5351.,    3332.,    2050., $M= .85
                        11940.,    9849.,    7608.,    5578.,    3487.,    2141., $M= .90
                        11680.,    9701.,    7610.,    5699.,    3598.,    2203., $M= .95
                        11400.,    9547.,    7521.,    5719.,    3710.,    2256., $M=1.
    ...
```

```
      I.0, = 1,
      ITO2X= 12,
      ITO2Y=  9,
      ITO2Z=  6,
      TTABO2=5.00,   10.00,   20.00,   30.00,   40.00,   50.00,
             60.00,  70.00,   80.00,   90.00,   95.00,  100.00,
      0.00,   .20,     .40,     .50,     .80,     .85,    .90,    .95,   1.00,
              0.,    10000.,  20000.,  30000.,  40000.,  50000.,
```

$ ALTITUDE =   0.

1.357,	1.135,	.835,	.706,	.736,	.725, $M=0.00
.723,	.731,	.747,	.758,	.763,	.768,
2.138,	1.354,	1.012,	.900,	.847,	.817, $M= .20
.802,	.806,	.812,	.817,	.818,	.820,
2.669,	1.681,	1.205,	1.041,	.960,	.916, $M= .40
.891,	.888,	.386,	.884,	.884,	.883,
3.716,	2.221,	1.467,	1.216,	1.096,	1.033, $M= .60
.997,	.982,	.970,	.961,	.957,	.953,
5.343,	3.008,	1.837,	1.473,	1.293,	1.195, $M= .80
1.138,	1.104,	1.078,	1.058,	1.050,	1.042,
5.827,	3.238,	1.949,	1.551,	1.353,	1.242, $M= .85
1.179,	1.139,	1.109,	1.085,	1.075,	1.066,
6.427,	3.536,	2.106,	1.653,	1.429,	1.303, $M= .90
1.230,	1.182,	1.147,	1.119,	1.107,	1.096,
7.396,	4.023,	2.363,	1.816,	1.555,	1.404, $M= .95
1.317,	1.257,	1.212,	1.176,	1.161,	1.148,
8.548,	4.599,	2.654,	2.005,	1.698,	1.518, $M=1.00
1.415,	1.346,	1.285,	1.242,	1.223,	1.207,

$ ALTITUDE =   10000.

1.134,	1.102,	.815,	.747,	.716,	.709, $M=0.00
.708,	.710,	.733,	.755,	.764,	.773,
1.867,	1.276,	.965,	.861,	.814,	.787, $M= .20
.779,	.775,	.795,	.810,	.816,	.822,
2.408,	1.535,	1.116,	.975,	.907,	.870, $M= .40
.854,	.852,	.863,	.871,	.875,	.878,
3.233,	1.961,	1.323,	1.116,	1.020,	.969, $M= .60
.942,	.937,	.937,	.936,	.936,	.936,
4.534,	2.590,	1.630,	1.326,	1.182,	1.106, $M= .80
1.062,	1.041,	1.026,	1.014,	1.009,	1.004,
4.878,	2.752,	1.712,	1.363,	1.224,	1.140, $M= .85
1.091,	1.067,	1.049,	1.034,	1.028,	1.023,
5.321,	2.969,	1.821,	1.458,	1.281,	1.185, $M= .90
1.129,	1.100,	1.078,	1.061,	1.054,	1.048,
6.100,	3.371,	2.019,	1.593,	1.380,	1.261, $M= .95
1.194,	1.156,	1.127,	1.105,	1.096,	1.088,
7.002,	3.824,	2.250,	1.742,	1.491,	1.346, $M=1.00
1.266,	1.219,	1.184,	1.156,	1.145,	1.134,

$ ALTITUDE =   20000.

1.155,	1.156,	.964,	.853,	.802,	.773, $M=0.00
.763,	.760,	.776,	.788,	.793,	.798,
1.155,	1.156,	.964,	.853,	.802,	.773, $M= .20
.763,	.760,	.776,	.788,	.793,	.798,
1.913,	1.516,	1.095,	.954,	.887,	.849, $M= .40
.834,	.827,	.839,	.848,	.852,	.856,
2.991,	1.829,	1.246,	1.056,	.977,	.930, $M= .60
.910,	.897,	.907,	.915,	.919,	.922,
3.838,	2.234,	1.445,	1.202,	1.093,	1.031, $M= .80
.995,	.984,	.985,	.987,	.987,	.988,
4.124,	2.374,	1.517,	1.250,	1.127,	1.059, $M= .85
1.019,	1.006,	1.005,	1.003,	1.003,	1.002,
4.491,	2.563,	1.615,	1.316,	1.176,	1.098, $M= .90
1.050,	1.036,	1.030,	1.025,	1.023,	1.021,
5.159,	2.893,	1.792,	1.426,	1.253,	1.160, $M= .95
1.102,	1.083,	1.070,	1.060,	1.056,	1.052,
5.907,	3.263,	1.965,	1.547,	1.341,	1.231, $M=1.00
1.162,	1.136,	1.117,	1.102,	1.096,	1.091,

$ ALTITUDE =   30000.

```
          1.100,    1.....,   1.100,     .956,     .883,     .841,
           .824,     .816,     .825,     .831,     .834,     .836,
          1.100,    1.100,    1.100,     .956,     .883,     .841, SM= .20
           .824,     .816,     .825,     .831,     .834,     .836,
          1.100,    1.100,    1.100,     .956,     .883,     .841, SM= .40
           .824,     .816,     .825,     .831,     .834,     .836,
          1.725,    1.725,    1.233,    1.040,     .959,     .912, SM= .60
           .883,     .878,     .884,     .889,     .891,     .893,
          3.685,    2.147,    1.393,    1.160,    1.060,    1.000, SM= .80
           .968,     .948,     .954,     .959,     .961,     .963,
          3.823,    2.211,    1.429,    1.185,    1.077,    1.013, SM= .85
           .980,     .956,     .965,     .971,     .973,     .975,
          4.036,    2.320,    1.487,    1.223,    1.106,    1.036, SM= .90
          1.001,     .978,     .985,     .991,     .993,     .996,
          4.469,    2.548,    1.601,    1.300,    1.162,    1.081, SM= .95
          1.039,    1.013,    1.020,    1.025,    1.027,    1.029,
          5.038,    2.830,    1.742,    1.393,    1.229,    1.136, SM=1.00
          1.084,    1.059,    1.062,    1.064,    1.065,    1.066,
$ ALTITUDE =   40000.
           .842,     .842,     .842,     .842,     .842,     .842, SM=0.00
           .827,     .816,     .822,     .827,     .829,     .831,
           .842,     .842,     .842,     .842,     .842,     .842, SM= .20
           .827,     .816,     .822,     .827,     .829,     .831,
           .842,     .842,     .842,     .842,     .842,     .842, SM= .40
           .827,     .816,     .822,     .827,     .829,     .831,
           .966,     .966,     .966,     .966,     .957,     .910, SM= .60
           .885,     .870,     .875,     .878,     .880,     .881,
          1.286,    1.286,    1.286,    1.161,    1.056,     .994, SM= .80
           .960,     .938,     .942,     .946,     .947,     .948,
          1.456,    1.456,    1.397,    1.178,    1.068,    1.003, SM= .85
           .967,     .947,     .952,     .956,     .958,     .959,
          1.760,    1.760,    1.478,    1.213,    1.095,    1.024, SM= .90
           .989,     .966,     .971,     .975,     .977,     .979,
          2.609,    2.482,    1.582,    1.283,    1.146,    1.065, SM= .95
          1.024,     .998,    1.004,    1.009,    1.011,    1.012,
          4.863,    2.739,    1.691,    1.357,    1.201,    1.111, SM=1.00
          1.064,    1.036,    1.042,    1.046,    1.048,    1.050,
$ ALTITUDE =   50000.
           .877,     .877,     .877,     .877,     .877,     .877, SM=0.00
           .876,     .876,     .876,     .876,     .876,     .878,
           .877,     .877,     .877,     .877,     .877,     .877, SM= .20
           .876,     .876,     .876,     .876,     .876,     .878,
           .877,     .877,     .877,     .877,     .877,     .877, SM= .40
           .876,     .876,     .876,     .876,     .876,     .878,
           .895,     .896,     .897,     .898,     .899,     .900, SM= .60
           .901,     .902,     .903,     .906,     .914,     .920,
           .991,     .990,     .990,     .990,     .990,     .990, SM= .80
           .990,     .983,     .984,     .984,     .985,     .985,
          1.011,    1.010,    1.010,    1.010,    1.010,    1.010, SM= .85
          1.007,     .984,     .986,     .988,     .989,     .990,
          1.054,    1.054,    1.054,    1.054,    1.053,    1.053, SM= .90
           .940,    1.002,    1.005,    1.007,    1.008,    1.009,
          1.127,    1.127,    1.127,    1.127,    1.126,    1.112, SM= .95
          1.066,    1.034,    1.037,    1.040,    1.041,    1.042,
          1.231,    1.231,    1.231,    1.231,    1.231,    1.162, SM=1.00
          1.107,    1.077,    1.078,    1.079,    1.079,    1.079,
...
   INOT11= 1,
   IT11X= 12,
   IT11Y=  9,
   IT11Z=  6,
   TTAB11=5.00,   10.00,    20.00,    30.00,    40.00,    50.00,
          60.00,   70.00,    80.00,    90.00,    95.00,   100.00,
   0.00,    .20,     .40,     .60,     .80,     .85,     .90,     .95,    1.00,
            0.,   10000.,   20000.,   30000.,   40000.,   50000.,
$ ALTITUDE =       0.
```

581.,	1178.,	2358.,	3537.,	4716.,	5895.,	$M=0.00
7074.,	8253.,	9432.,	10611.,	11201.,	11790.,	
1127.,	1868.,	3269.,	4613.,	5926.,	7226.,	$M= .20
8511.,	9769.,	11023.,	12276.,	12903.,	13530.,	
2127.,	2936.,	4452.,	5907.,	7312.,	8697.,	$M= .40
10064.,	11373.,	12632.,	13991.,	14646.,	15366.,	
3924.,	4737.,	6301.,	7819.,	9312.,	10787.,	$M= .60
12230.,	13618.,	15005.,	16393.,	17086.,	17780.,	
6706.,	7480.,	9013.,	10529.,	12043.,	13554.,	$M= .80
15017.,	16446.,	17874.,	19302.,	20016.,	20730.,	
7652.,	8408.,	9919.,	11423.,	12929.,	14449.,	$M= .85
15909.,	17337.,	18765.,	20192.,	20906.,	21620.,	
8679.,	9423.,	10911.,	12397.,	13888.,	15395.,	$M= .90
16838.,	18256.,	19674.,	21092.,	21801.,	22510.,	
10021.,	10739.,	12178.,	13618.,	15065.,	16519.,	$M= .95
17915.,	19301.,	20688.,	22074.,	22767.,	23460.,	
11509.,	12194.,	13570.,	14947.,	16353.,	17765.,	$M=1.00
19116.,	20467.,	21818.,	23169.,	23845.,	24520.,	

$ ALTITUDE = 10000.

826.,	867.,	1735.,	2602.,	3470.,	4337.,	$M=0.00
5204.,	6072.,	6939.,	7807.,	8240.,	8674.,	
885.,	1385.,	2437.,	3448.,	4437.,	5419.,	$M= .20
6387.,	7354.,	8303.,	9251.,	9726.,	10200.,	
1525.,	2148.,	3315.,	4435.,	5519.,	6594.,	$M= .40
7650.,	8689.,	9702.,	10716.,	11223.,	11730.,	
2739.,	3362.,	4573.,	5745.,	6897.,	8042.,	$M= .60
9180.,	10274.,	11356.,	12438.,	12979.,	13520.,	
4645.,	5251.,	6458.,	7661.,	8862.,	10070.,	$M= .80
11274.,	12410.,	13547.,	14684.,	15252.,	15820.,	
5298.,	5900.,	7115.,	8334.,	9554.,	10783.,	$M= .85
11998.,	13156.,	14314.,	15472.,	16051.,	16630.,	
6012.,	6608.,	7828.,	9056.,	10287.,	11533.,	$M= .90
12754.,	13923.,	15092.,	16261.,	16846.,	17430.,	
6939.,	7523.,	8716.,	9912.,	11109.,	12320.,	$M= .95
13507.,	14688.,	15828.,	16989.,	17570.,	18150.,	
7967.,	8533.,	9091.,	10852.,	12017.,	13199.,	$M=1.00
14364.,	15518.,	16672.,	17826.,	18403.,	18980.,	

$ ALTITUDE = 20000.

1102.,	1102.,	1629.,	2306.,	2968.,	3625.,	$M=0.00
4273.,	4918.,	5552.,	6186.,	6503.,	6820.,	
1102.,	1102.,	1629.,	2306.,	2968.,	3625.,	$M= .20
4273.,	4918.,	5552.,	6186.,	6503.,	6820.,	
1182.,	1449.,	2243.,	3005.,	3741.,	4473.,	$M= .40
5191.,	5905.,	6594.,	7283.,	7627.,	7972.,	
1870.,	2325.,	3212.,	4006.,	4907.,	5747.,	$M= .60
6579.,	7408.,	8195.,	8982.,	9376.,	9769.,	
3150.,	3631.,	4577.,	5519.,	6467.,	7416.,	$M= .80
8366.,	9282.,	10168.,	11054.,	11497.,	11940.,	
3579.,	4051.,	4994.,	5941.,	6896.,	7850.,	$M= .85
8802.,	9721.,	10621.,	11520.,	11970.,	12420.,	
4052.,	4520.,	5461.,	6412.,	7373.,	8330.,	$M= .90
9281.,	10205.,	11120.,	12035.,	12493.,	12950.,	
4689.,	5144.,	6066.,	6997.,	7934.,	8874.,	$M= .95
9815.,	10735.,	11653.,	12572.,	13031.,	13490.,	
5384.,	5826.,	6724.,	7638.,	8554.,	9477.,	$M=1.00
10401.,	11320.,	12240.,	13160.,	13620.,	14080.,	

$ ALTITUDE = 30000.

1476.,	1476.,	1476.,	1949.,	2427.,	2903.,	$M=0.00
3370.,	3833.,	4279.,	4726.,	4950.,	5173.,	
1476.,	1476.,	1476.,	1949.,	2427.,	2903.,	$M= .20
3370.,	3833.,	4279.,	4726.,	4950.,	5173.,	
1476.,	1476.,	1476.,	1949.,	2427.,	2903.,	$M= .40
3370.,	3833.,	4279.,	4726.,	4950.,	5173.,	
1563.,	1563.,	2086.,	2642.,	3191.,	3740.,	$M= .60
4283.,	4820.,	5331.,	5842.,	6097.,	6353.,	
2048.,	2373.,	3015.,	3655.,	4298.,	4944.,	$M= .80

5580.,	6212.,	6560.,	7404.,	7702.,	8000.,
2335.,	2606.,	3326.,	3990.,	4658.,	5327.,	$M= .85
5990.,	6650.,	7274.,	7890.,	8210.,	8522.,
2654.,	2993.,	3679.,	4309.,	5063.,	5758.,	$M= .90
6453.,	7146.,	7801.,	8456.,	8783.,	9111.,
3071.,	3414.,	4109.,	4800.,	5503.,	6207.,	$M= .95
6917.,	7524.,	8304.,	8984.,	9324.,	9664.,
3524.,	3863.,	4543.,	5233.,	5933.,	6637.,	$M=1.00
7350.,	8058.,	8755.,	9453.,	9801.,	10156.,

$ ALTITUDE = 40000.

1859.,	1859.,	1860.,	1860.,	1859.,	1859.,	$M=0.00
2075.,	2360.,	2635.,	2911.,	3048.,	3186.,
1859.,	1859.,	1860.,	1860.,	1859.,	1859.,	$M= .20
2075.,	2360.,	2635.,	2911.,	3048.,	3186.,
1859.,	1859.,	1860.,	1860.,	1859.,	1859.,	$M= .40
2075.,	2360.,	2635.,	2911.,	3048.,	3186.,
1919.,	1919.,	1919.,	1919.,	1965.,	2300.,	$M= .60
2632.,	2963.,	3278.,	3592.,	3750.,	3907.,
2016.,	2016.,	2017.,	2265.,	2665.,	3064.,	$M= .80
3458.,	3850.,	4219.,	4589.,	4773.,	4958.,
2035.,	2035.,	2035.,	2479.,	2896.,	3313.,	$M= .85
3726.,	4137.,	4525.,	4913.,	5107.,	5301.,
2069.,	2069.,	2291.,	2721.,	3156.,	3590.,	$M= .90
4025.,	4457.,	4865.,	5274.,	5479.,	5683.,
2107.,	2107.,	2565.,	3003.,	3447.,	3892.,	$M= .95
4341.,	4787.,	5215.,	5643.,	5857.,	6071.,
2203.,	2422.,	2864.,	3311.,	3766.,	4222.,	$M=1.00
4687.,	5149.,	5598.,	6046.,	6271.,	6495.,

$ ALTITUDE = 50000.

1856.,	1857.,	1859.,	1860.,	1862.,	1863.,	$M=0.00
1865.,	1866.,	1868.,	1869.,	1871.,	1942.,
1856.,	1857.,	1859.,	1860.,	1862.,	1863.,	$M= .20
1865.,	1866.,	1868.,	1869.,	1871.,	1942.,
1856.,	1857.,	1859.,	1860.,	1862.,	1863.,	$M= .40
1865.,	1866.,	1868.,	1869.,	1871.,	1942.,
2151.,	2153.,	2154.,	2156.,	2158.,	2160.,	$M= .60
2162.,	2163.,	2165.,	2222.,	2314.,	2406.,
2249.,	2250.,	2252.,	2253.,	2254.,	2255.,	$M= .80
2257.,	2371.,	2577.,	2827.,	2941.,	3055.,
2269.,	2269.,	2269.,	2269.,	2269.,	2269.,	$M= .85
2291.,	2543.,	2782.,	3022.,	3141.,	3261.,
2296.,	2296.,	2296.,	2296.,	2296.,	2296.,	$M= .90
2296.,	2736.,	2987.,	3239.,	3364.,	3490.,
2331.,	2330.,	2329.,	2328.,	2327.,	2386.,	$M= .95
2660.,	2934.,	3197.,	3460.,	3592.,	3723.,
2353.,	2353.,	2353.,	2354.,	2354.,	2581.,	$M=1.00
2862.,	3141.,	3414.,	3688.,	3824.,	3961.,

...
...   F-15 MAX A/B (FN WITH SFC AND FG -- 100%)
...

      INDTO5= 1,
      ITO5X= 13,
      ITO5Y= 22,
      TTABO5=   0.,   5000., 10000., 15000., 20000., 25000.,
               30000., 35000., 40000., 45000., 50000., 55000.,
               60000.,
               0.00, .20, .40, .50, .60, .70, .80, .90,1.00,1.10,
               1.20,1.30,1.40,1.50,1.60,1.80,1.90,2.00,2.20,2.30,
               2.40,2.50,

18790.,	16430.,	14070.,	11670.,	9755.,	7901.,	$M=0.00
6211.,	5057.,	4072.,	3455.,	2812.,	2530.,
1731.,
20350.,	18100.,	15600.,	12930.,	10730.,	8884.,	$M= .20
6775.,	5057.,	4072.,	3455.,	2812.,	2530.,
1731.,
21670.,	19150.,	16800.,	14290.,	11770.,	9744.,	$M= .40

7870..,	5714..,	4553..,	3455..,	2512..,	2530..,	
1731..,						
22680..,	19840..,	17630..,	15230..,	12570..,	10360..,	$M= .50
8486..,	6155..,	4899..,	3694..,	2812..,	2530..,	
1731.,						
23720..,	20870..,	18450..,	16110..,	13020..,	11170..,	$M= .60
9186..,	6771..,	5354..,	4064..,	3084..,	2530..,	
1731.,						
24610..,	22170..,	19330..,	17060..,	14610..,	12100..,	$M= .70
9973..,	7522..,	6016..,	4486..,	3367..,	2530..,	
1731.,						
25940..,	23260..,	20510..,	18020..,	15800..,	13380..,	$M= .80
10940..,	8452..,	6756..,	5012..,	3793..,	2851..,	
1940.,						
27330..,	24690..,	22010..,	19170..,	16800..,	14500..,	$M= .90
12140..,	9411..,	7715..,	5792..,	4300..,	3205..,	
2241.,						
28370..,	25850..,	23240..,	20470..,	17870..,	15480..,	$M=1.00
13070..,	10400..,	8626..,	6541..,	4699..,	3425..,	
2396.,						
29580..,	26360..,	24250..,	21620..,	18900..,	16400..,	$M=1.10
14050..,	11290..,	9283..,	7109..,	4998..,	3646..,	
2537.,						
31660..,	28590..,	25920..,	23200..,	20320..,	17890..,	$M=1.20
15310..,	12420..,	10140..,	7786..,	5747..,	4058..,	
2838.,						
33330..,	30500..,	27520..,	24870..,	22070..,	19270..,	$M=1.30
16710..,	13640..,	11090..,	8541..,	6453..,	4595..,	
3132.,						
31730..,	33020..,	30070..,	26700..,	23740..,	20770..,	$M=1.40
18060..,	15070..,	12160..,	9335..,	7030..,	5012..,	
3462.,						
31730..,	34440..,	32880..,	29120..,	25650..,	22540..,	$M=1.50
19760..,	16320..,	13230..,	10090..,	7658..,	5559..,	
3826.,						
31730..,	34440..,	35310..,	32010..,	28240..,	24690..,	$M=1.60
21320..,	17630..,	14210..,	10880..,	8325..,	6156..,	
4214.,						
31730..,	34440..,	35310..,	34420..,	32670..,	29020..,	$M=1.80
25120..,	20550..,	16800..,	12810..,	9684..,	7216..,	
5231.,						
31730..,	34440..,	35310..,	35900..,	33330..,	30490..,	$M=1.90
26760..,	21980..,	18050..,	13730..,	10440..,	7799..,	
5742.,						
31730..,	34440..,	35310..,	35900..,	34430..,	31250..,	$M=2.00
28040..,	23350..,	19090..,	14620..,	11160..,	8442..,	
6229..,						
31730..,	34440..,	35310..,	35900..,	34430..,	32110..,	$M=2.20
29810..,	25200..,	20730..,	16140..,	12510..,	9675..,	
7248.,						
31730..,	34440..,	35310..,	35900..,	34430..,	30360..,	$M=2.30
29860..,	25840..,	21480..,	16710..,	12980..,	9944..,	
7455.,						
31730..,	34440..,	35310..,	35900..,	34430..,	30360..,	$M=2.40
29020..,	26110..,	21720..,	17050..,	13240..,	10060..,	
7488.,						
31730..,	34440..,	35310..,	35900..,	34430..,	30360..,	$M=2.50
29020..,	25650..,	21550..,	16940..,	13050..,	9956..,	
7474.,						

INOTO6= 1,
ITO6X= 13,
ITO6Y= 22,
TTAB06=   0.., 5000.., 10000.., 15000.., 20000.., 25000..,
30000.., 36090.., 40000.., 45000.., 50000.., 55000..,
60000..,
       0.00, .20, .40, .50, .60, .70, .80, .90,1.00,1.10,

```
1.20,1.30,1.40,...,...,1.80,1...,...,...,...,
2.40,2.50,
```

2.356,	2.284,	2.201,	2.153,	2.099,	2.042,	SM=0.00
1.955,	1.897,	1.806,	1.836,	1.895,	1.936,	
2.143,						
2.403,	2.312,	2.247,	2.172,	2.174,	2.080,	SM= .20
1.993,	1.897,	1.806,	1.836,	1.895,	1.936,	
2.143,						
2.450,	2.388,	2.314,	2.227,	2.174,	2.122,	SM= .40
2.056,	1.951,	1.905,	1.836,	1.895,	1.936,	
2.143,						
2.466,	2.420,	2.331,	2.251,	2.175,	2.135,	SM= .50
2.083,	1.979,	1.952,	1.849,	1.895,	1.936,	
2.143,						
2.488,	2.435,	2.359,	2.281,	2.186,	2.141,	SM= .60
2.084,	1.991,	1.989,	1.900,	1.869,	1.936,	
2.143,						
2.521,	2.442,	2.386,	2.302,	2.219,	2.140,	SM= .70
2.090,	2.013,	1.980,	1.952,	1.859,	1.936,	
2.143,						
2.543,	2.468,	2.409,	2.326,	2.237,	2.145,	SM= .80
2.094,	2.034,	1.992,	1.992,	1.910,	1.891,	
2.074,						
2.574,	2.484,	2.414,	2.348,	2.263,	2.173,	SM= .90
2.091,	2.030,	2.016,	1.973,	1.962,	1.874,	
1.986,						
2.636,	2.536,	2.446,	2.381,	2.290,	2.205,	SM=1.00
2.114,	2.038,	2.025,	2.003,	2.021,	1.948,	
1.987,						
2.679,	2.597,	2.520,	2.437,	2.362,	2.263,	SM=1.10
2.169,	2.071,	2.063,	2.064,	2.105,	2.052,	
2.030,						
2.708,	2.634,	2.544,	2.468,	2.401,	2.287,	SM=1.20
2.196,	2.070,	2.070,	2.074,	2.074,	2.098,	
2.057,						
2.779,	2.696,	2.600,	2.501,	2.412,	2.320,	SM=1.30
2.218,	2.097,	2.071,	2.071,	2.087,	2.061,	
2.086,						
2.900,	2.736,	2.626,	2.544,	2.440,	2.370,	SM=1.40
2.257,	2.116,	2.084,	2.080,	2.102,	2.087,	
2.109,						
2.900,	2.679,	2.624,	2.549,	2.473,	2.380,	SM=1.50
2.279,	2.154,	2.125,	2.106,	2.122,	2.126,	
2.137,						
2.900,	2.679,	2.569,	2.547,	2.464,	2.391,	SM=1.60
2.320,	2.209,	2.187,	2.147,	2.154,	2.198,	
2.204,						
2.900,	2.679,	2.569,	2.585,	2.495,	2.434,	SM=1.80
2.364,	2.310,	2.232,	2.253,	2.243,	2.285,	
2.328,						
2.900,	2.679,	2.569,	2.542,	2.550,	2.462,	SM=1.90
2.402,	2.339,	2.332,	2.306,	2.271,	2.304,	
2.365,						
2.900,	2.679,	2.569,	2.542,	2.535,	2.533,	SM=2.00
2.451,	2.378,	2.389,	2.378,	2.341,	2.329,	
2.389,						
2.900,	2.679,	2.569,	2.542,	2.535,	2.625,	SM=2.20
2.593,	2.513,	2.522,	2.534,	2.516,	2.468,	
2.457,						
2.900,	2.679,	2.569,	2.542,	2.535,	2.781,	SM=2.30
2.676,	2.602,	2.606,	2.612,	2.627,	2.588,	
2.570,						
2.900,	2.679,	2.569,	2.542,	2.535,	2.781,	SM=2.40
2.759,	2.713,	2.706,	2.707,	2.722,	2.729,	
2.722,						
2.900,	2.679,	2.569,	2.542,	2.535,	2.781,	SM=2.50

```
                          2.759,    2.855,    2.819,    2.825,    2.850,    2.886,
                          2.889,
              INDT13= 1,
              IT13X= 13,
              IT13Y= 22,
              TTAB13=  0.,     5000.,   10000.,   15000.,   20000.,   25000.,
                       30000.,  36090.,  40000.,   45000.,   50000.,   55000.,
                       60000.,
                      0.00,  .20,  .40,  .50,  .60,  .70,  .80,  .90,1.00,1.10,
                      1.20,1.30,1.40,1.50,1.60,1.80,1.90,2.00,2.20,2.30,
                      2.40,2.50,
              18790.,   16430.,   14070.,   11670.,    9755.,    7961., $M=0.00
               6211.,    5404.,    4359.,    3957.,    3335.,    3199.,
               2248.,
              21850.,   19370.,   16680.,   13810.,   11450.,    9462., $M= .20
               7437.,    5404.,    4359.,    3957.,    3335.,    3199.,
               2248.,
              24960.,   21930.,   19160.,   16260.,   13360.,   11030., $M= .40
               8897.,    6486.,    5197.,    3957.,    3335.,    3199.,
               2248.,
              27030.,   23510.,   20730.,   17840.,   14690.,   12080., $M= .50
               9855.,    7183.,    5750.,    4362.,    3335.,    3199.,
               2248.,
              29250.,   25560.,   22390.,   19440.,   16370.,   13390., $M= .60
              10950.,    8098.,    6453.,    4927.,    3761.,    3199.,
               2248.,
              31450.,   28000.,   24220.,   21170.,   18030.,   14940., $M= .70
              12190.,    9190.,    7398.,    5573.,    4220.,    3199.,
               2248.,
              34300.,   30380.,   26510.,   23040.,   19990.,   16830., $M= .80
              13700.,   10520.,    8470.,    6362.,    4853.,    3684.,
               2579.,
              37500.,   33340.,   29310.,   25250.,   21860.,   18690., $M= .90
              15530.,   11960.,    9828.,    7455.,    5612.,    4233.,
               3033.,
              40620.,   36290.,   32010.,   27780.,   23920.,   20440., $M=1.00
              17130.,   13480.,   11180.,    8552.,    6276.,    4658.,
               3354.,
              42570.,   38270.,   34330.,   30210.,   26090.,   22340., $M=1.10
              18850.,   14960.,   12340.,    9507.,    6929.,    5162.,
               3738.,
              47050.,   41980.,   37550.,   33300.,   28940.,   24940., $M=1.20
              21080.,   16790.,   13760.,   10630.,    7993.,    5847.,
               4233.,
              52440.,   46760.,   41250.,   36600.,   31980.,   27490., $M=1.30
              23460.,   18780.,   15330.,   11860.,    9043.,    6630.,
               4728.,
              54830.,   52520.,   46220.,   40360.,   35220.,   30460., $M=1.40
              25960.,   21070.,   17120.,   13190.,   10030.,    7370.,
               5313.,
              54830.,   57060.,   51720.,   45020.,   38940.,   33580., $M=1.50
              28760.,   23290.,   18980.,   14570.,   11150.,    8301.,
               6021.,
              54830.,   57060.,   57100.,   50450.,   43560.,   37320., $M=1.60
              31750.,   25830.,   20960.,   16130.,   12430.,    9393.,
               6831.,
              54830.,   57060.,   57100.,   59360.,   53110.,   46060., $M=1.80
              39090.,   31420.,   25760.,   19860.,   15250.,   11630.,
               8720.,
              54830.,   57060.,   57100.,   64370.,   56640.,   49930., $M=1.90
              42780.,   34450.,   28290.,   21850.,   16770.,   12790.,
               9685.,
              54830.,   57060.,   57100.,   64370.,   61020.,   53500., $M=2.00
              46540.,   37670.,   30870.,   23870.,   18390.,   14120.,
              10770.,
              54830.,   57060.,   57100.,   64370.,   61020.,   61230., $M=2.20
```

54010.,	44130.,	38350.,	28350.,	22980.,	17100.,	
13080.,						
54830.,	57060.,	57100.,	64370.,	61020.,	63850.,	$M=2.30$
57090.,	47020.,	39450.,	30690.,	23910.,	18460.,	
14100.,						
54830.,	57060.,	57100.,	64370.,	61020.,	63850.,	$M=2.40$
59700.,	50810.,	42040.,	32900.,	25620.,	19080.,	
15000.,						
54830.,	57060.,	57100.,	64370.,	61020.,	63850.,	$M=2.50$
59700.,	53200.,	44040.,	34530.,	26760.,	20620.,	
15790.,						

...

```
     WT=35000.,
     XUSW=608.,
     AMLIM=2.5,
     CLMAX=1.6,
     GLIMIT=9.0,
     NUMENG=2,
     ULIM=2131.,
     XCL=12.,
     ZCL=-2.,
     XNL=-20.,
     ZNL=0.,
20.18.44.UCLP, CA, N1609H5,      0.896KLNS.
```

APPENDIX B

Results From Using the Traditional Equations of Motion

F-15 STOL

TURN RATE VS MACH

CONFIGURATION:

MILITARY POWER AND
MAXIMUM A/B POWER
ANGLE OF ATTACK
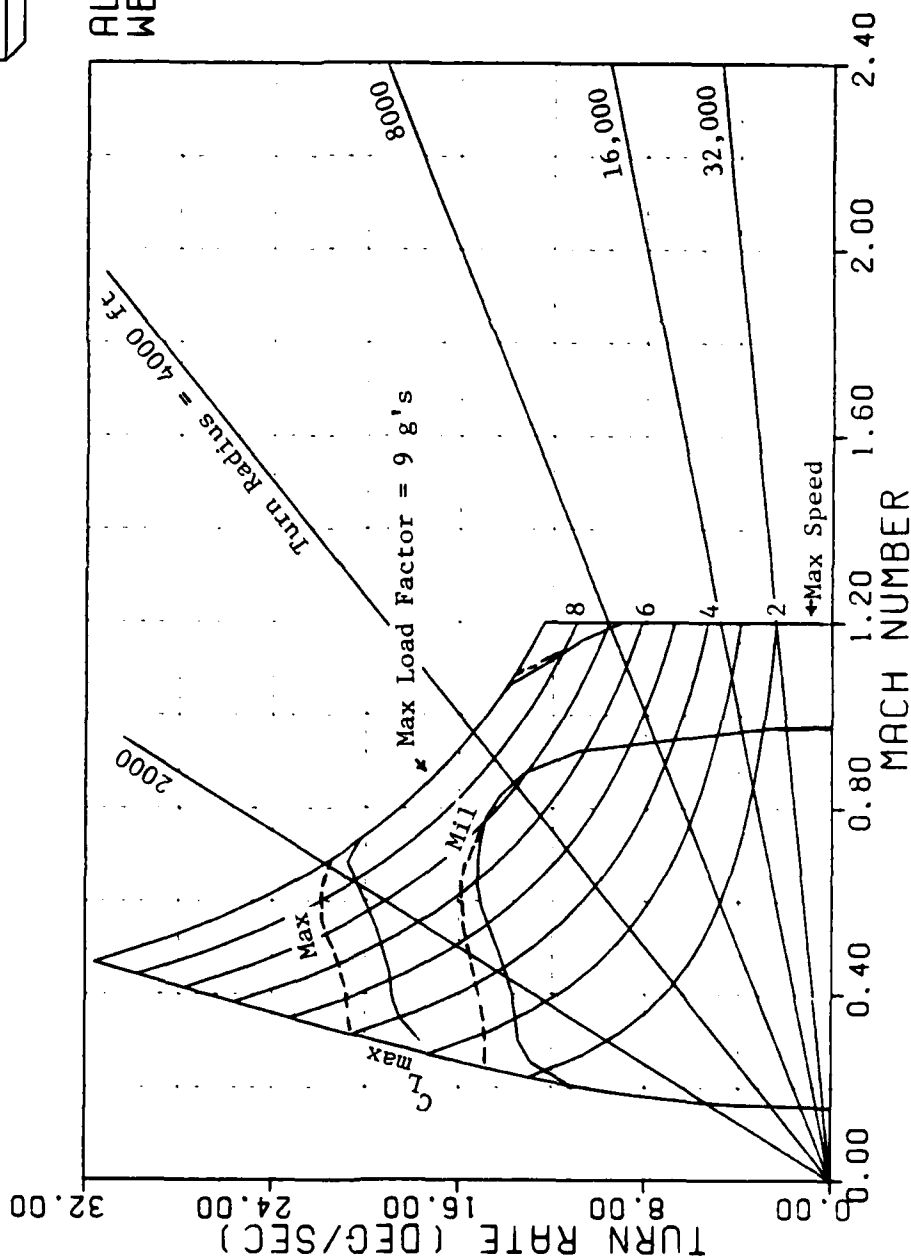AND THRUST VECTOR
ANGLE NEGLECTED

ALT = 0.
WEIGHT=35000.
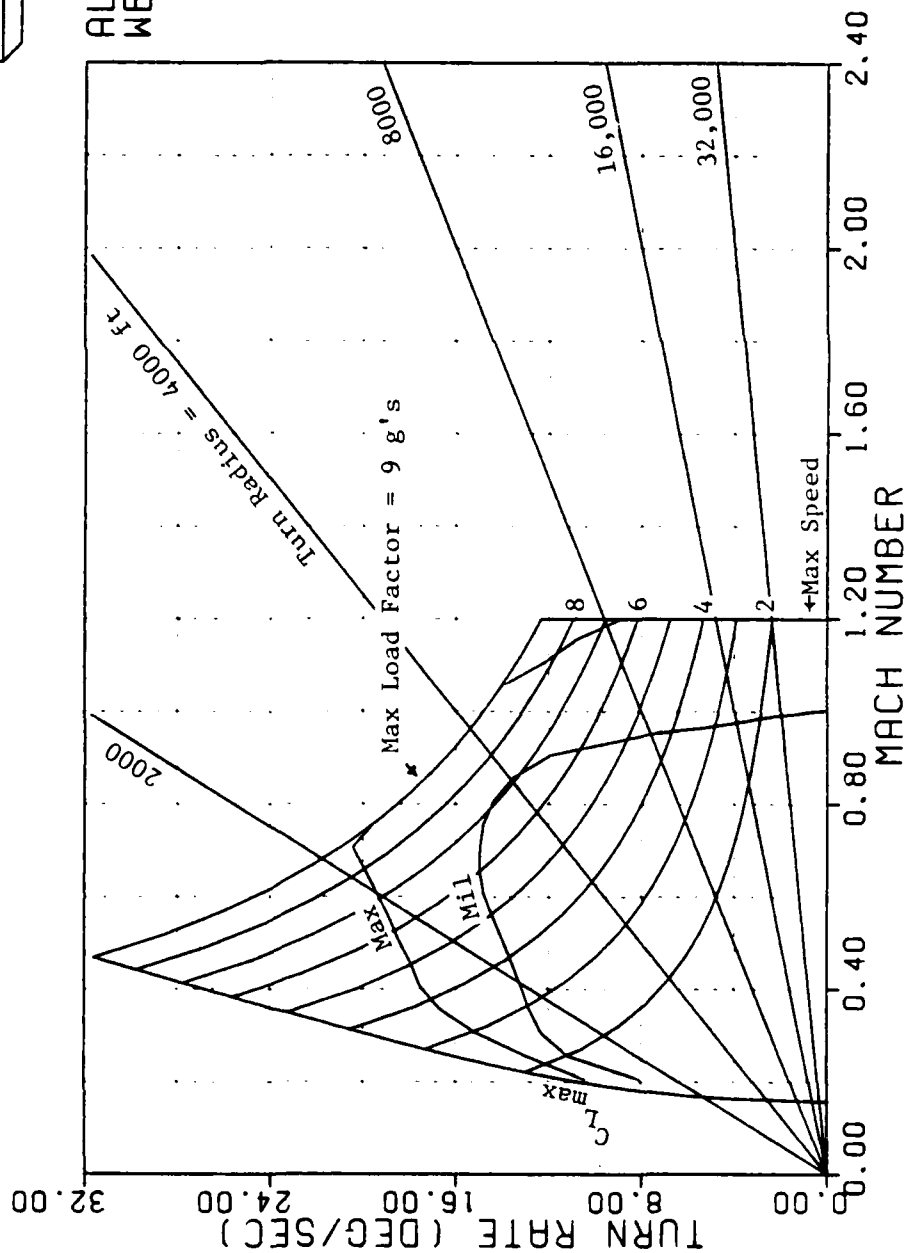
Figure 7 -- Sustained Turn Rate, Sea Level (Case 1)

68

F-15 STOL

TURN RATE VS MACH

CONFIGURATION:

MILITARY POWER AND
MAXIMUM A/B POWER
ANGLE OF ATTACK
AND THRUST VECTOR
ANGLE NEGLECTED

ALT = 10000.
WEIGHT = 35000.
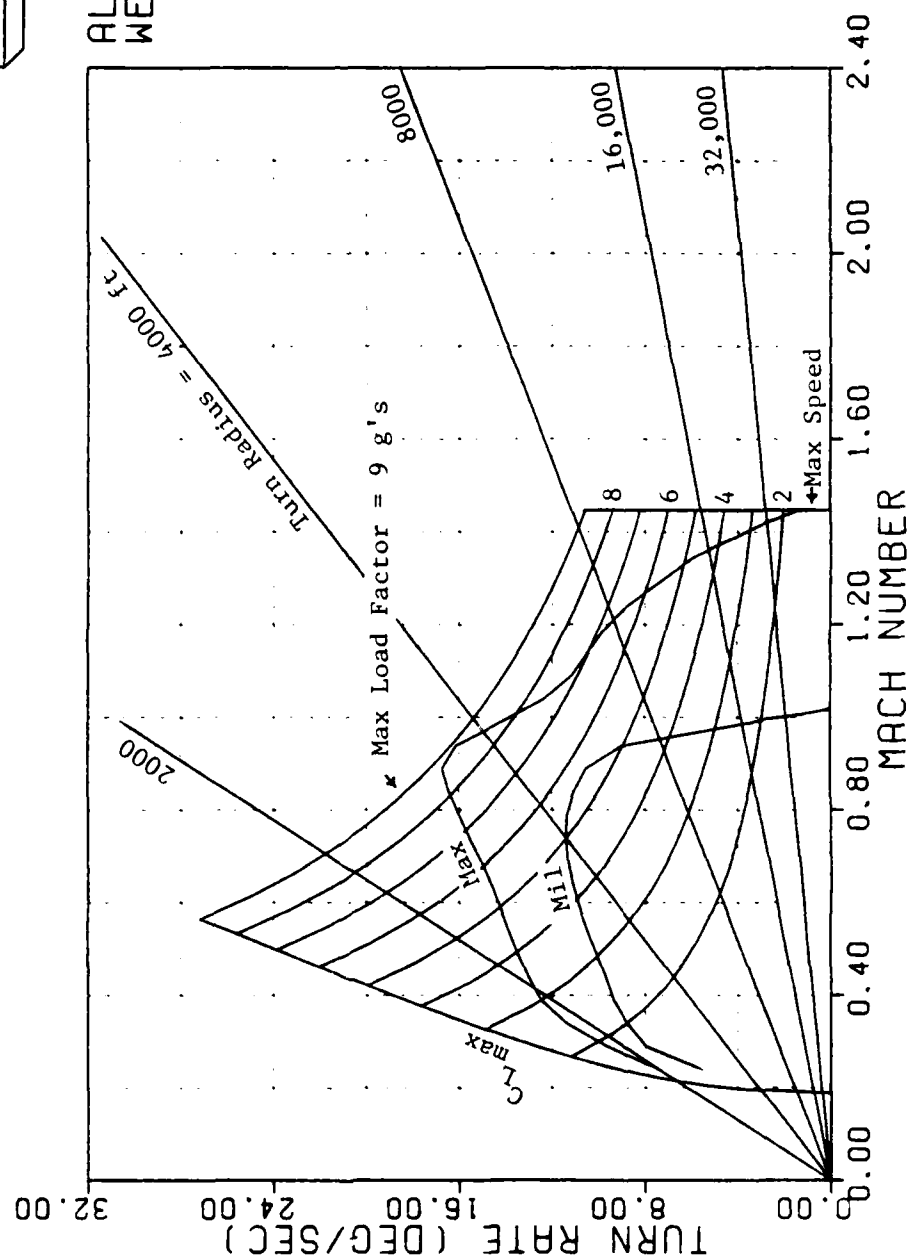
Figure 8 -- Sustained Turn Rate, 10,000 ft (Case 1)

Figure 9 -- Sustained Turn Rate, 20,000 ft (Case 1)

70

Figure 10 -- Sustained Turn Rate, 30,000 ft (Case 1)

71

F-15 STOL
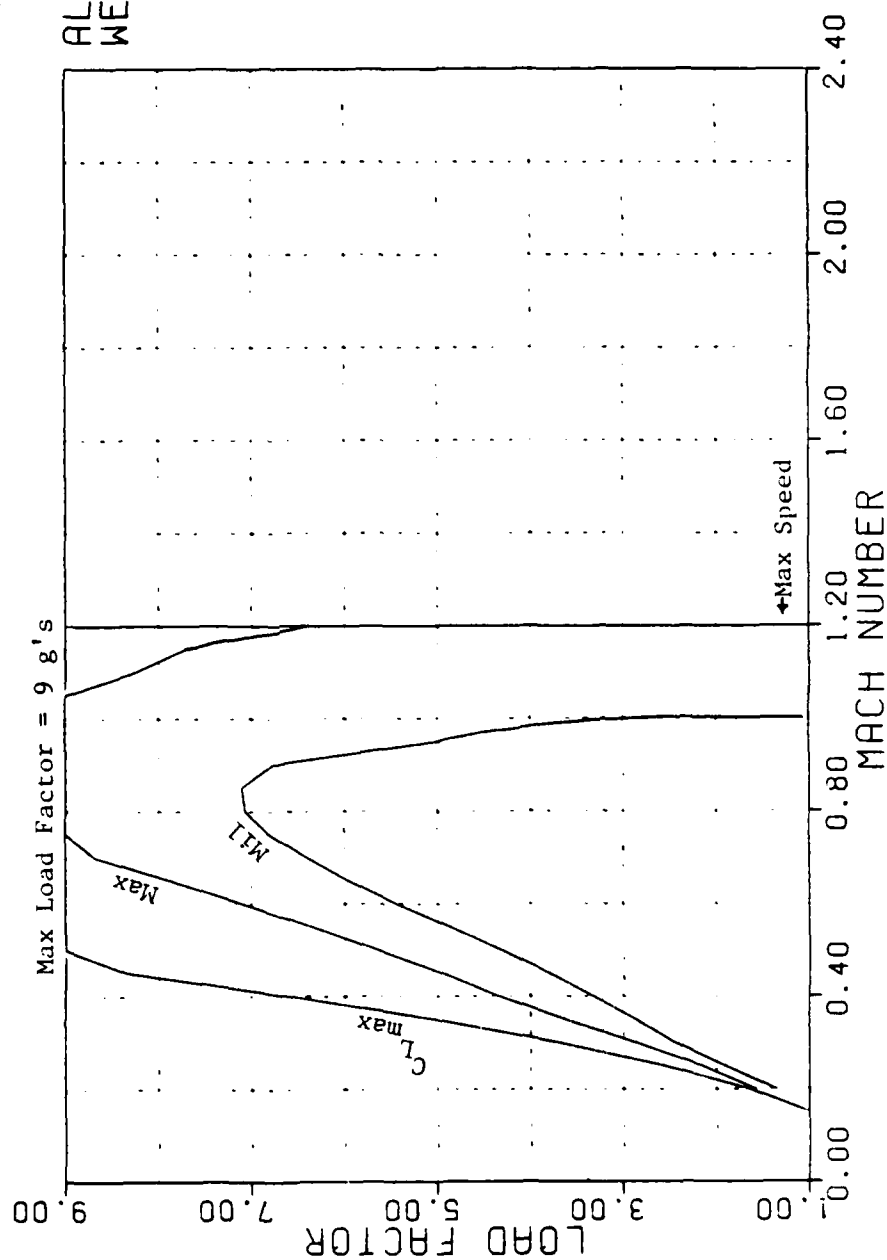
LOAD FACTOR VS MACH

Figure 11 -- Sustained Load Factor, Sea Level (Case 1)
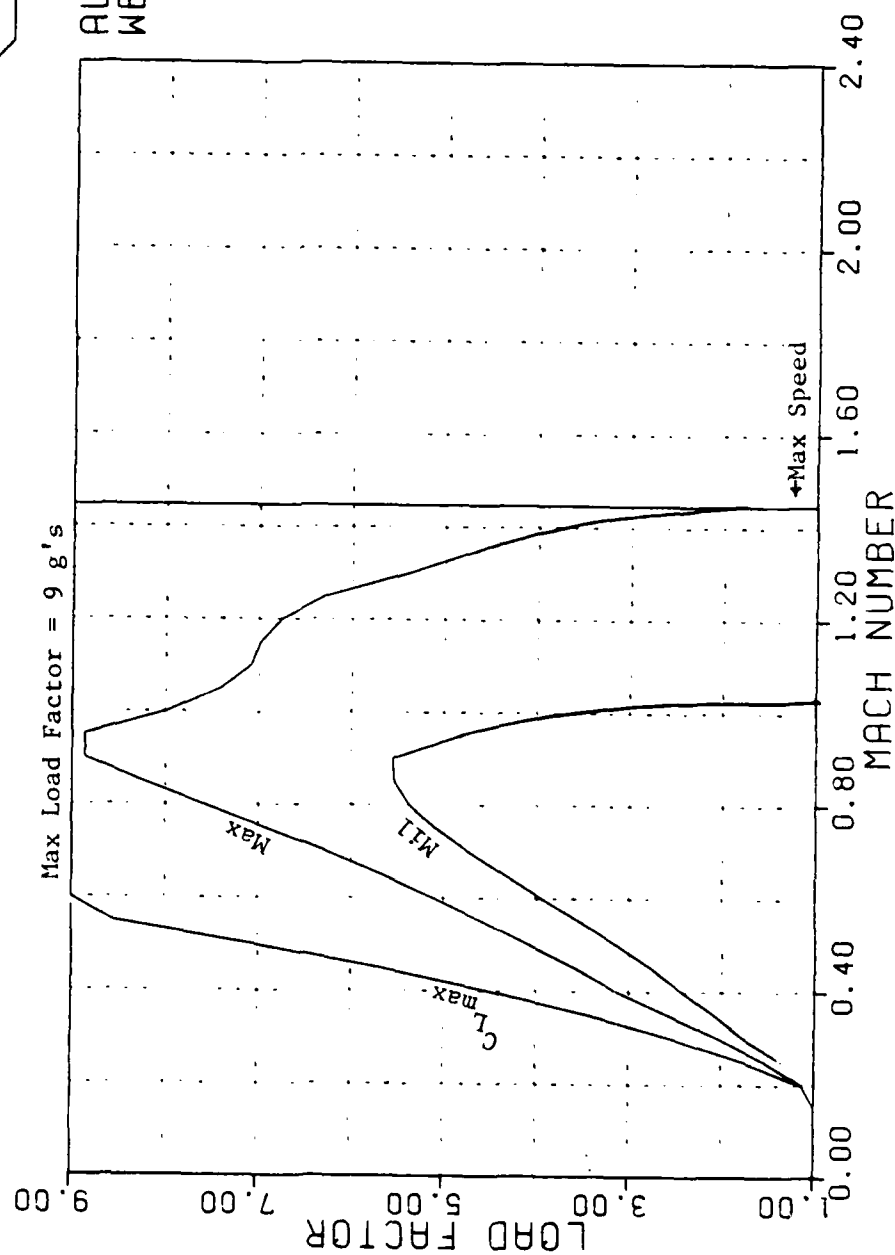
Figure 12 -- Sustained Load Factor, 10,000 ft (Case 1)

73

F-15 STOL

LOAD FACTOR VS MACH

CONFIGURATION:

MILITARY POWER AND
MAXIMUM A/B POWER
ANGLE OF ATTACK
AND THRUST VECTOR
ANGLE NEGLECTED

ALT   =20000.
WEIGHT=35000.

Max Load Factor = 9 g's

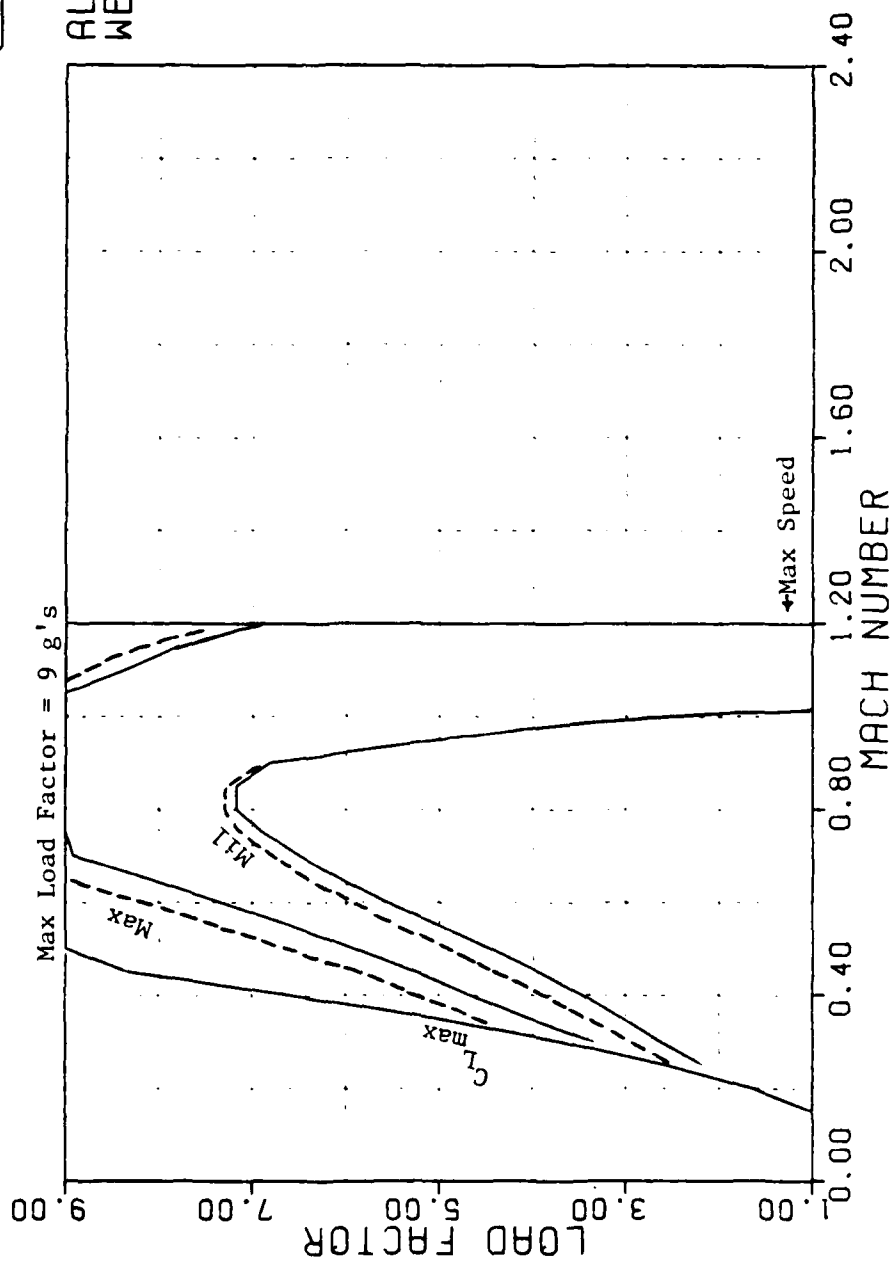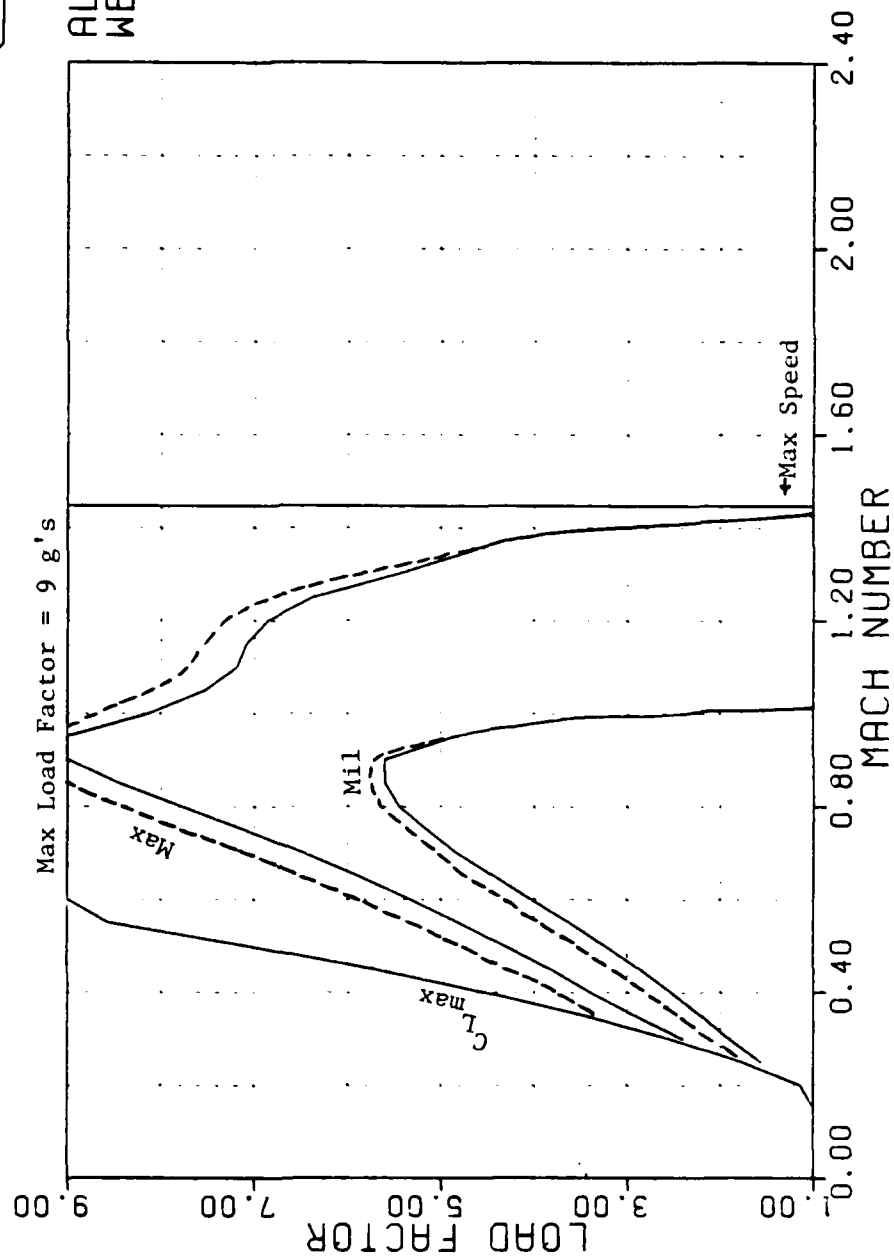$C_{L_{max}}$

Max

Mil

Max Speed

LOAD FACTOR

MACH NUMBER
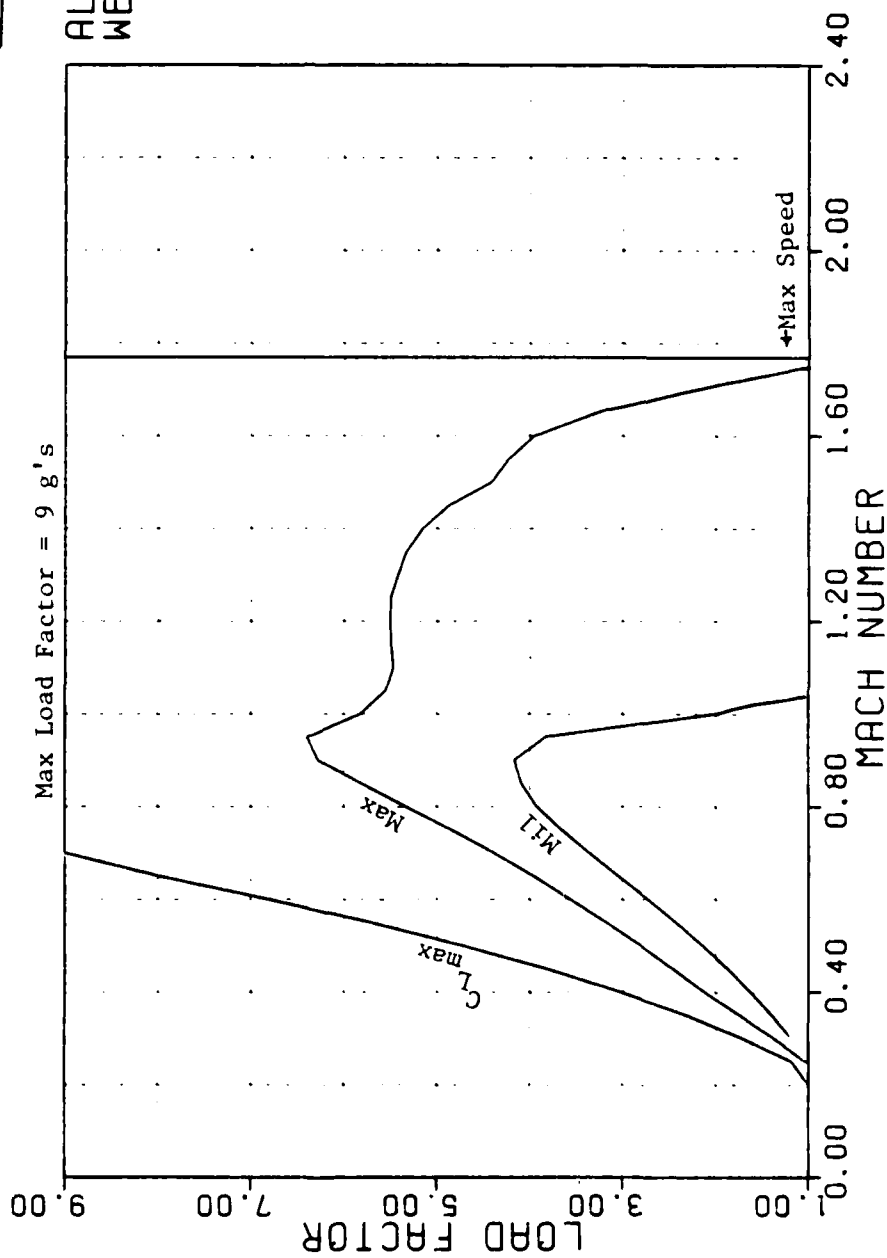
Figure 13 -- Sustained Load Factor, 20,000 ft (Case 1)

74

F-15 STOL

LOAD FACTOR VS MACH

CONFIGURATION:

MILITARY POWER AND
MAXIMUM A/B POWER
ANGLE OF ATTACK
AND THRUST VECTOR
ANGLE NEGLECTED

ALT =30000.
WEIGHT=35000.
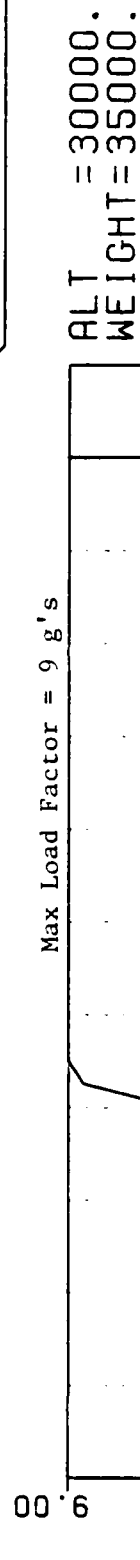
Figure 14 -- Sustained Load Factor, 30,000 ft (Case 1)

75
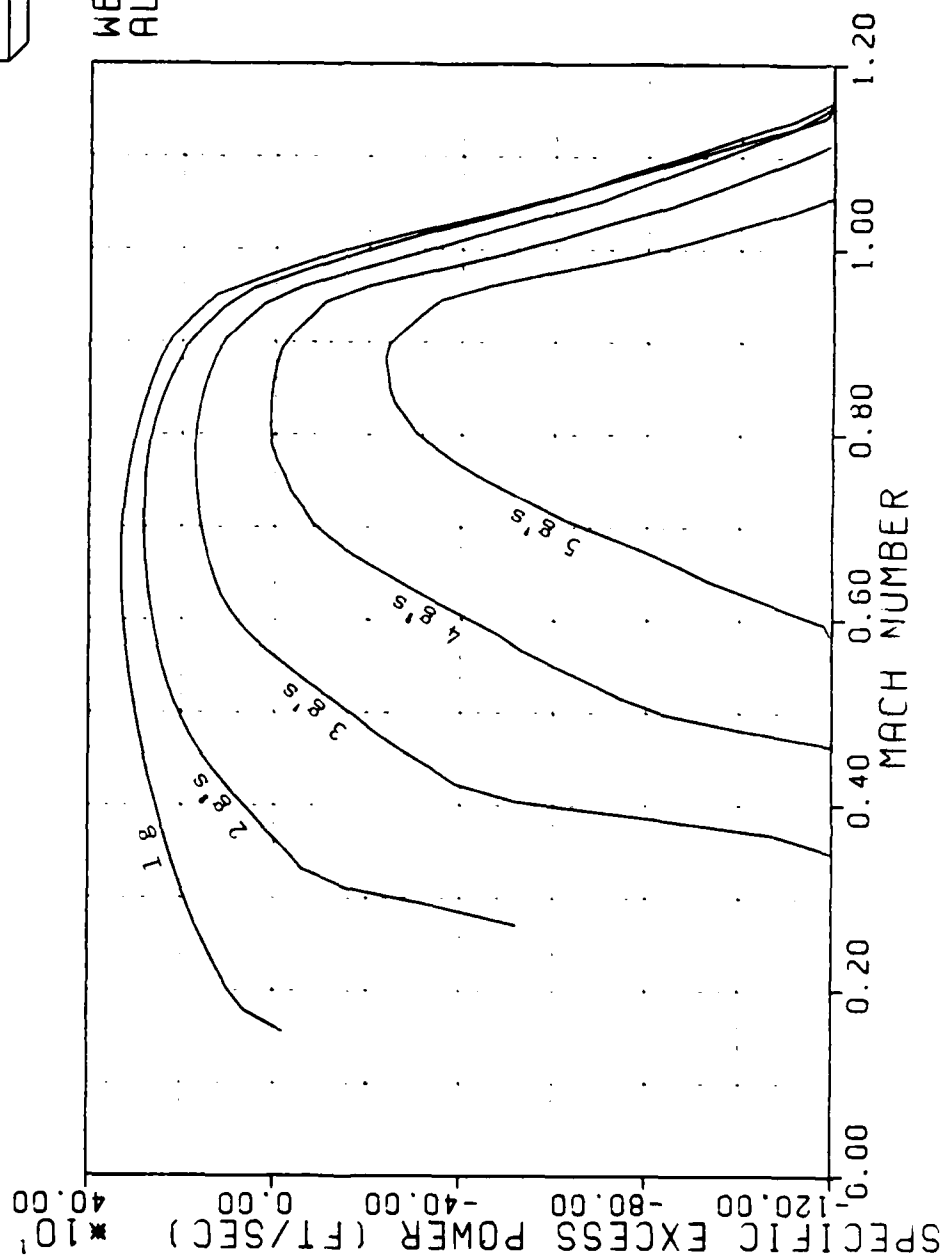
Figure 15 -- Specific Excess Power, Sea Level (Case 1)

76

F-15 STOL

ACCELERATION VS MACH MAP

CONFIGURATION:

MILITARY POWER
ANGLE OF ATTACK
AND THRUST VECTOR
ANGLE NEGLECTED

WEIGHT=35000.
ALT =10000.
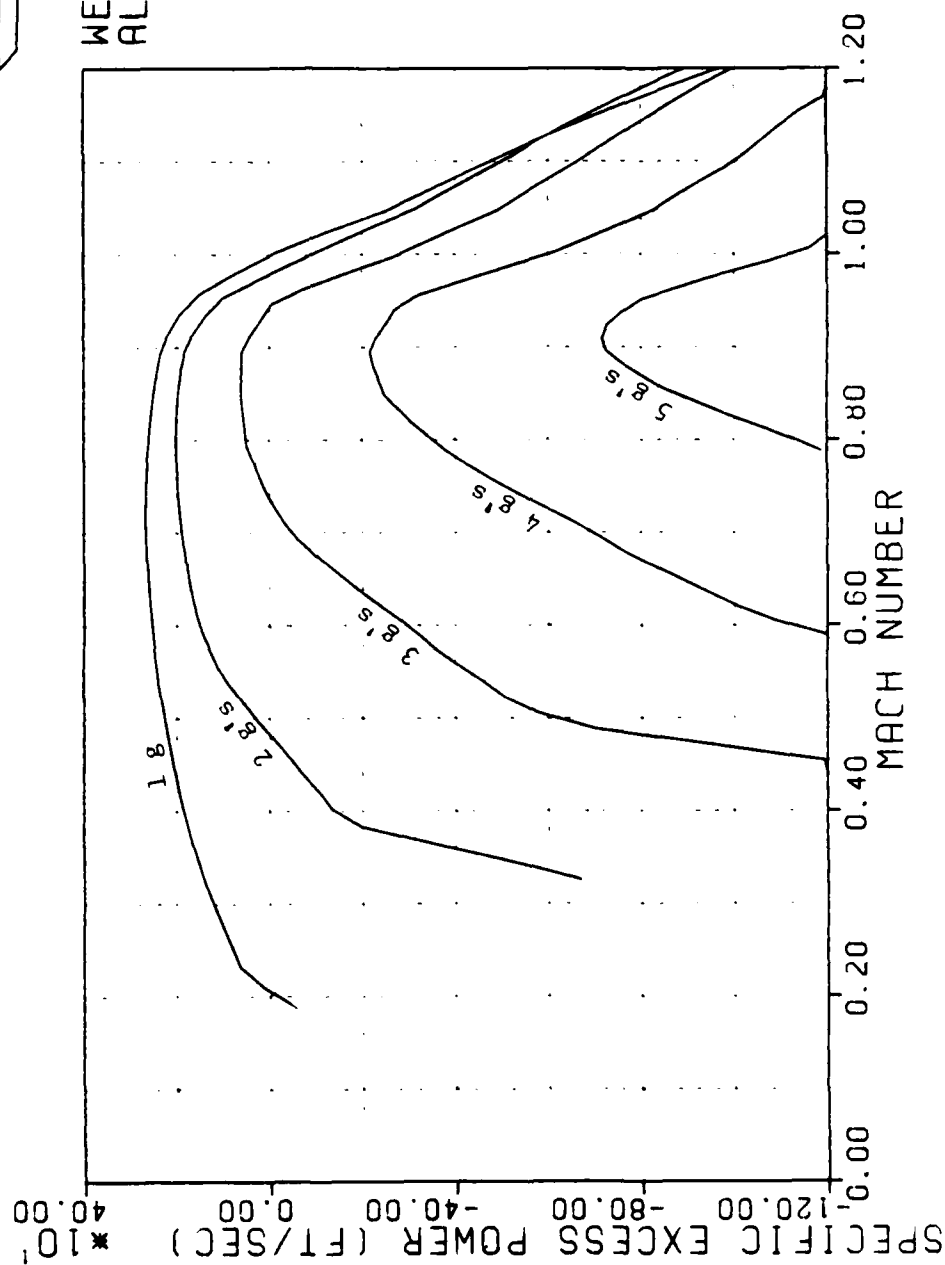
Figure 16 -- Specific Excess Power, 10,000 ft (Case 1)

77

F-15 STOL

ACCELERATION VS MACH MAP

CONFIGURATION:

MILITARY POWER
ANGLE OF ATTACK
AND THRUST VECTOR
ANGLE NEGLECTED

WEIGHT=35000.
ALT =20000.
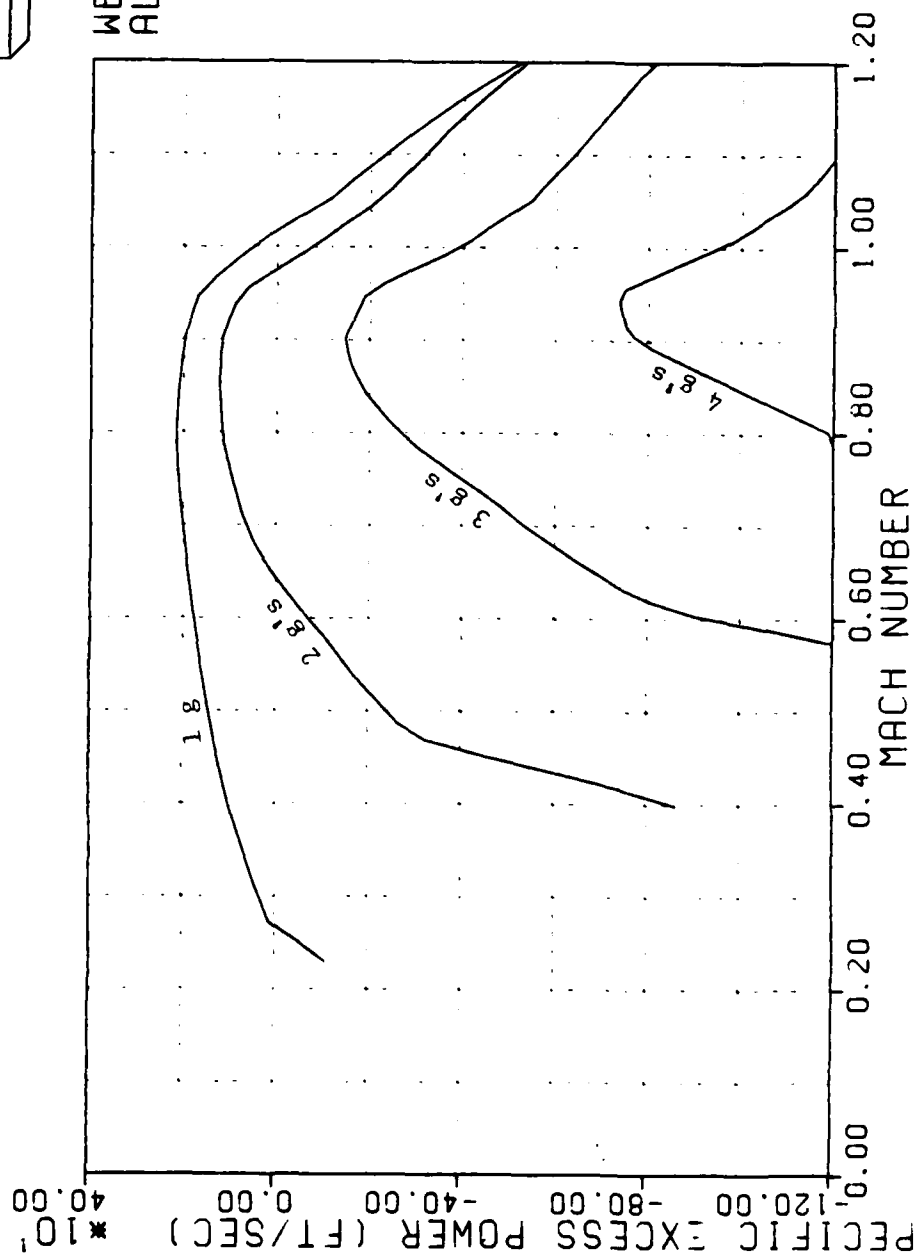
Figure 17 -- Specific Excess Power, 20,000 ft (Case 1)

78

F-15 STOL

ACCELERATION VS MACH MAP

CONFIGURATION:

MILITARY POWER
ANGLE OF ATTACK
AND THRUST VECTOR
ANGLE NEGLECTED

WEIGHT = 35000.
ALT = 30000.
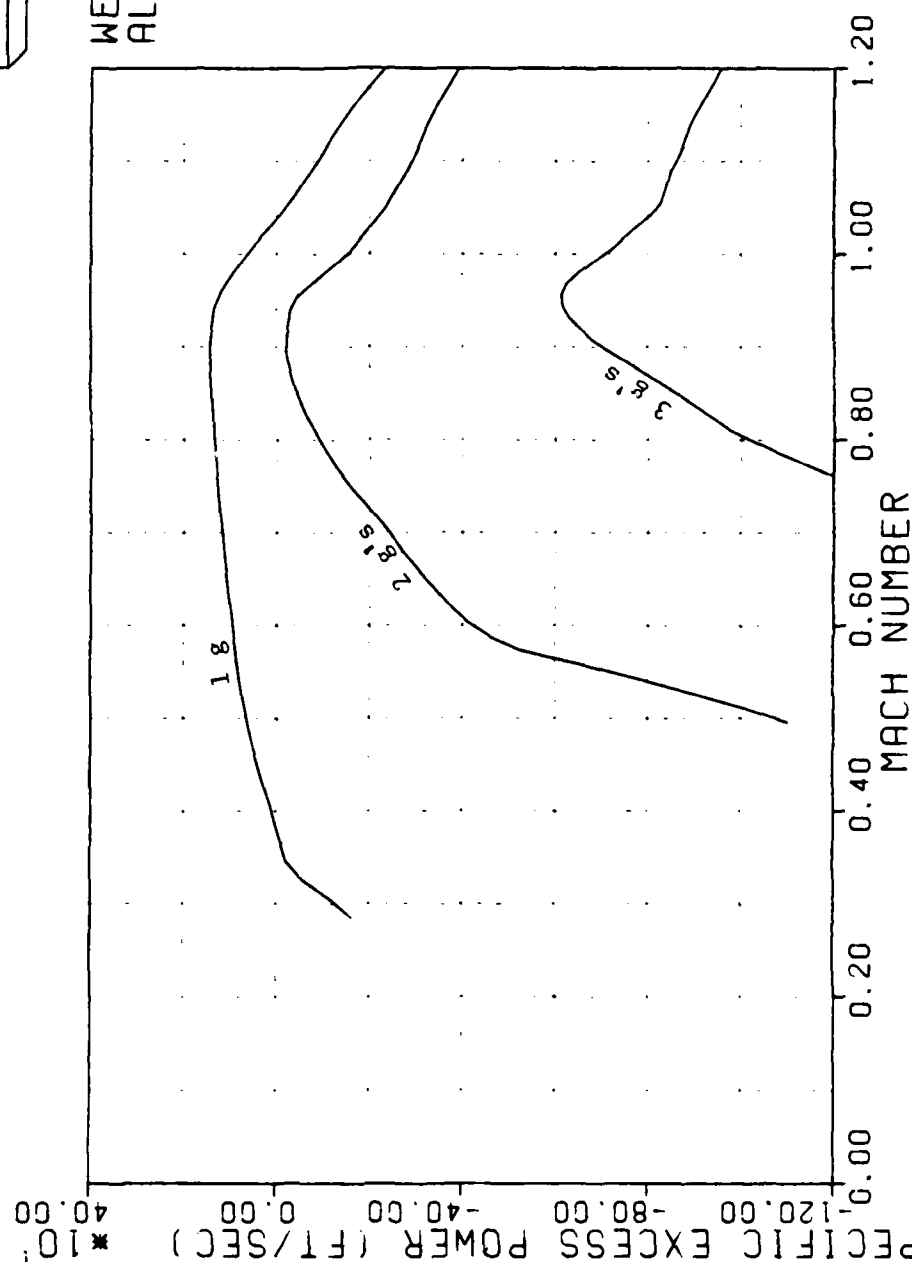
Figure 18 -- Specific Excess Power, 30,000 ft (Case 1)

79
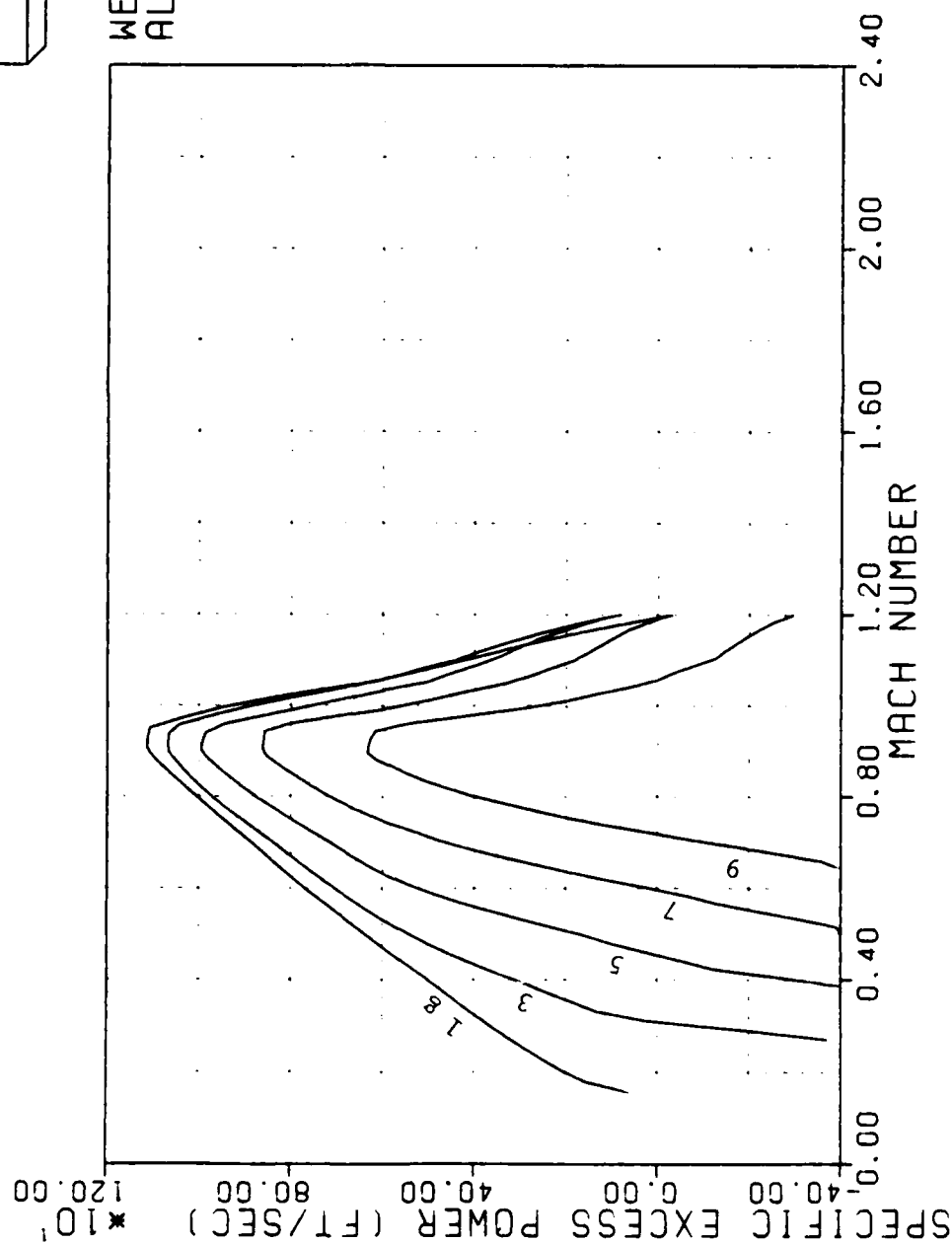
Figure 19 -- Specific Excess Power, Sea Level (Case 1)
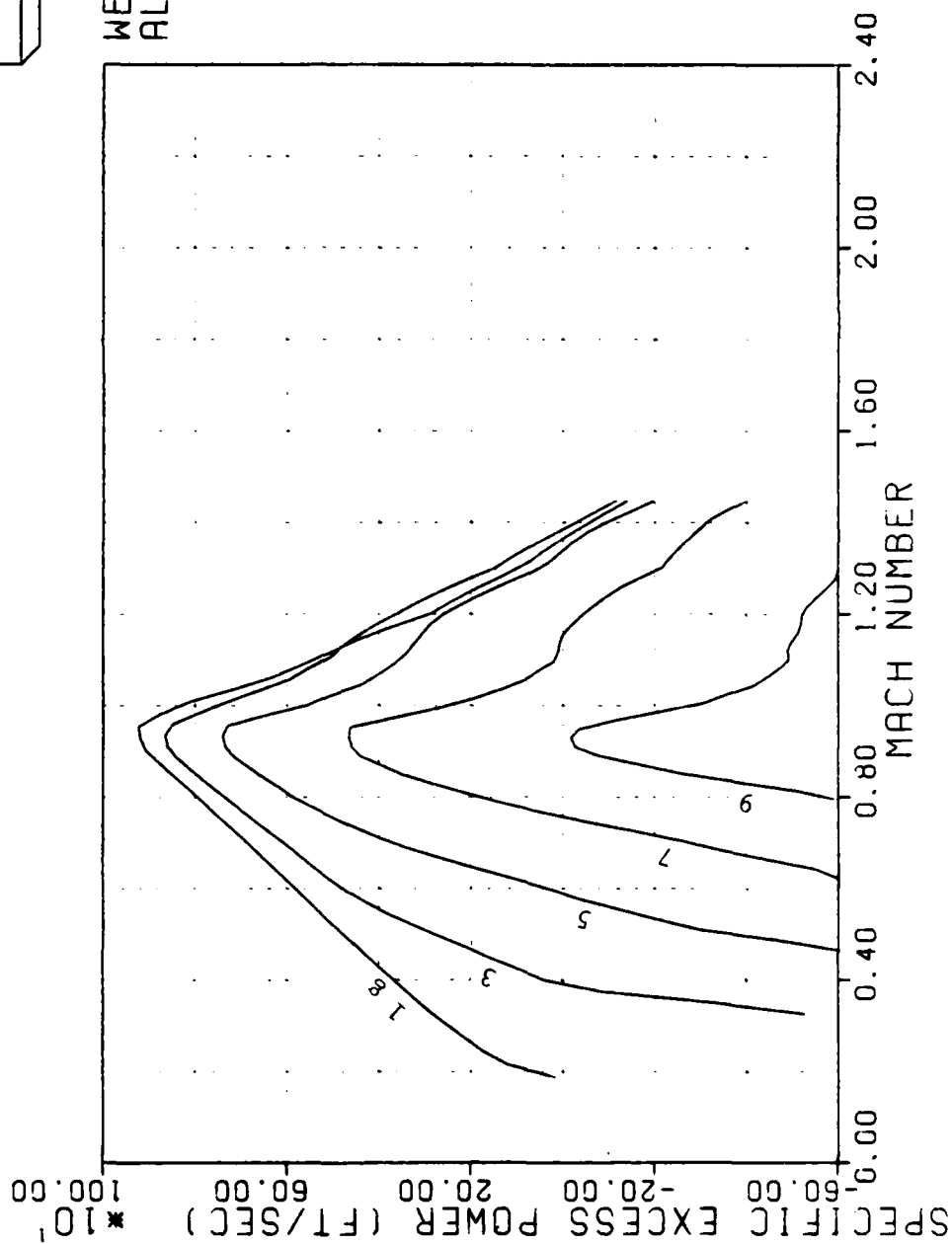
Figure 20 -- Specific Excess Power, 10,000 ft (Case 1)
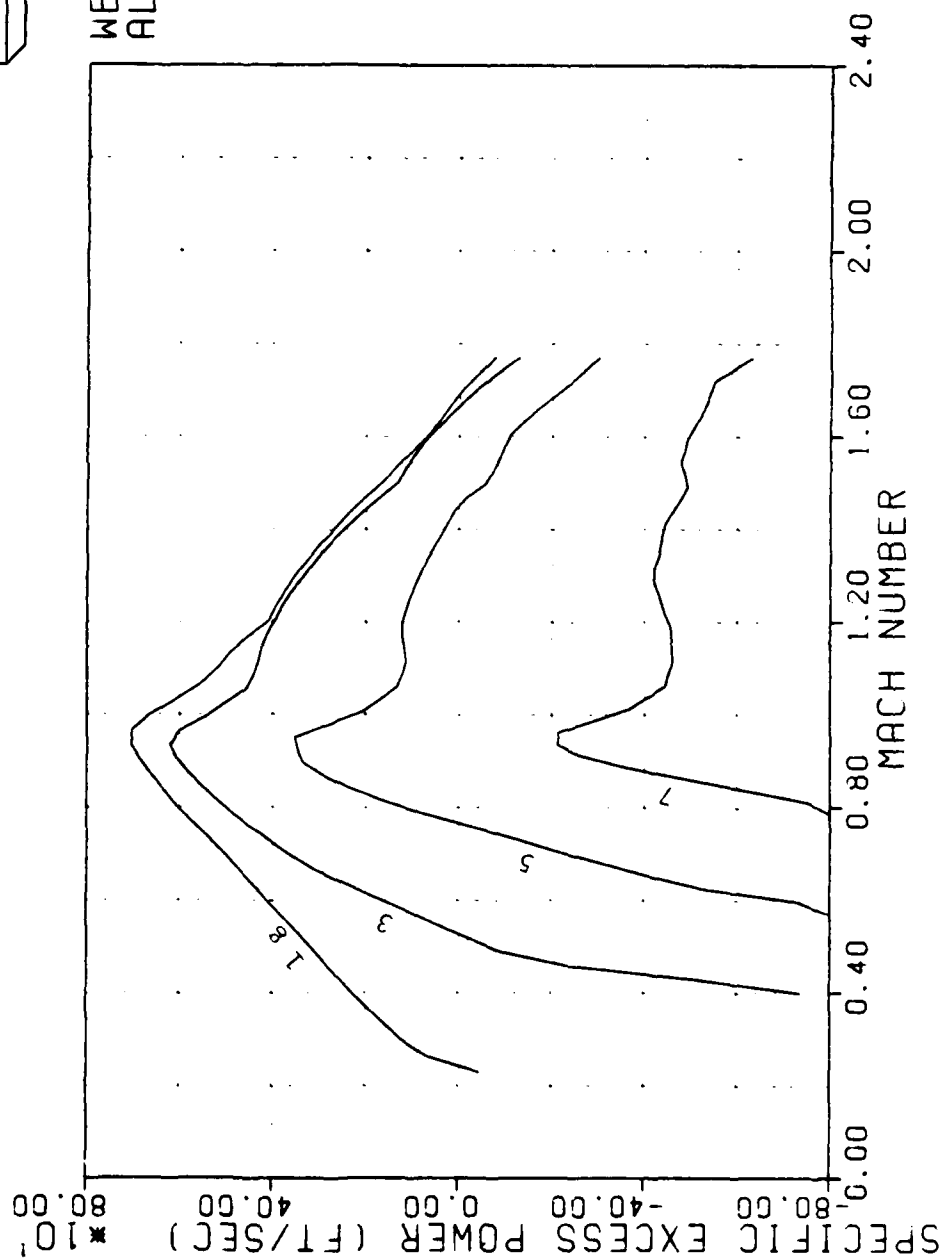
Figure 21 -- Specific Excess Power, 20,000 ft (Case 1)

82

F-15 STOL

ACCELERATION VS MACH MAP

CONFIGURATION:

MAXIMUM A/B POWER
ANGLE OF ATTACK
AND THRUST VECTOR
ANGLE NEGLECTED

WEIGHT=35000.
ALT =30000.
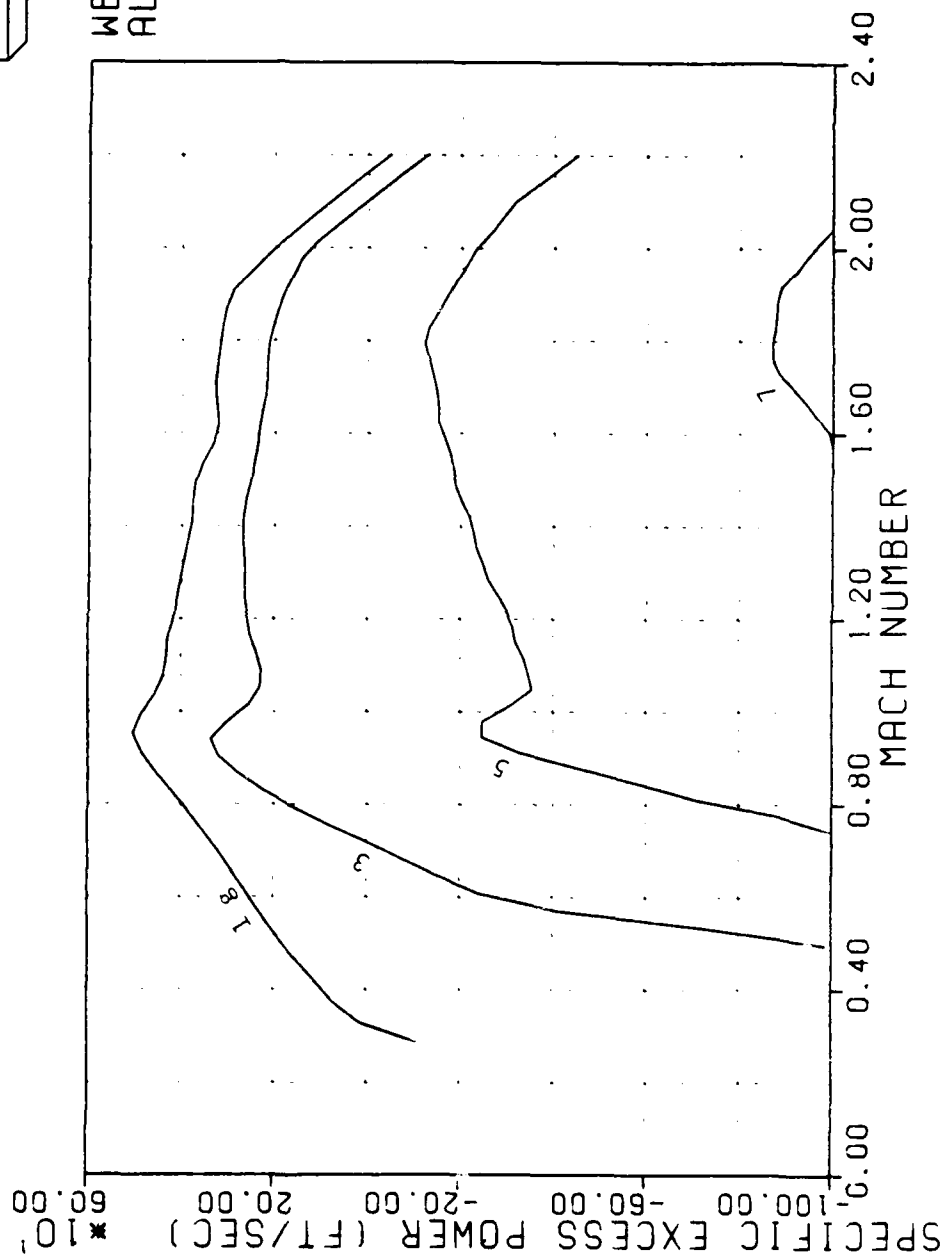
Figure 22 -- Specific Excess Power, 30,000 ft (Case 1)
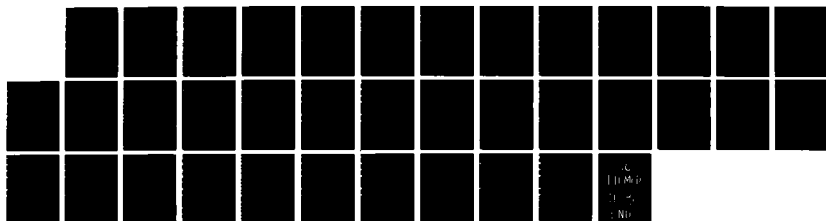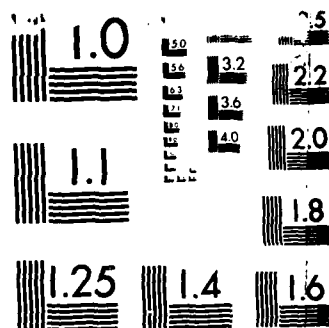
MICROCOPY RESOLUTION TEST CHART
NATIONAL BUREAU OF STANDARDS-1963-A

F-15 STOL

SPEED-POWER MAP

CONFIGURATION:

MILITARY POWER
ANGLE OF ATTACK
AND THRUST VECTOR
ANGLE NEGLECTED

ALT = 0.
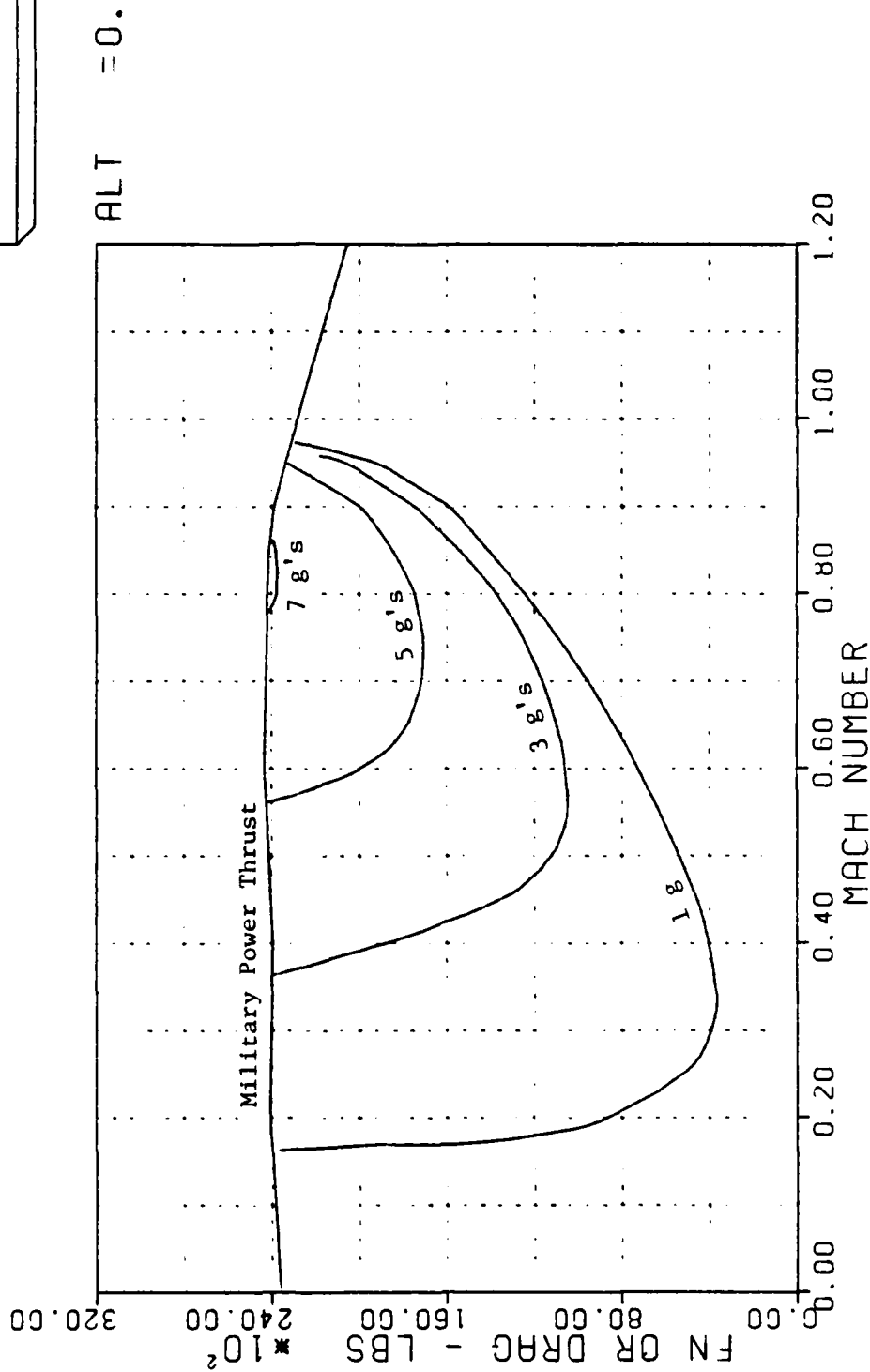
Figure 23 -- Thrust Required, Sea Level (Case 1)

84

F-15 STOL

SPEED-POWER MAP

CONFIGURATION:

MILITARY POWER
ANGLE OF ATTACK
AND THRUST VECTOR
ANGLE NEGLECTED

ALT = 10000.
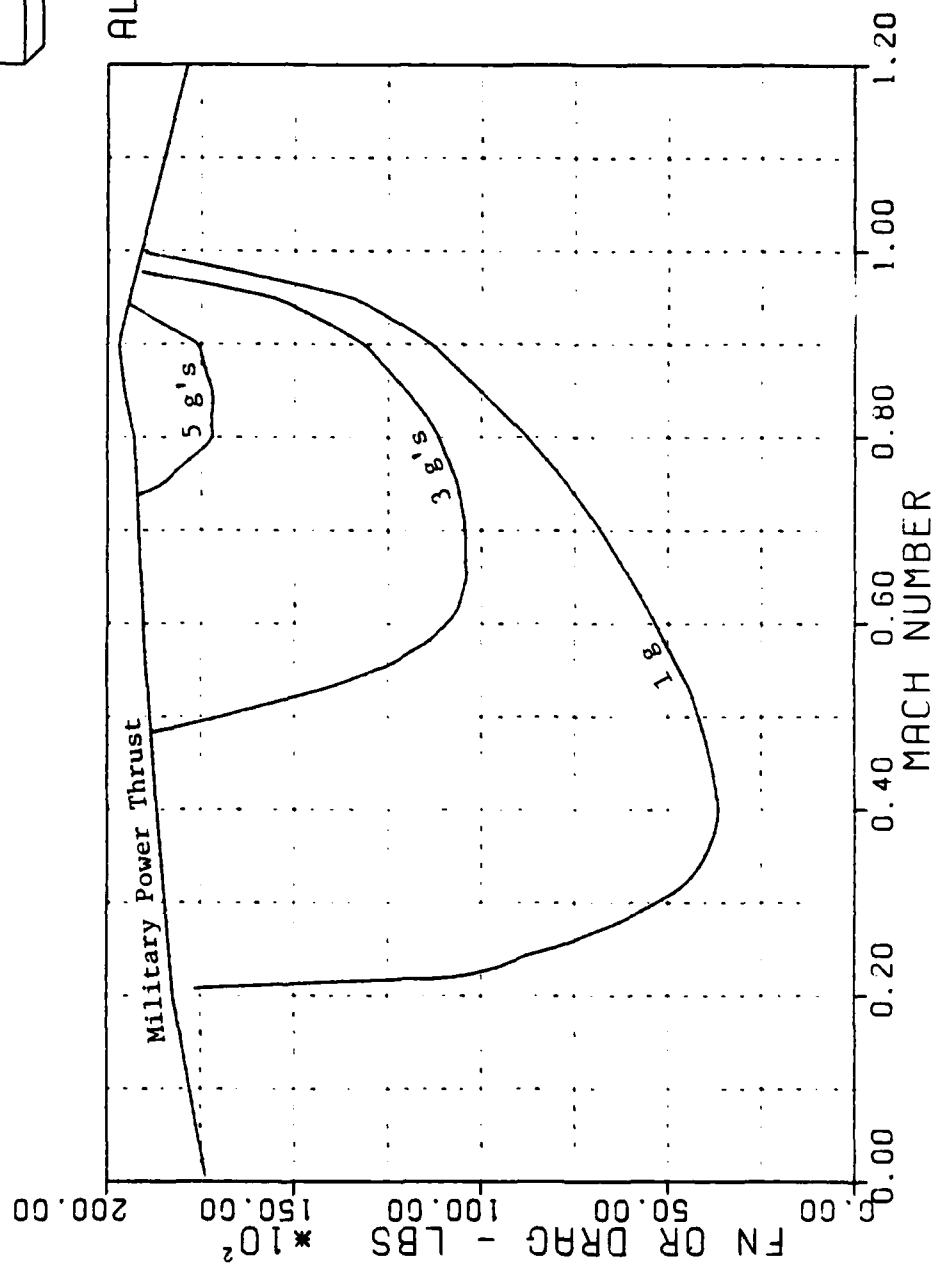
Figure 24 -- Thrust Required, 10,000 ft (Case 1)

F-15 STOL

SPEED-POWER MAP

CONFIGURATION:

MILITARY POWER
ANGLE OF ATTACK
AND THRUST VECTOR
ANGLE NEGLECTED

ALT = 20000.
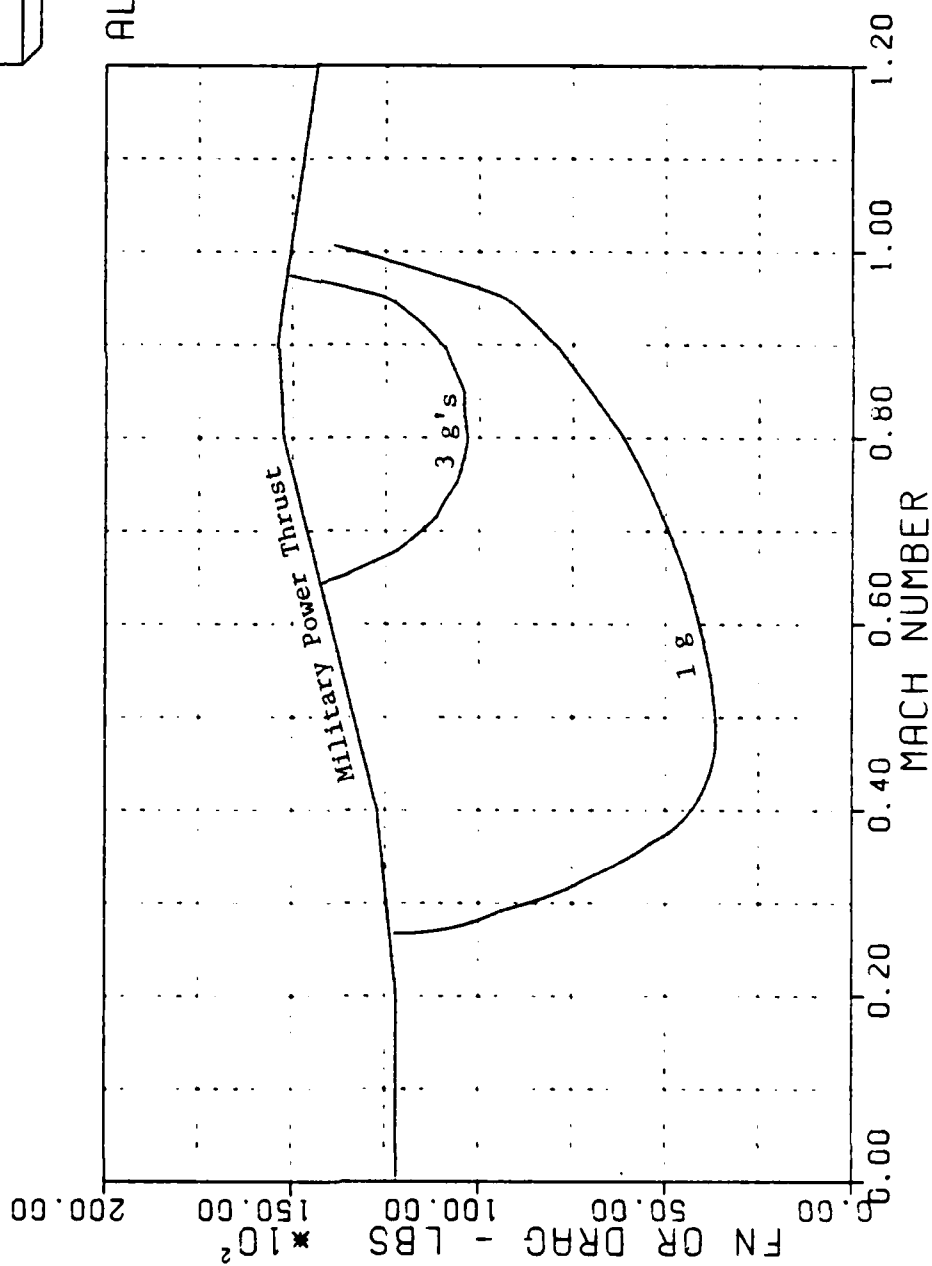
Figure 25 -- Thrust Required, 20,000 ft (Case 1)

86

F-15 STOL

SPEED-POWER MAP

CONFIGURATION:

MILITARY POWER
ANGLE OF ATTACK
AND THRUST VECTOR
ANGLE NEGLECTED

ALT = 30000.
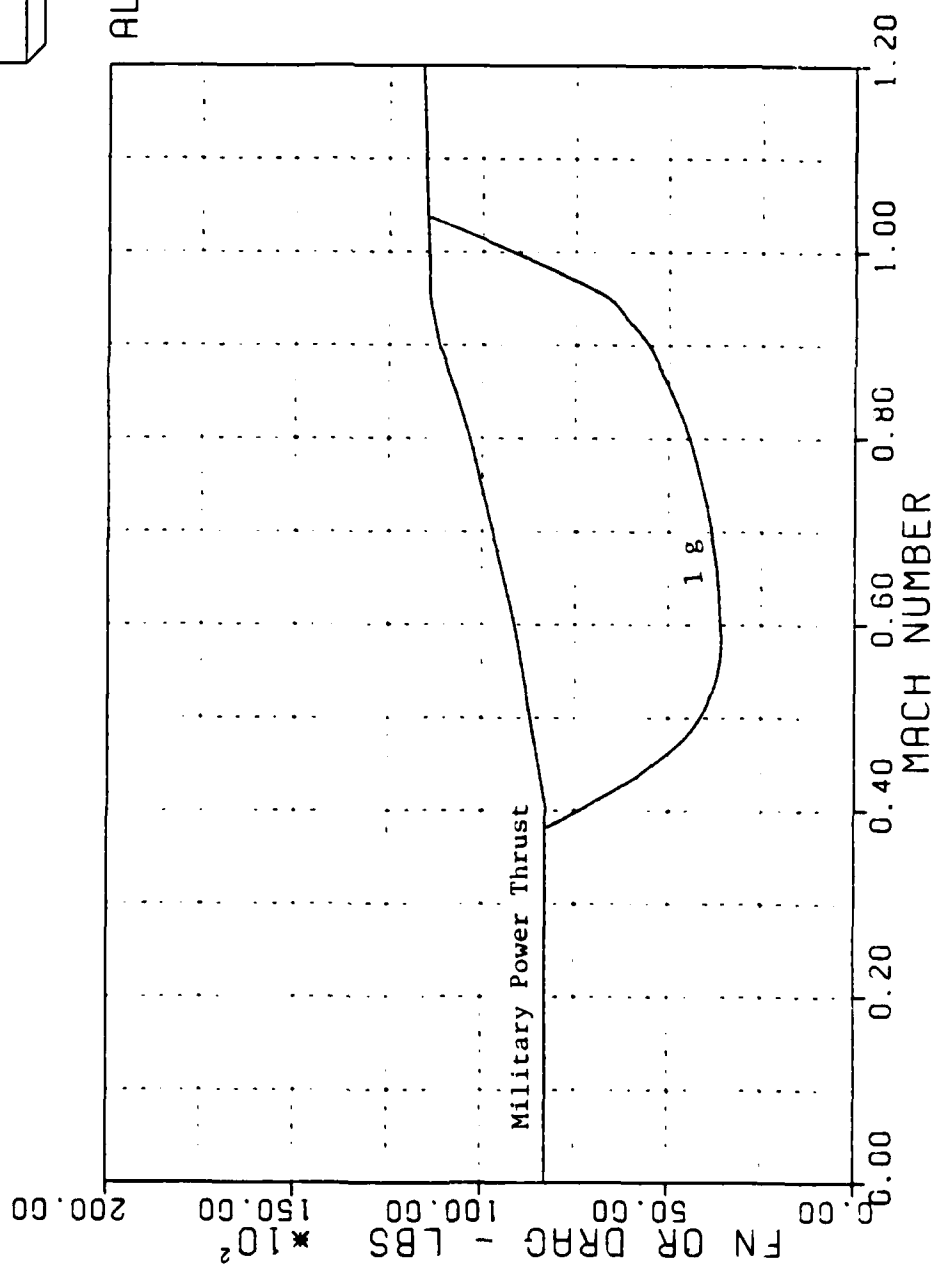
Figure 26 -- Thrust Required, 30,000 ft (Case 1)

87

APPENDIX C

Results From Using the Complete Equations of Motion

F-15 STOL

TURN RATE VS MACH

Figure 27 -- Sustained Turn Rate, Sea Level (Cases 2&3)

F-15 STOL

TURN RATE VS MACH

CONFIGURATION:
MILITARY POWER AND
MAXIMUM A/B POWER
— NO THRUST VECTOR
    ANGLE
-- OPTIMUM THRUST
    VECTOR ANGLE

ALT = 10000.
WEIGHT = 35000.
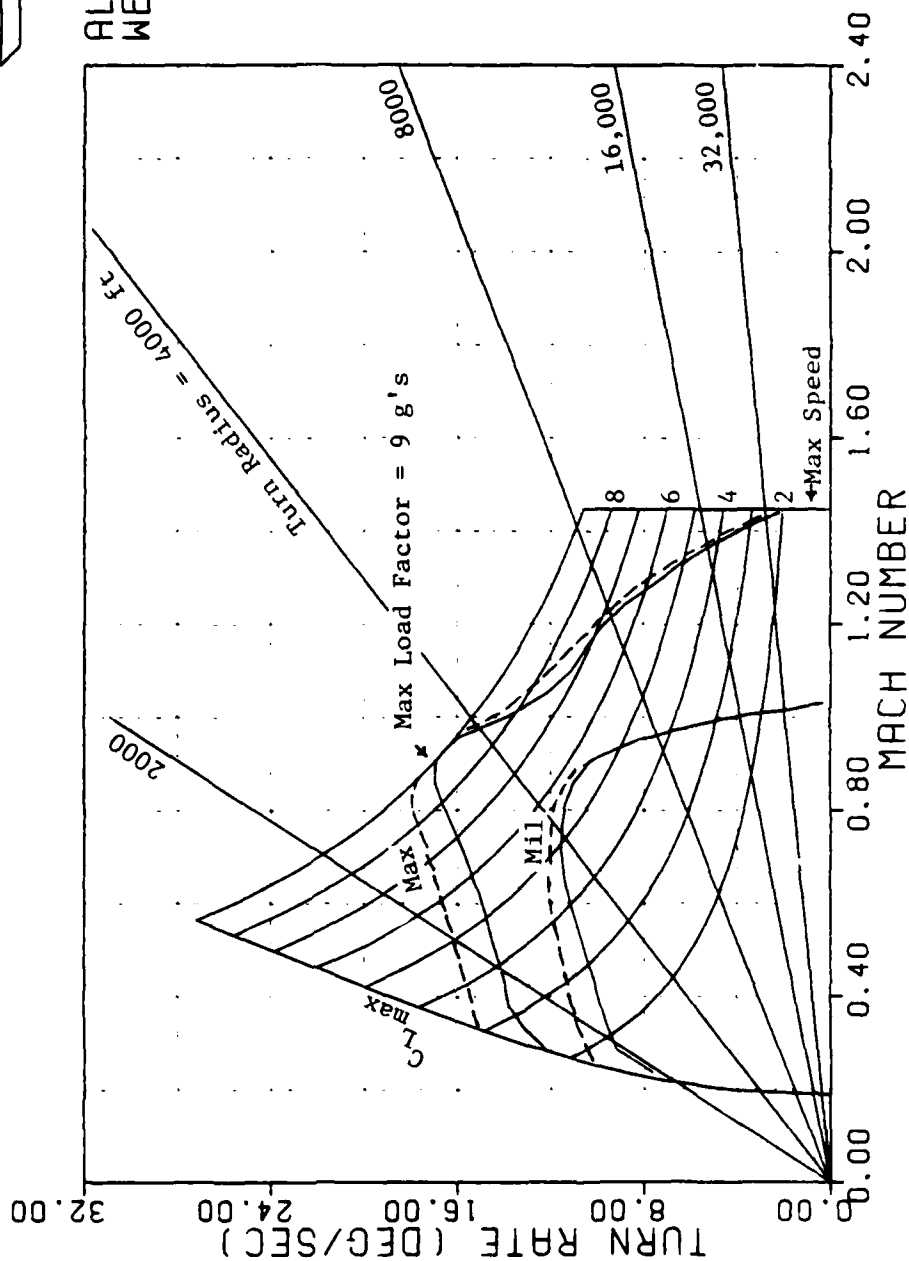
Figure 28 -- Sustained Turn Rate, 10,000 ft (Cases 2&3)

90

F-15 STOL

TURN RATE VS MACH

CONFIGURATION:
MILITARY POWER AND
MAXIMUM A/B POWER
— NO THRUST VECTOR
  ANGLE
-- OPTIMUM THRUST
  VECTOR ANGLE

ALT =20000.
WEIGHT=35000.
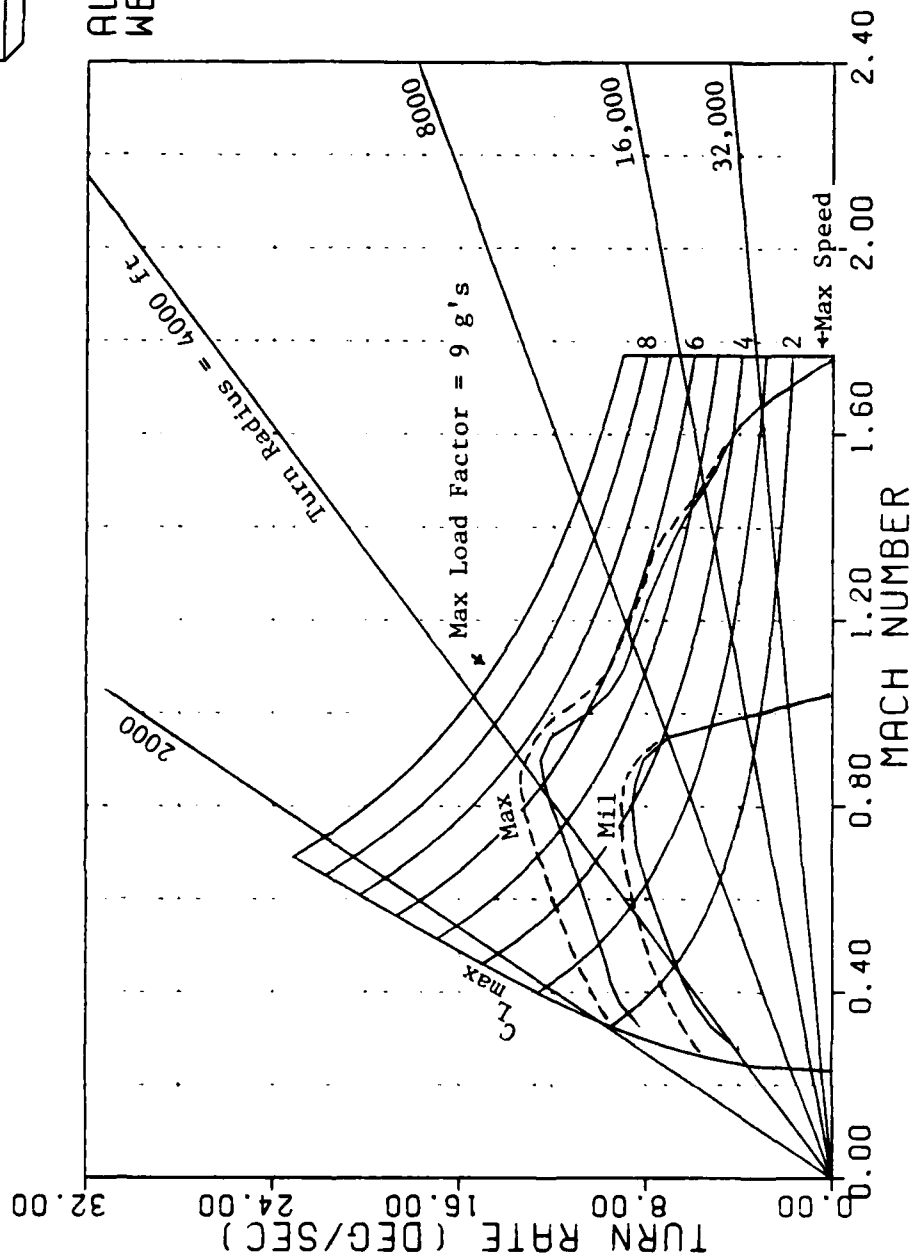
Figure 29 -- Sustained Turn Rate, 20,000 ft (Cases 2&3)

16

F-15 STOL

TURN RATE VS MACH

CONFIGURATION:
MILITARY POWER AND
MAXIMUM A/B POWER
— NO THRUST VECTOR
ANGLE
-- OPTIMUM THRUST
VECTOR ANGLE
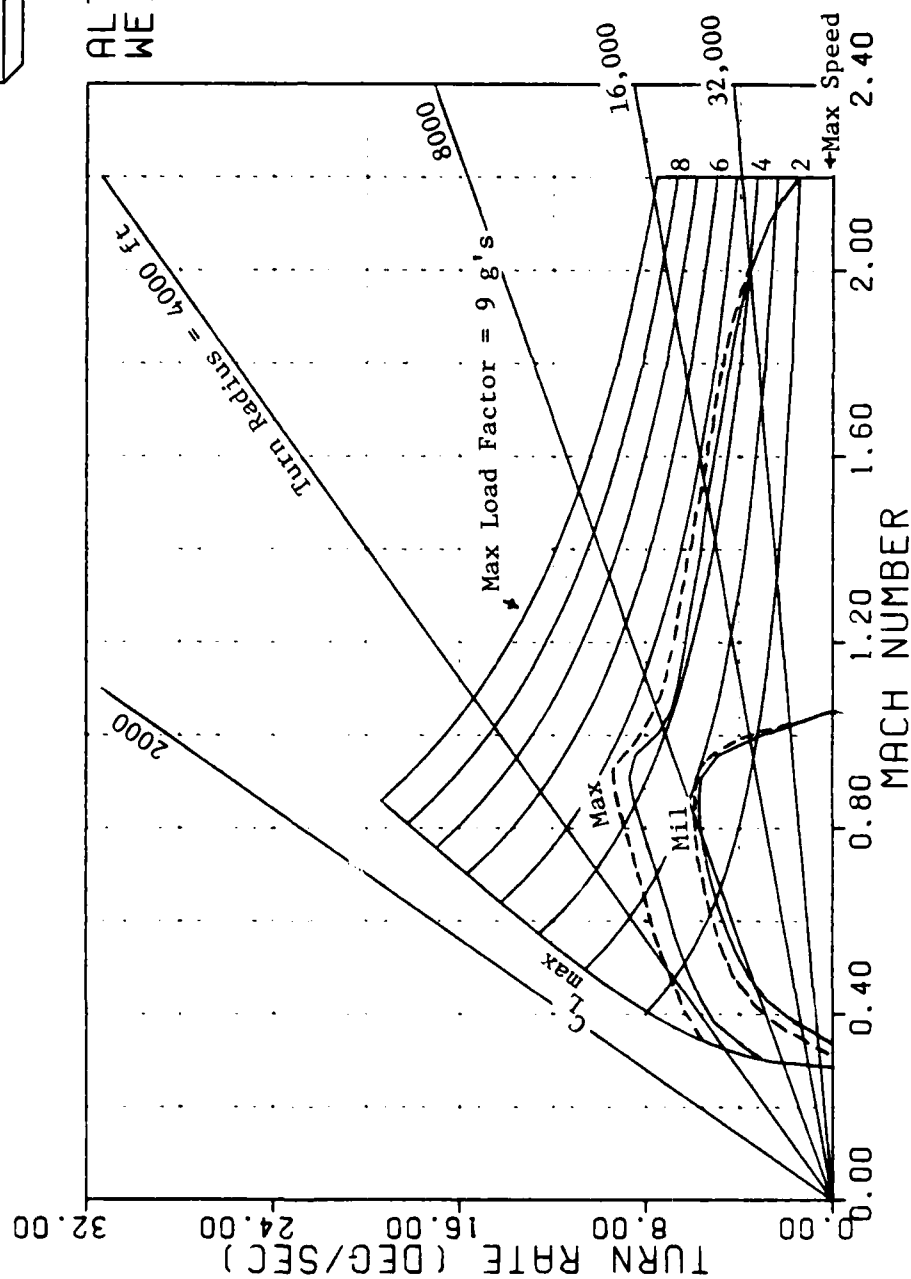
ALT =30000.
WEIGHT=35000.

Figure 30 -- Sustained Turn Rate, 30,000 ft (Cases 2&3)

F-15 STOL

LOAD FACTOR VS MACH

CONFIGURATION:
MILITARY POWER AND
MAXIMUM A/B POWER
— NO THRUST VECTOR
ANGLE
-- OPTIMUM THRUST
VECTOR ANGLE

ALT = 0.
WEIGHT = 35000.

Figure 31 -- Sustained Load Factor, Sea Level (Cases 2&3)

93

F-15 STOL

LOAD FACTOR VS MACH

CONFIGURATION:
MILITARY POWER AND
MAXIMUM A/B POWER
— NO THRUST VECTOR
 ANGLE
-- OPTIMUM THRUST
 VECTOR ANGLE

ALT = 10000.
WEIGHT=35000.

Figure 32 -- Sustained Load Factor, 10,000 ft (Cases 2&3)

94

F-15 STOL

LOAD FACTOR VS MACH

CONFIGURATION:
MILITARY POWER AND
MAXIMUM A/B POWER
— NO THRUST VECTOR
   ANGLE
-- OPTIMUM THRUST
   VECTOR ANGLE

ALT   =20000.
WEIGHT=35000.

Max Load Factor = 9 g's

Max

Mil

$C_{L_{max}}$

Max Speed

MACH NUMBER
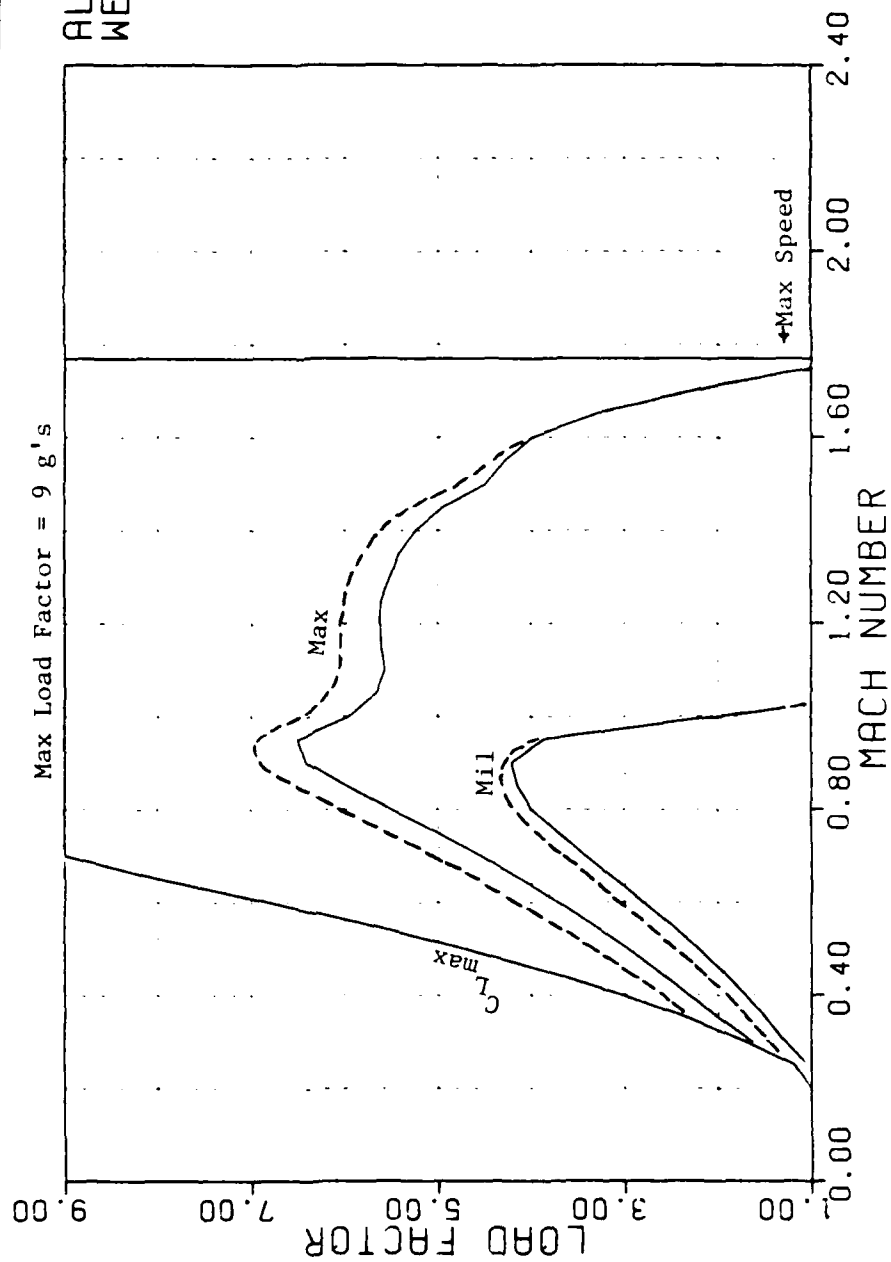
LOAD FACTOR

Figure 33 -- Sustained Load Factor, 20,000 ft (Cases 2&3)

95

F-15 STOL

LOAD FACTOR VS MACH

CONFIGURATION:
MILITARY POWER AND
MAXIMUM A/B POWER
— NO THRUST VECTOR
ANGLE
-- OPTIMUM THRUST
VECTOR ANGLE

ALT =30000.
WEIGHT=35000.

Max Load Factor = 9 g's

Max

Mil

$C_{L_{max}}$

+Max Speed

MACH NUMBER

LOAD FACTOR

Figure 34 -- Sustained Load Factor, 30,000 ft (Cases 2&3)

96

F-15 STOL

ACCELERATION VS MACH MAP
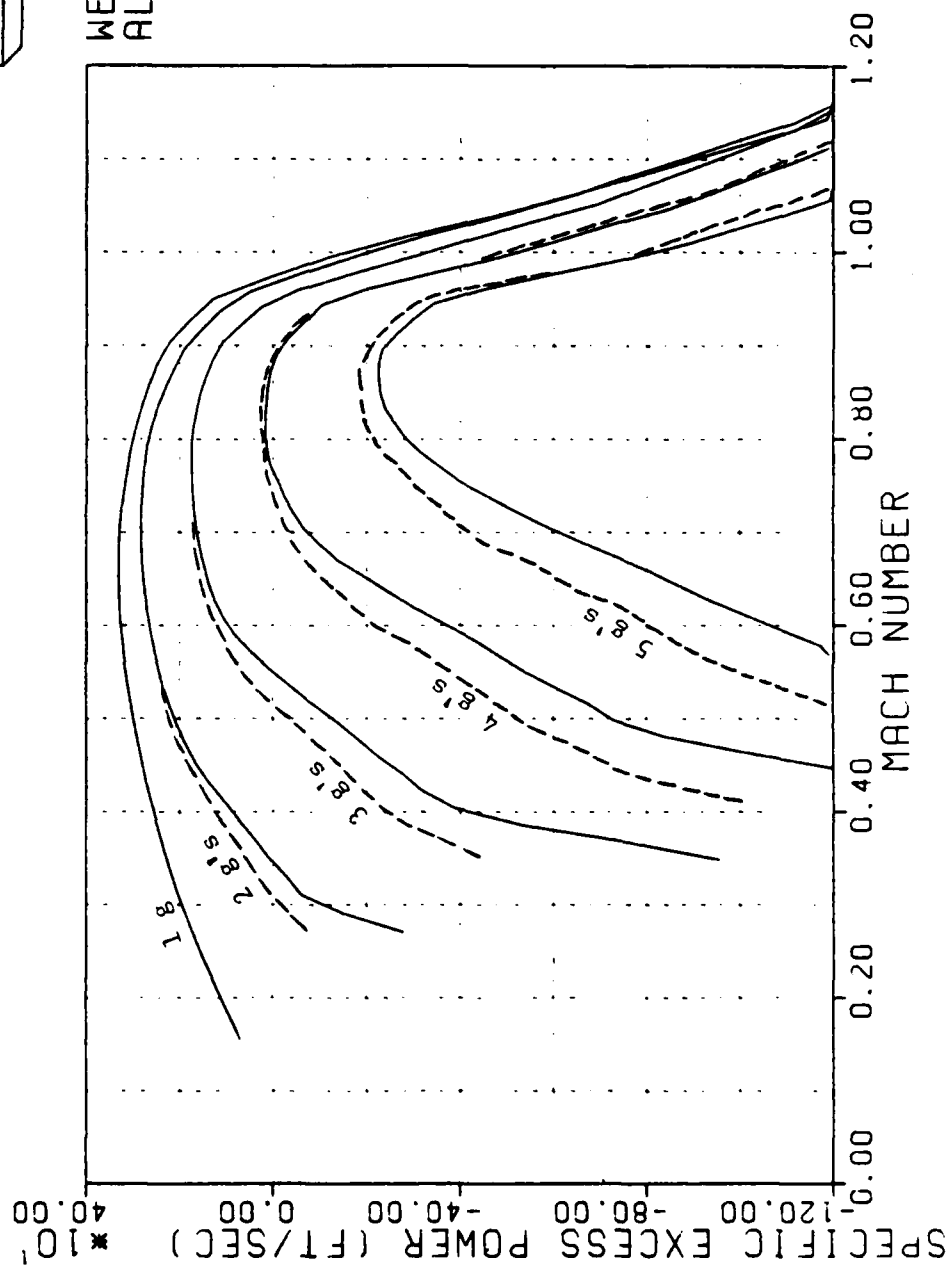
Figure 35 -- Specific Excess Power, Sea Level (Cases 2&3)

CONFIGURATION:

MILITARY POWER
— NO THRUST VECTOR
  ANGLE
-- OPTIMUM THRUST
   VECTOR ANGLE

WEIGHT=35000.
ALT =0.

F-15 STOL

ACCELERATION VS MACH MAP

CONFIGURATION:

MILITARY POWER
— NO THRUST VECTOR
  ANGLE
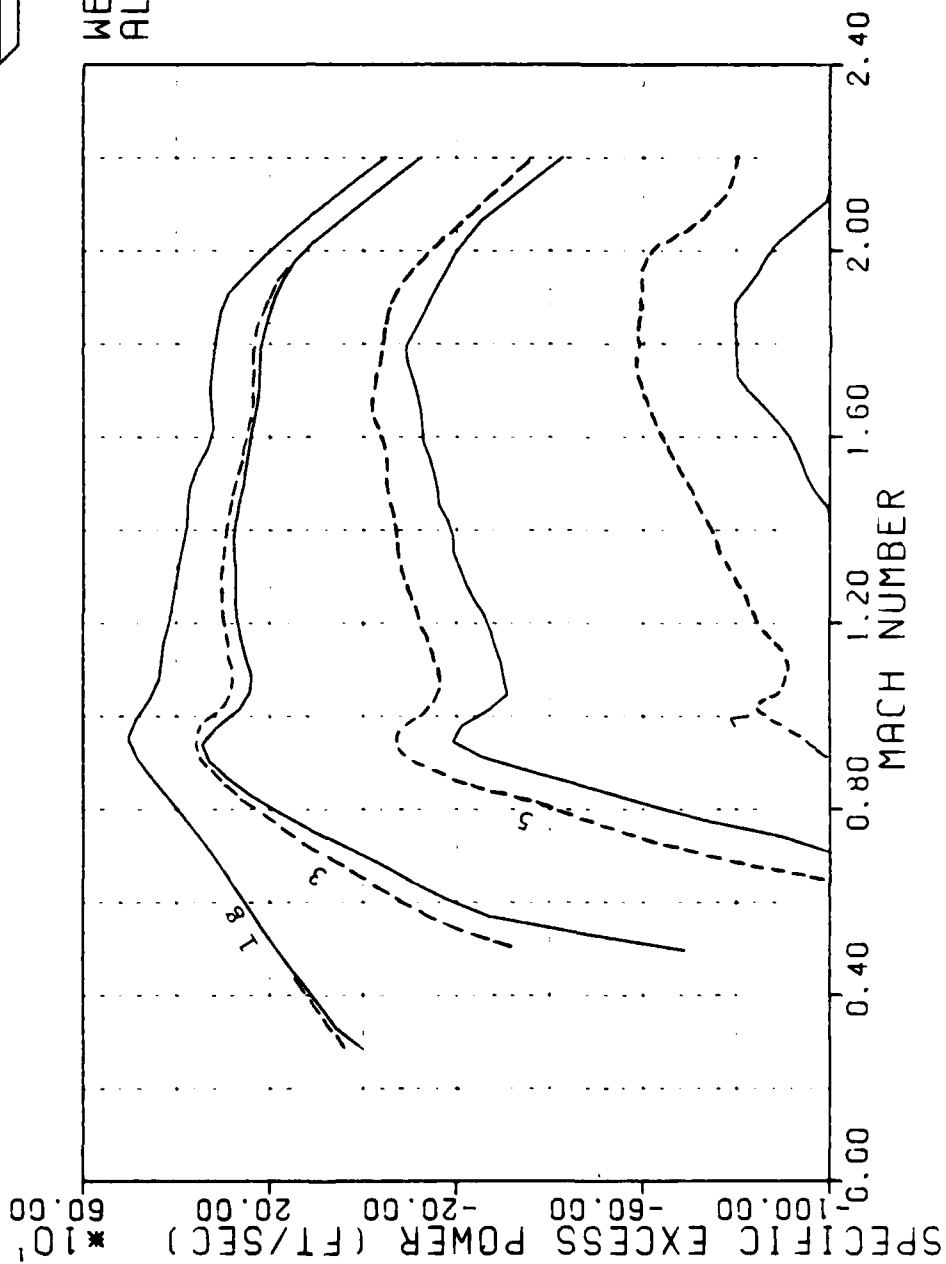-- OPTIMUM THRUST
   VECTOR ANGLE

WEIGHT=35000.
ALT =10000.
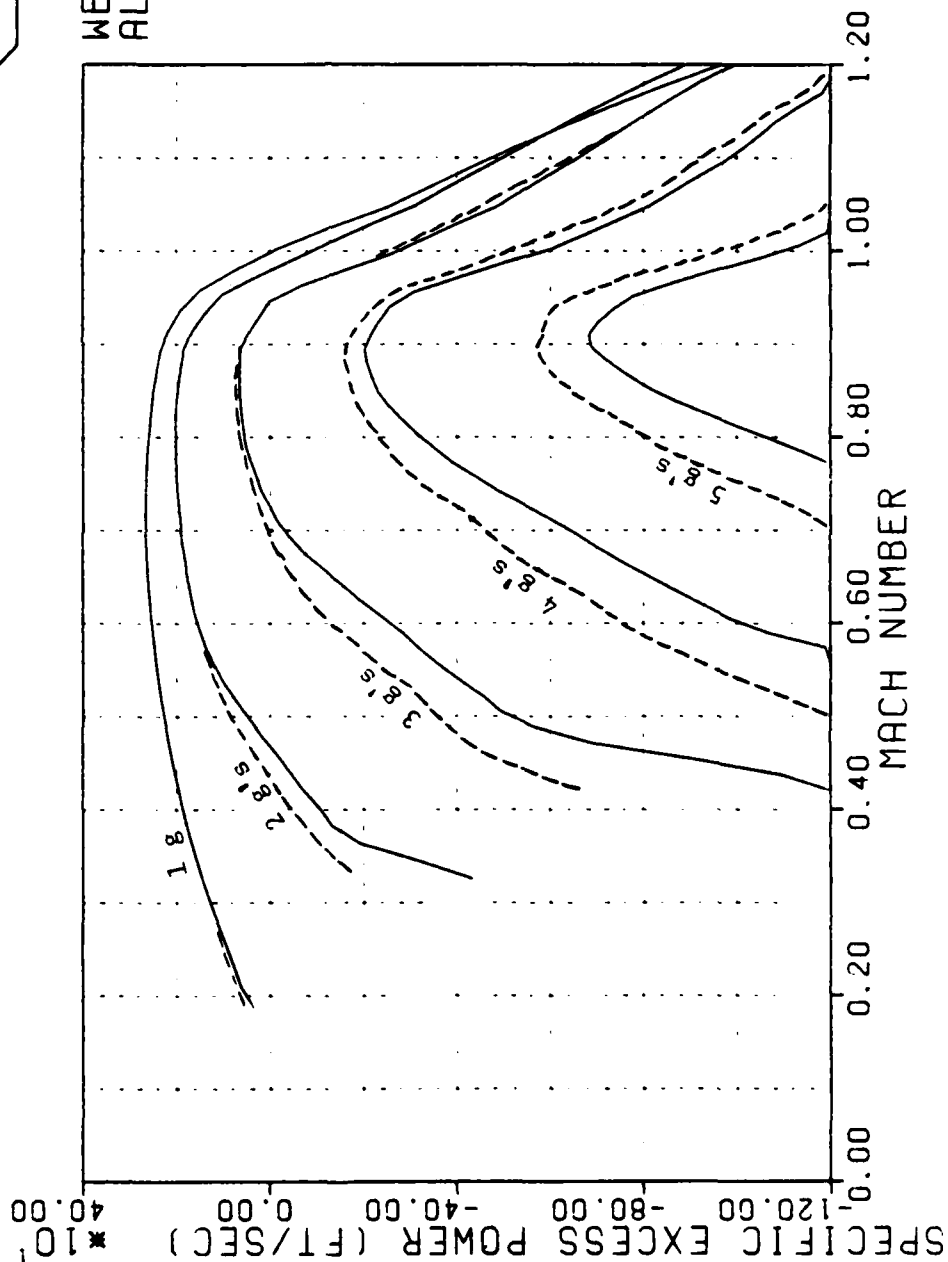
Figure 36 -- Specific Excess Power, 10,000 ft (Cases 2&3)

F-15 STOL

ACCELERATION VS MACH MAP

CONFIGURATION:

MILITARY POWER
— NO THRUST VECTOR ANGLE
-- OPTIMUM THRUST VECTOR ANGLE

WEIGHT=35000.
ALT =20000.
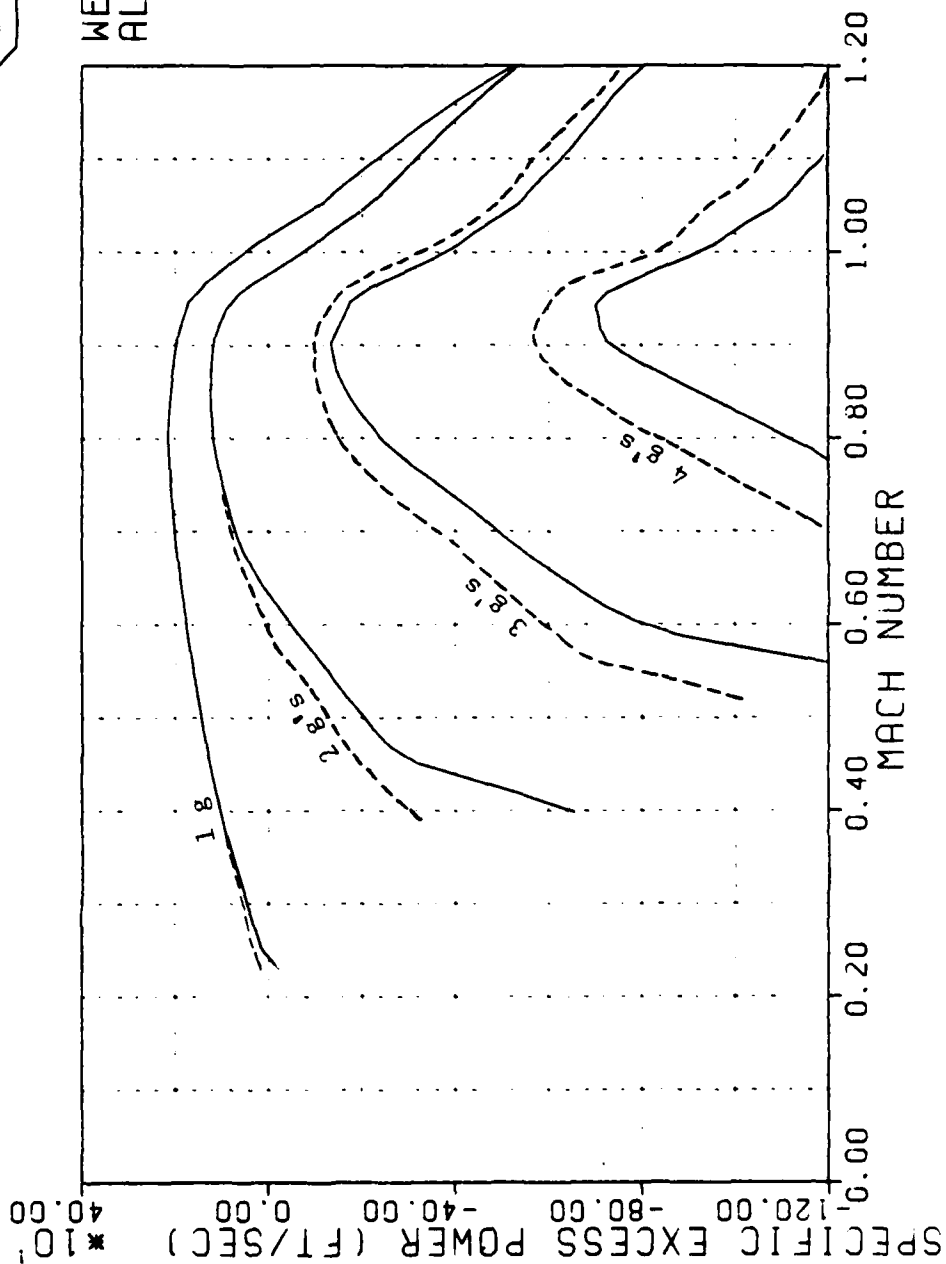
Figure 37 -- Specific Excess Power, 20,000 ft (Cases 2&3)
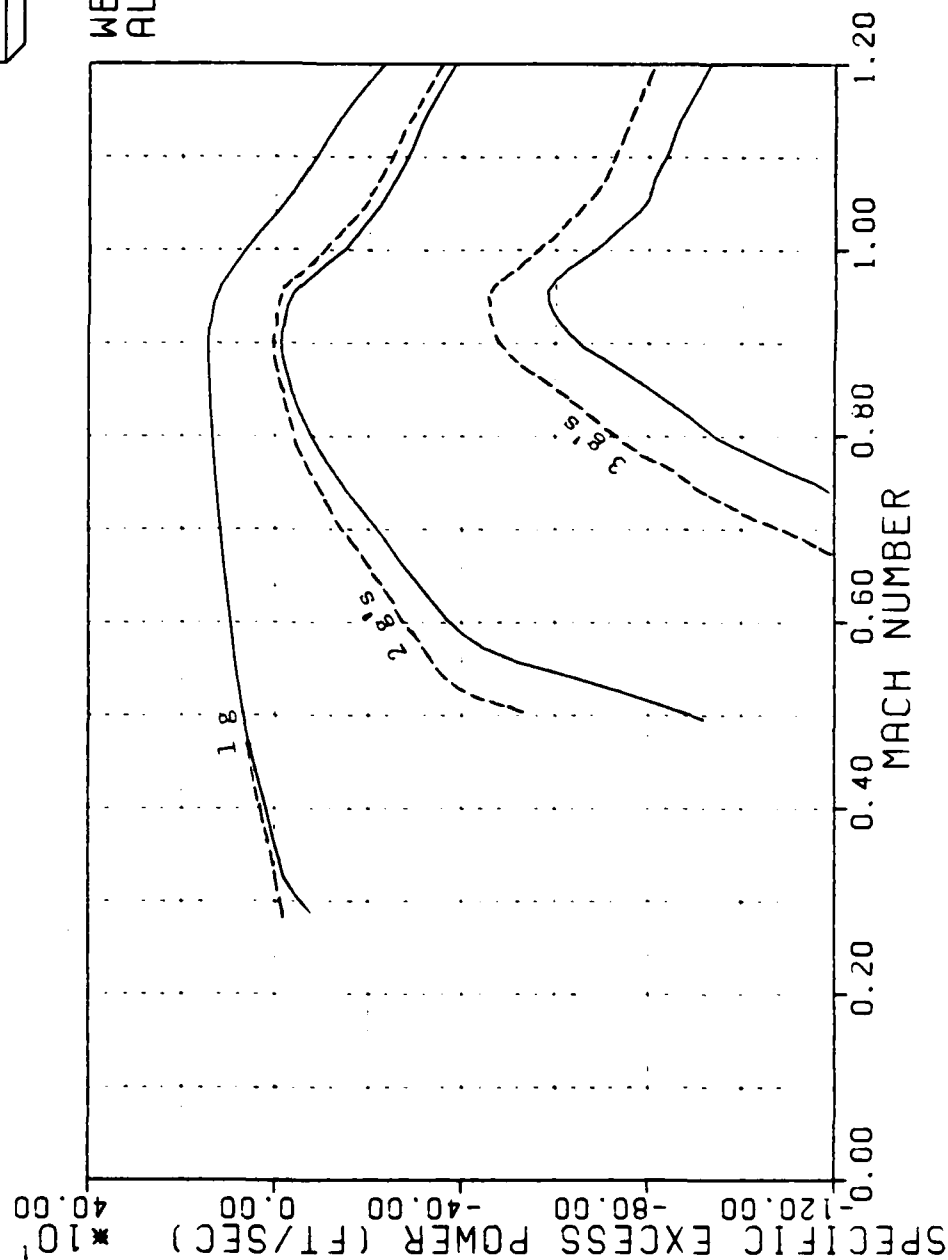
Figure 38 -- Specific Excess Power, 30,000 ft (Cases 2&3)

F-15 STOL

ACCELERATION VS MACH MAP
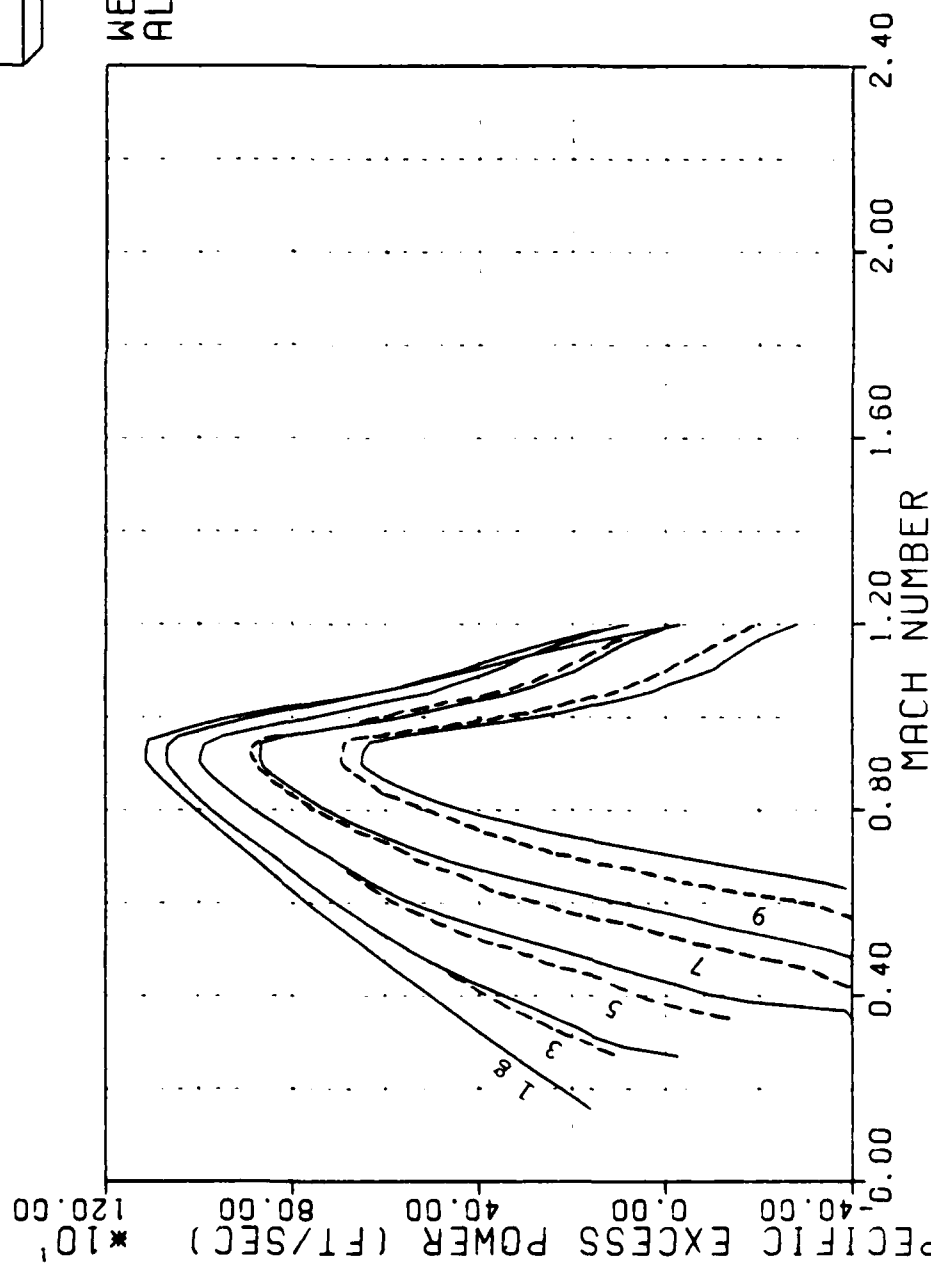
Figure 39 -- Specific Excess Power, Sea Level (Cases 2&3)

F-15 STOL

ACCELERATION VS MACH MAP

CONFIGURATION:

MAXIMUM A/B POWER
— NO THRUST VECTOR
   ANGLE
-- OPTIMUM THRUST
   VECTOR ANGLE

WEIGHT = 35000.
ALT = 10000.
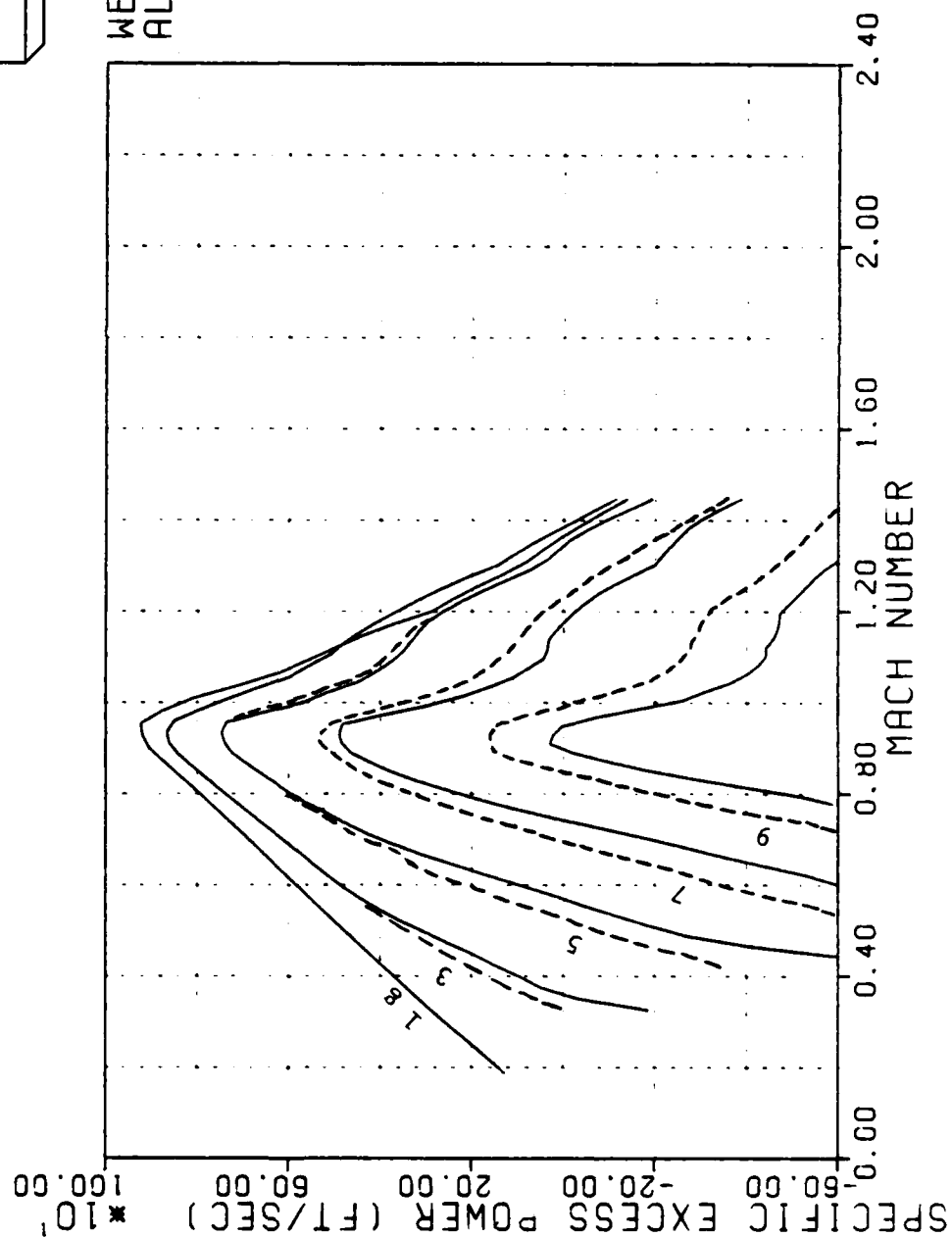
Figure 40 -- Specific Excess Power, 10,000 ft (Cases 2&3)

102

F-15 STOL

ACCELERATION VS MACH MAP

CONFIGURATION:

MAXIMUM A/B POWER
— NO THRUST VECTOR ANGLE
-- OPTIMUM THRUST VECTOR ANGLE

WEIGHT=35000.
ALT =20000.
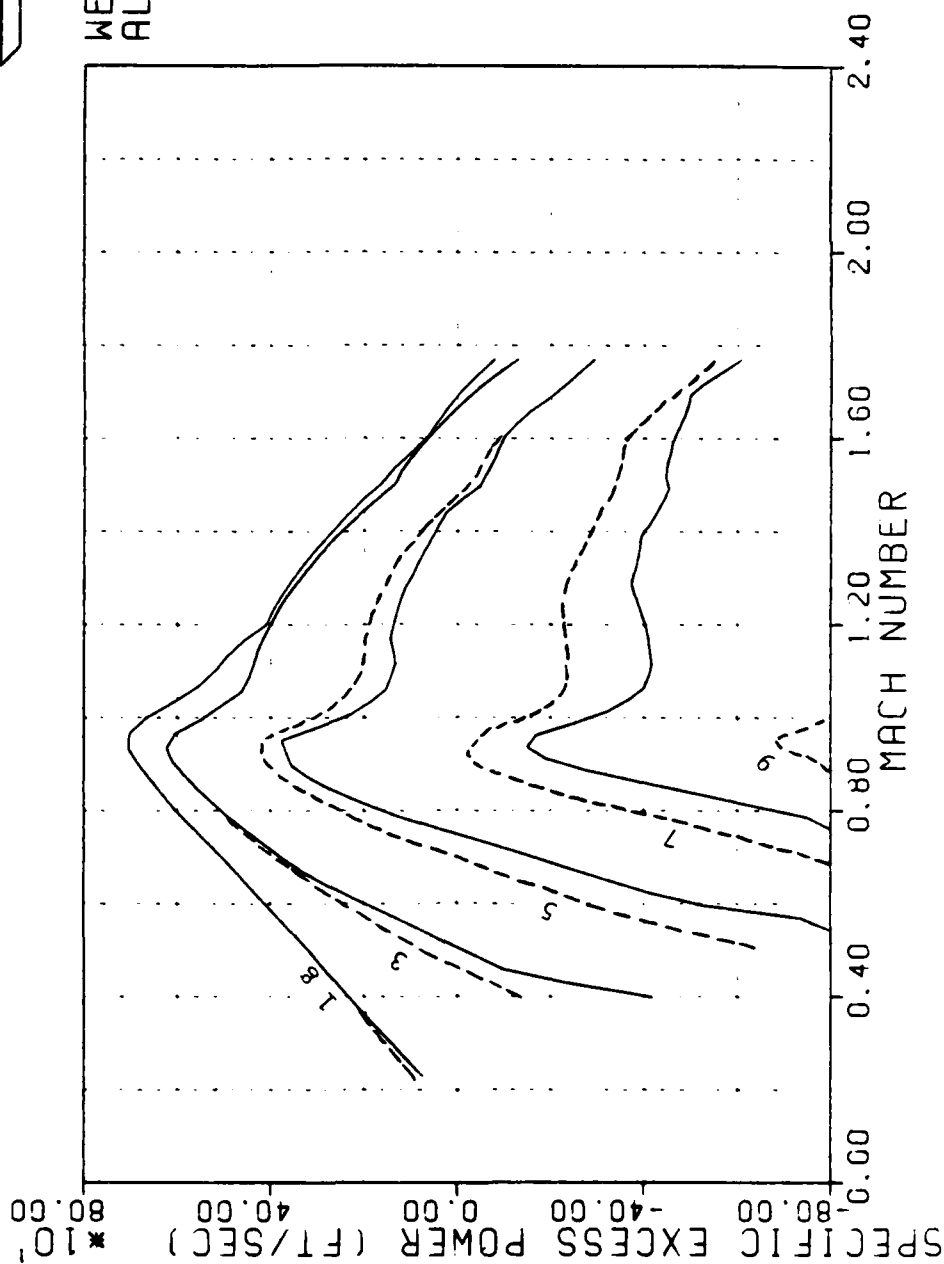
Figure 41 -- Specific Excess Power, 20,000 ft (Cases 2&3)

F-15 STOL

ACCELERATION VS MACH MAP

Figure 42 -- Specific Excess Power, 30,000 ft (Cases 2&3)

104

F-15 STOL

SPEED-POWER MAP

CONFIGURATION:

MILITARY POWER
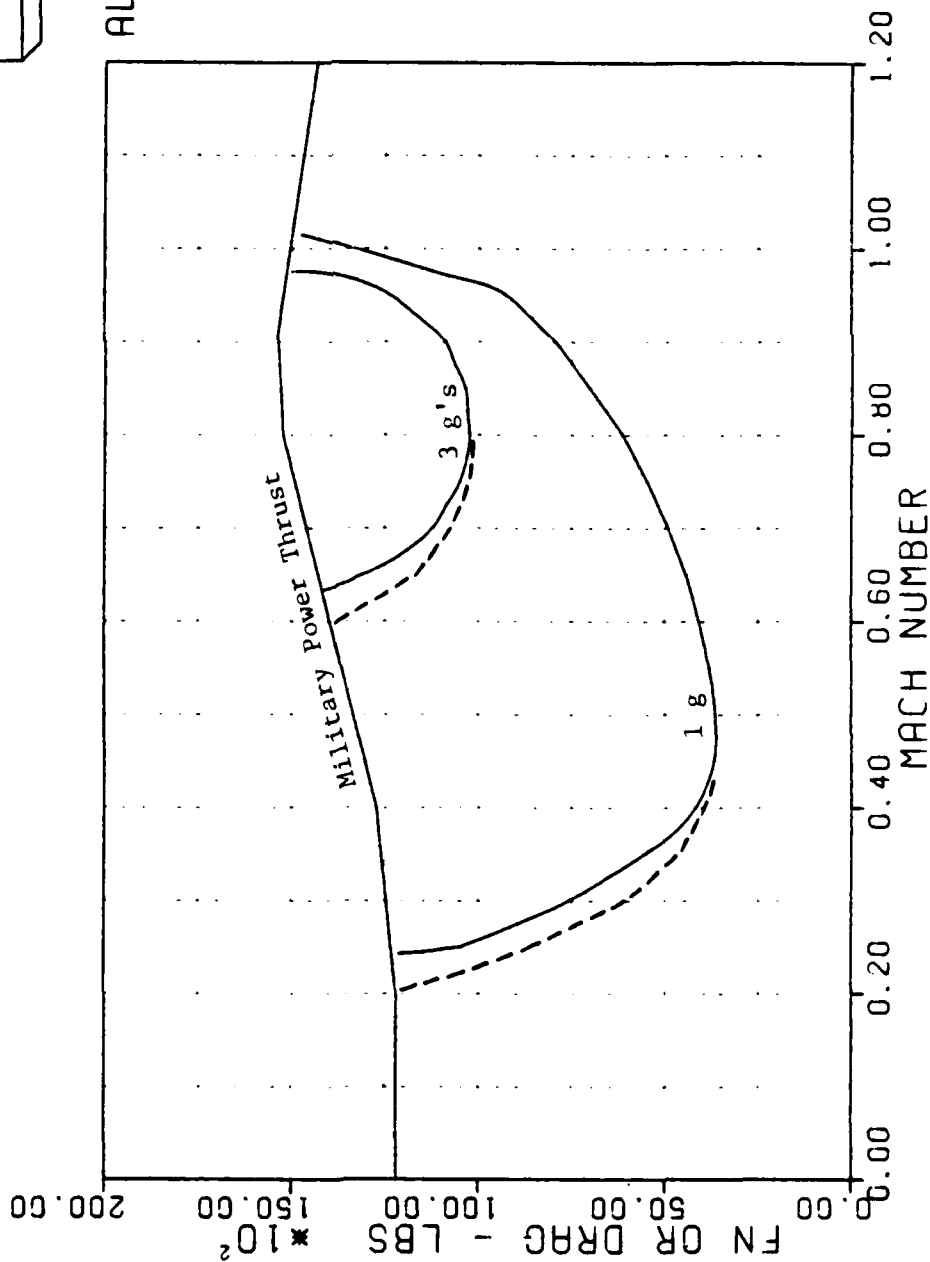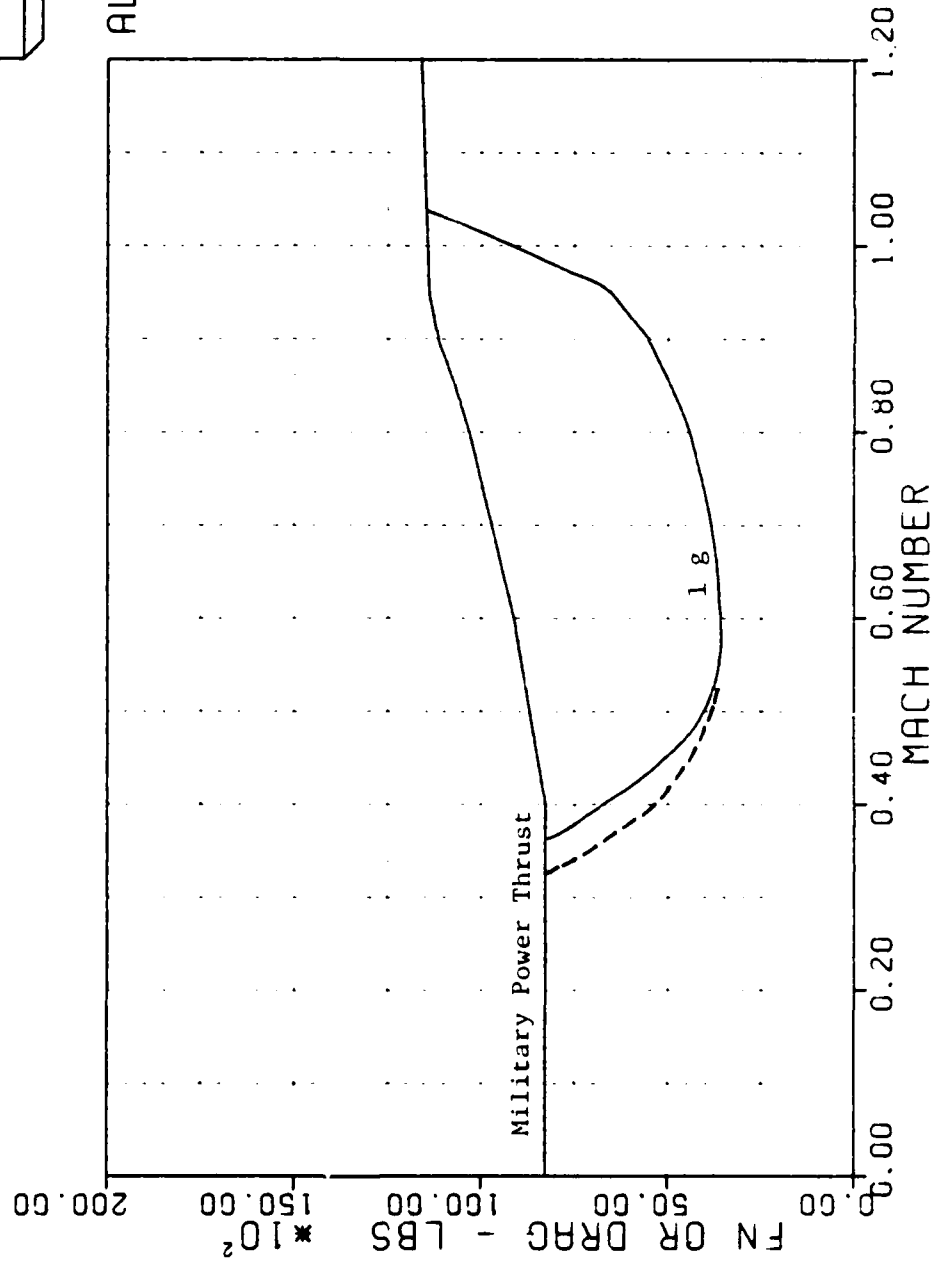— NO THRUST VECTOR
  ANGLE
-- OPTIMUM THRUST
  VECTOR ANGLE

ALT = 0.
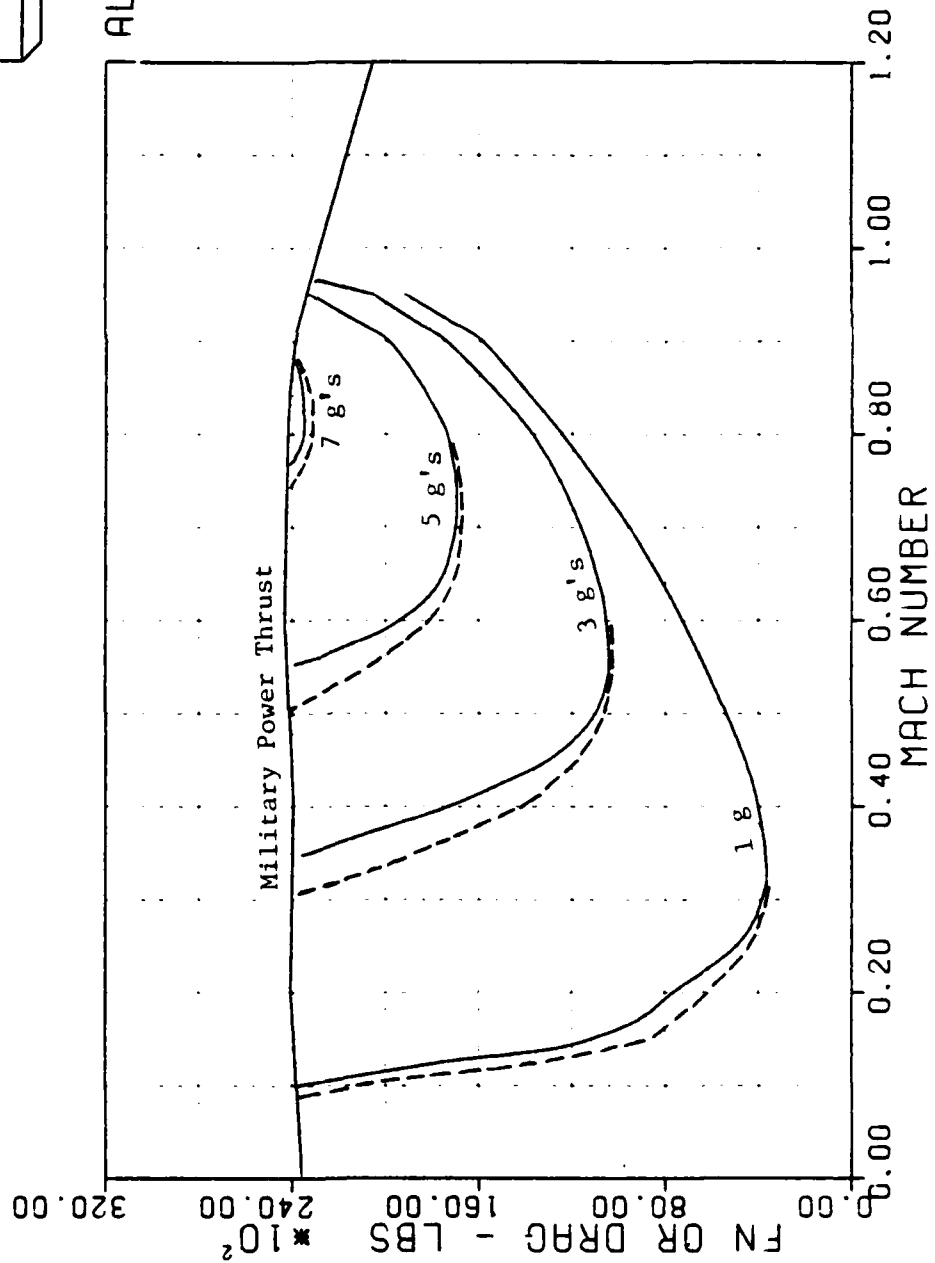
Figure 43 -- Thrust Required, Sea Level (Cases 2&3)

105

F-15 STOL

SPEED-POWER MAP

CONFIGURATION:

MILITARY POWER
— NO THRUST VECTOR
  ANGLE
-- OPTIMUM THRUST
  VECTOR ANGLE

ALT = 10000.
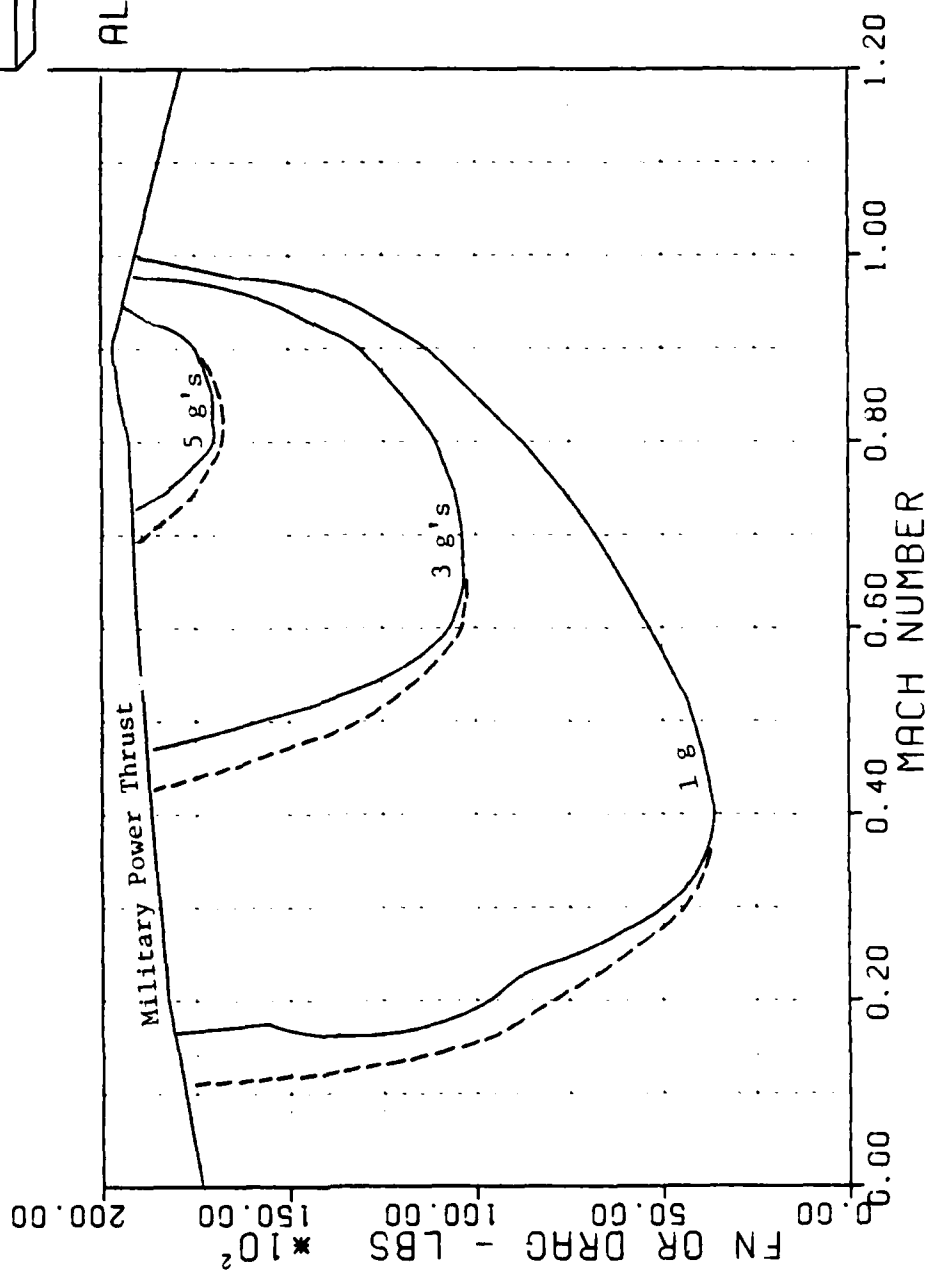
Figure 44 -- Thrust Required, 10,000 ft (Cases 2&3)

F-15 STOL

SPEED-POWER MAP

CONFIGURATION:

MILITARY POWER
— NO THRUST VECTOR
  ANGLE
-- OPTIMUM THRUST
   VECTOR ANGLE

ALT = 20000.

Figure 45 -- Thrust Required, 20,000 ft (Cases 2&3)

107

F-15 STOL

SPEED-POWER MAP

CONFIGURATION:

MILITARY POWER
— NO THRUST VECTOR
   ANGLE
-- OPTIMUM THRUST
   VECTOR ANGLE

ALT = 30000.

Military Power Thrust

1 g

FN OR DRAG - LBS *10²

MACH NUMBER

0.00   0.20   0.40   0.60   0.80   1.00   1.20

0.00   50.00   100.00   150.00   200.00

Figure 46 -- Thrust Required, 30,000 ft (Cases 2&3)

108

APPENDIX D

Results for Subsonic Cruise
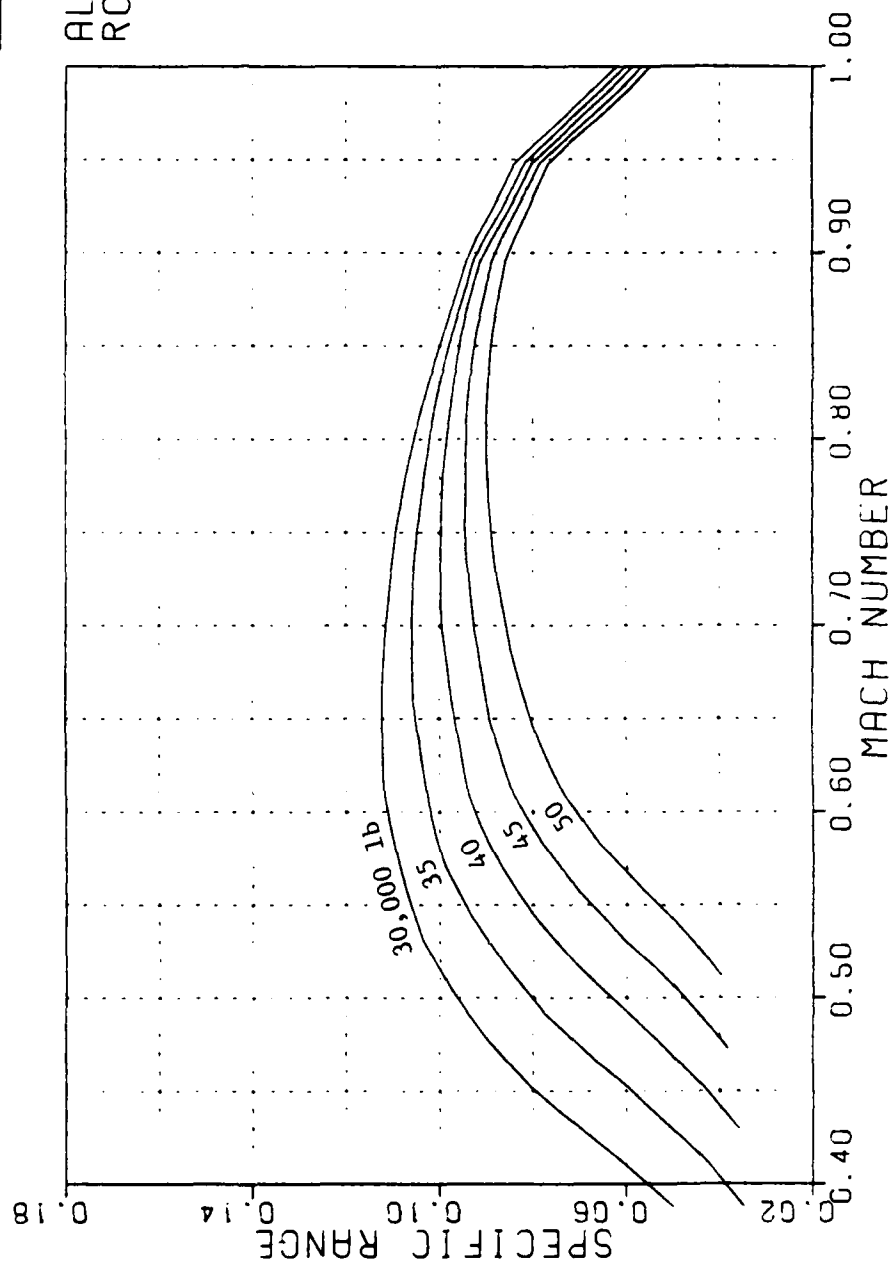
Figure 47 -- Specific Range, 30,000 ft (Case 1)

F-15 STOL

SPECIFIC RANGE VS MACH MAP

CONFIGURATION:

MILITARY POWER
ANGLE OF ATTACK
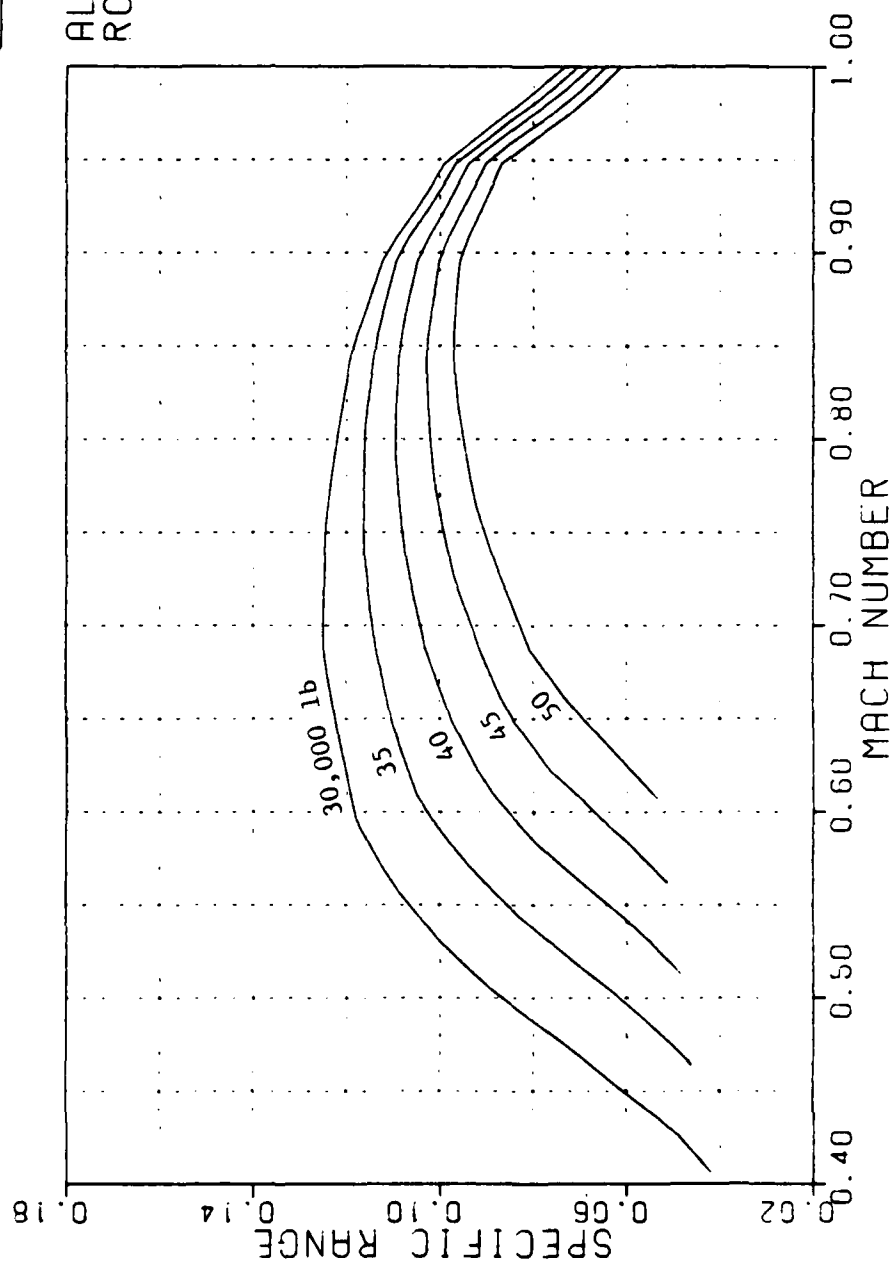AND THRUST VECTOR
ANGLE NEGLECTED

ALT   = 35000.
RCSC = 0.0

Figure 48 -- Specific Range, 35,000 ft (Case 1)

F-15 STOL

SPECIFIC RANGE VS MACH MAP

CONFIGURATION:

MILITARY POWER
ANGLE OF ATTACK
AND THRUST VECTOR
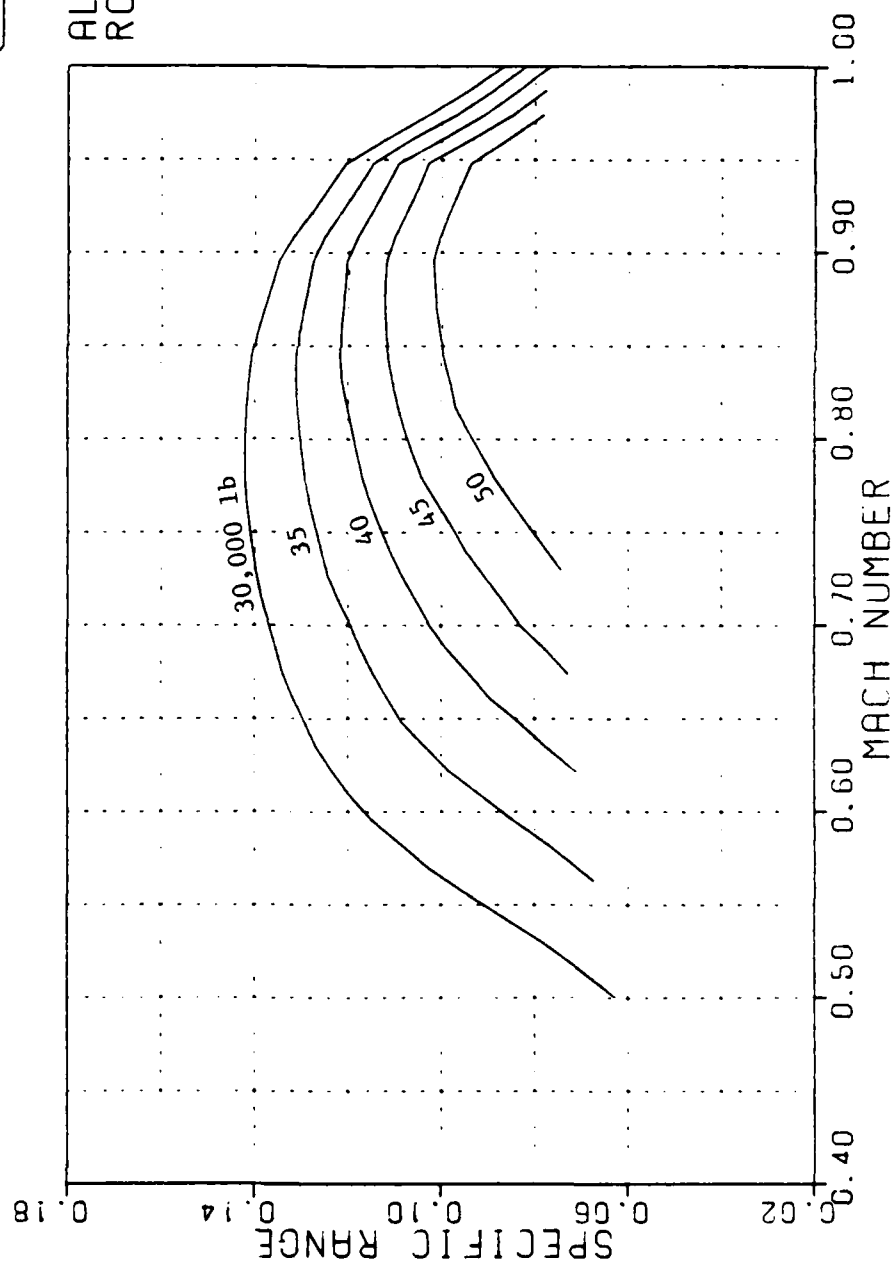ANGLE NEGLECTED

ALT = 40000.
RCSC = 0.0

Figure 49 -- Specific Range, 40,000 ft (Case 1)

112

F-15 STOL

SPECIFIC RANGE VS MACH MAP

CONFIGURATION:

MILITARY POWER
— NO THRUST VECTOR
    ANGLE
-- OPTIMUM THRUST
    VECTOR ANGLE

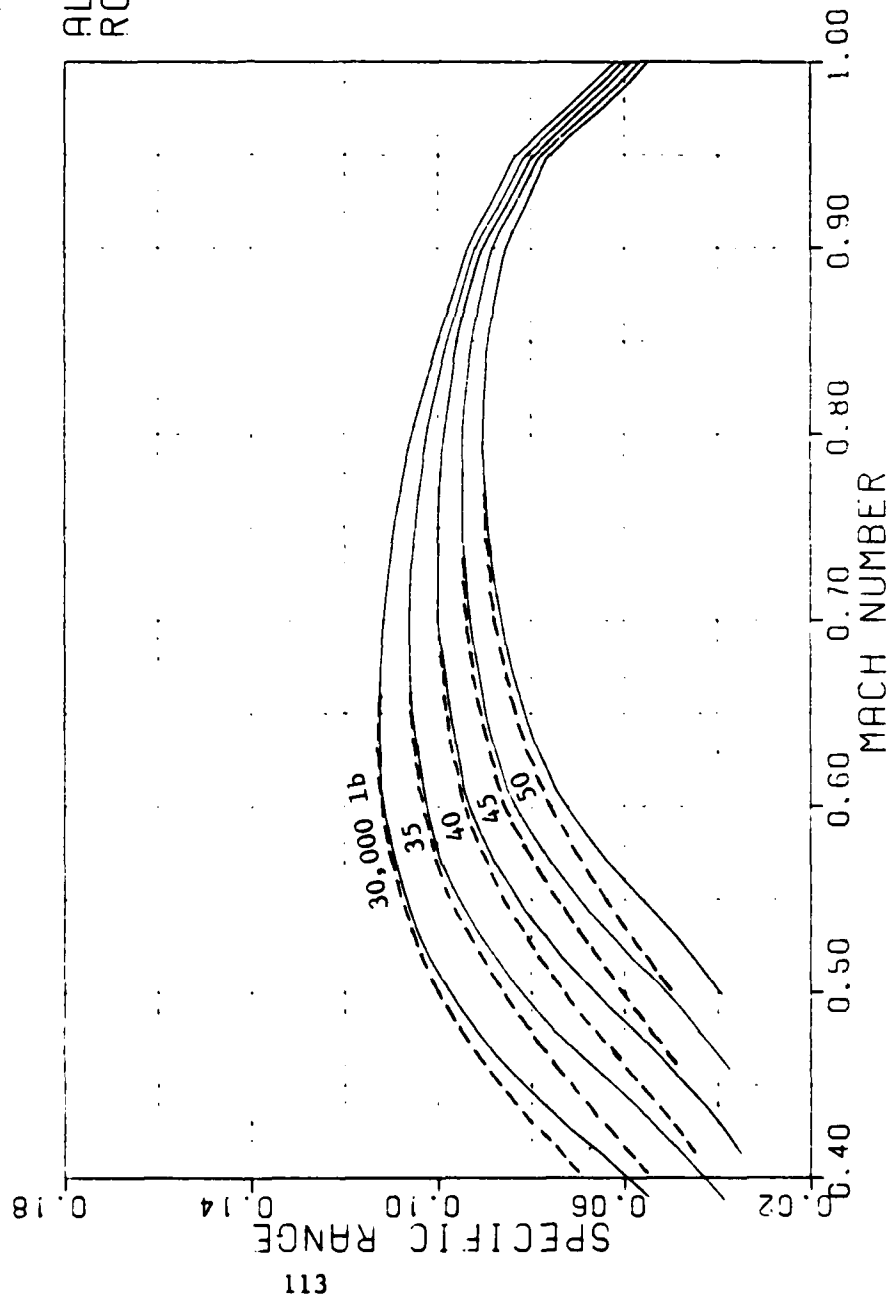ALT = 30000.
RCSC = 0.0

Figure 50 -- Specific Range, 30,000 ft (Cases 2&3)

F-15 STOL

SPECIFIC RANGE VS MACH MAP

CONFIGURATION:

MILITARY POWER
— NO THRUST VECTOR
  ANGLE
-- OPTIMUM THRUST
   VECTOR ANGLE

ALT = 35000.
RCSC = 0.0

Figure 51 -- Specific Range, 35,000 ft (Cases 2&3)

114

F-15 STOL

SPECIFIC RANGE VS MACH MAP

CONFIGURATION:

MILITARY POWER
— NO THRUST VECTOR
   ANGLE
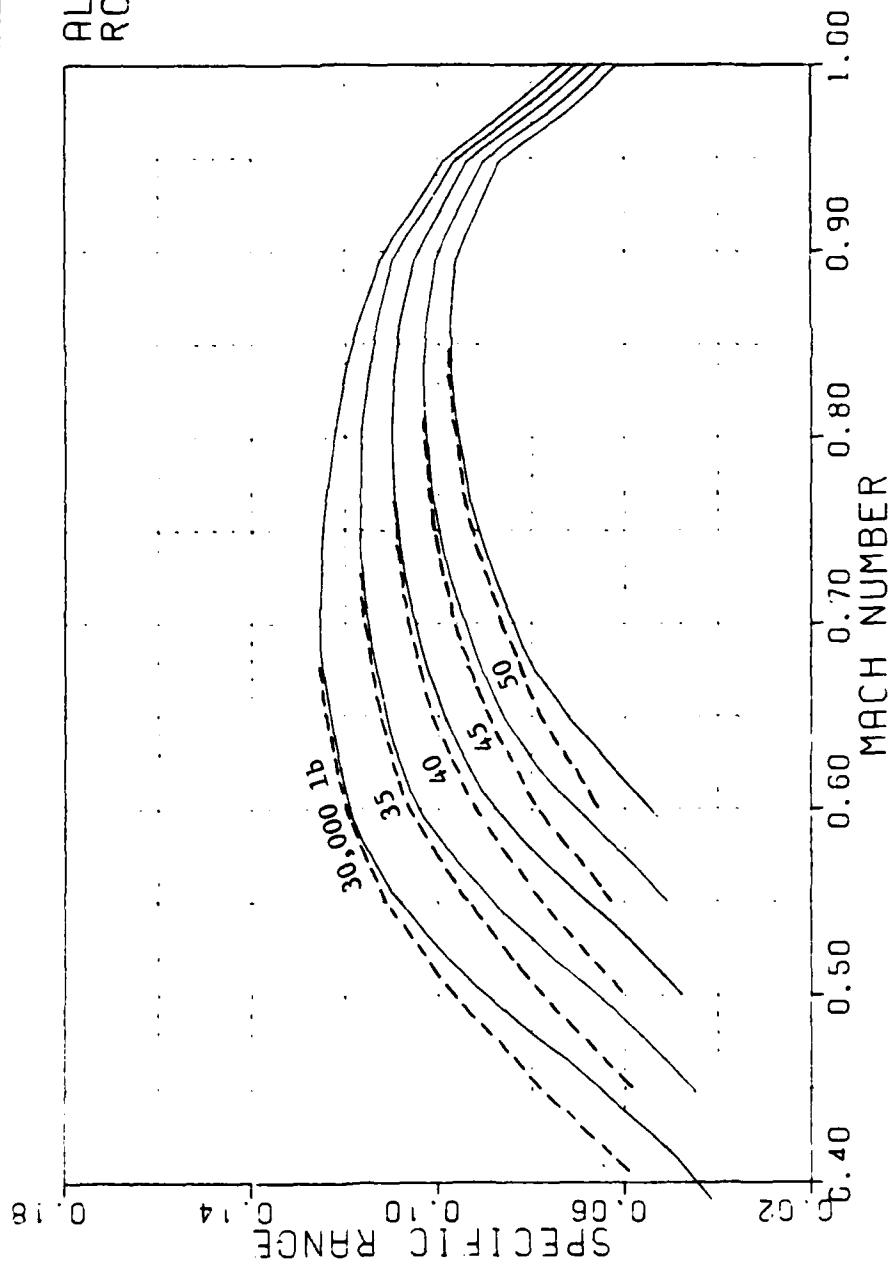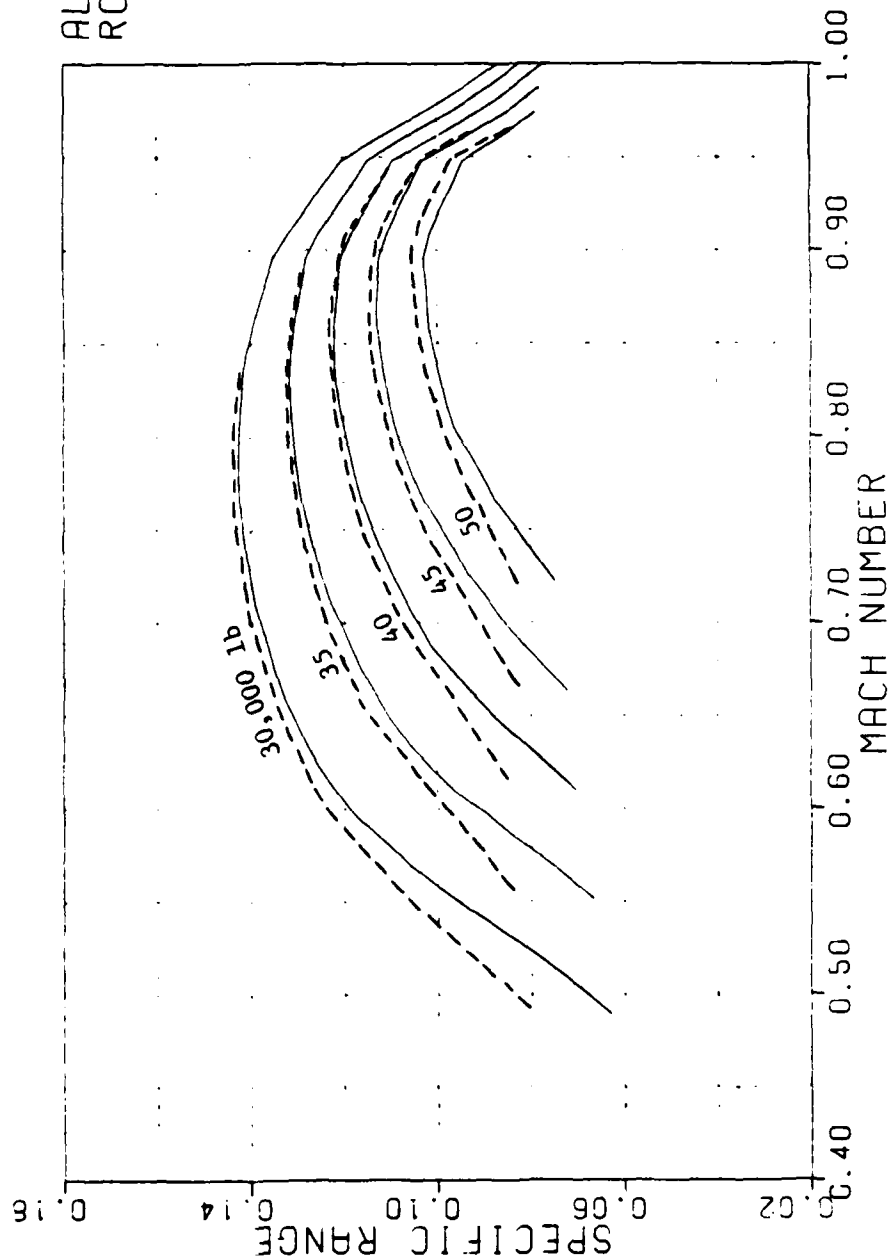-- OPTIMUM THRUST
   VECTOR ANGLE

ALT = 40000.
RCSC = 0.0

SPECIFIC RANGE

MACH NUMBER

30,000 lb
35
40
45
50

Figure 52 -- Specific Range, 40,000 ft (Cases 2&3)

Bibliography

1. Ropelewski, Robert R. "Modified F-15 Will Investigate Advanced Control Concepts," Aviation Week & Space Technology: 51-53 (February 11, 1985).

2. Kinnucan, Paul. "Superfighters," High Technology: 36-48 (April 1984).

3. Humphreys, Robert P., George R. Hennig, William A. Bolding, and Larry A. Helgeson. "Optimal 3-Dimensional Minimum Time Turns for an Aircraft," The Journal of the Astronautical Sciences, XX (2): 88-112 (September-October 1972).

4. Johnson, Capt Thomas L. Minimum Time Turns with Thrust Reversal, MS Thesis, School of Engineering, Air Force Institute of Technology (AU), Wright-Patterson AFB, OH, December 1979 (AD-A079.851)

5. Finnerty, Capt Christopher S. Minimum Time Turns Constrained to the Vertical Plane. MS Thesis. School of Engineering, Air Force Institute of Technology (AU), Wright-Patterson AFB, OH, December 1980 (AD-A111.096)

6. Brinson, Michael R. Minimum Time Turns with Direct Sideforce. MS Thesis. School of Engineering, Air Force Institute of Technology (AU), Wright-Patterson AFB, OH, December 1983 (AD-A136.958)

7. Schneider, Capt Garrett L. Minimum Time Turns Using Vectored Thrust. MS Thesis, School of Engineering, Air Force Institute of Technology (AU), Wright-Patterson AFB, OH, December 1984

8. NASA. U.S. Standard Atmosphere. Washington, D.C., December 1962.

9. Miele, Angelo. "Theory of Flight Paths," Flight Mechanics, 1. Massachusetts: Addison-Wesley Publishing Company, Inc., 1962.

10. Rutowski, Edward S. "Energy Approach to the General Aircraft Performance Problem," Journal of the Aeronautical Sciences, Vol 21: 187-95 (March 1954).

11. Fellows, Mark S. "NSEG--Segmented Mission Analysis Program, ASD/ENFTA User's Manual," ENFTA-TM-84-01, March 1984.

12. Parrott, Edward L. "Combat Performance Advantage: A Method of Evaluating Air Combat Performance Effectiveness," ASD-TR-78-36, December 1978.

VITA

Mark S. Fellows was born on 25 July 1957 in Dayton, Ohio. He graduated from high school in Kettering, Ohio in 1975 and attended the University of Cincinnati from which he received the degree of Bachelor of Science in Aerospace Engineering in June 1980. After graduation, he was employed as an aeronautical engineer in the Aerodynamics and Performance Branch, Flight Technology Division of the Deputy for Engineering within the Aeronautical Systems Division at Wright-Patterson Air Force Base until entering the School of Engineering, Air Force Institute of Technology in June 1984.

                    Permanent Address: 311 Kenderton Trail

                                          Beavercreek, Ohio 45430

SECURITY CLASSIFICATION OF THIS PAGE

ADA165388

REPORT DOCUMENTATION PAGE

1a. REPORT SECURITY CLASSIFICATION UNCLASSIFIED	1b. RESTRICTIVE MARKINGS
2a. SECURITY CLASSIFICATION AUTHORITY	3. DISTRIBUTION/AVAILABILITY OF REPORT Approved for public release; distribution unlimited
2b. DECLASSIFICATION/DOWNGRADING SCHEDULE	

4. PERFORMING ORGANIZATION REPORT NUMBER(S) AFIT/GAE/AA/85D-6	5. MONITORING ORGANIZATION REPORT NUMBER(S)

6a. NAME OF PERFORMING ORGANIZATION School of Engineering	6b. OFFICE SYMBOL (If applicable) AFIT/ENY	7a. NAME OF MONITORING ORGANIZATION

6c. ADDRESS (City, State and ZIP Code) Air Force Institute of Technology Wright-Patterson AFB, Ohio 45433	7b. ADDRESS (City, State and ZIP Code)

8a. NAME OF FUNDING/SPONSORING ORGANIZATION	8b. OFFICE SYMBOL (If applicable)	9. PROCUREMENT INSTRUMENT IDENTIFICATION NUMBER

8c. ADDRESS (City, State and ZIP Code)	10. SOURCE OF FUNDING NOS.

	PROGRAM ELEMENT NO.	PROJECT NO.	TASK NO.	WORK UNIT NO.

| 11. TITLE (Include Security Classification) See Box 19 | | | | |

12. PERSONAL AUTHOR(S)
Mark S. Fellows, B.S.

13a. TYPE OF REPORT MS Thesis	13b. TIME COVERED FROM _____ TO _____	14. DATE OF REPORT (Yr., Mo., Day) 1985 December 2	15. PAGE COUNT 117

16. SUPPLEMENTARY NOTATION

17. COSATI CODES			18. SUBJECT TERMS (Continue on reverse if necessary and identify by block number) Aircraft Performance, Optimization, Vectored Thrust, Thrust Vectoring.
FIELD	GROUP	SUB. GR.	
12	01		
01	03		

19. ABSTRACT (Continue on reverse if necessary and identify by block number)

TITLE: AIRCRAFT PERFORMANCE OPTIMIZATION WITH THRUST VECTOR CONTROL

THESIS ADVISOR: Dr. Curtis H. Spenny

Approved for public release: IAW AFR 190-1.

LYNN E. WOLAVER   16 JAN 86
Dean for Research and Professional Development
Air Force Institute of Technology (AFC)
Wright-Patterson AFB OH 45433

20. DISTRIBUTION/AVAILABILITY OF ABSTRACT UNCLASSIFIED/UNLIMITED ☒ SAME AS RPT. ☐ DTIC USERS ☐	21. ABSTRACT SECURITY CLASSIFICATION UNCLASSIFIED

22a. NAME OF RESPONSIBLE INDIVIDUAL Dr. Curtis H. Spenny	22b. TELEPHONE NUMBER (Include Area Code) 513-255-3517	22c. OFFICE SYMBOL AFIT/ENY

DD FORM 1473, 83 APR   EDITION OF 1 JAN 73 IS OBSOLETE.   UNCLASSIFIED

SECURITY CLASSIFICATION OF THIS PAGE

The objective of this ~~investigation~~ is to determine to what extent a highly-maneuverable aircraft's overall performance capability is enhanced by thrust-vectoring nozzles. The resulting performance capabilities are compared to a baseline configuration with non-thrust-vectoring nozzles to determine the effects and advantages of thrust vectoring.

The results indicate that the use of vectored thrust can significantly increase an aircraft's performance capability in turning flight. The greater the demand on the aircraft in a turning combat scenario, the more the aircraft utilizes its thrust-vectoring capability to complete the task. The results also indicate that the use of vectored thrust in other phases of flight -- such as cruise, acceleration and climb -- only slightly increases an aircraft's performance capability.

DTIC
FILMED

4-86
END